HOMOLOGOUS RECOMBINATION PROTEINS IN RESPONDING TO INTERSTRAND CROSS-LINKS AND DNA BREAKS

A Dissertation

Presented to the Faculty of the Graduate School of Cornell University

In Partial Fulfillment of the Requirements for the Degree of

Doctor of Philosophy

By

Joanna Maria Mleczko

August 2016

THE 9-1-1 DNA DAMAGE RESPONSE COMPLEX COORDINATES FANCONI ANEMIA AND HOMOLOGOUS RECOMBINATION PROTEINS IN RESPONDING TO INTERSTRAND CROSS-LINKS AND DNA BREAKS

Joanna Maria Mleczko

Cornell University 2016

Maintaining DNA integrity through genome surveillance and damage repair is crucial for cell survival. Thus, strategic infliction of DNA damage to cancer cells, for example using the DNA cross-linker Mitomycin C (MMC), has become a commonly employed approach in cancer chemotherapy. The 9-1-1 complex, a heterotrimeric PCNA-like scaffolding clamp consisting of RAD9, RAD1 and HUS1, localizes to damage sites and functions in DNA repair and ATR-mediated DNA damage checkpoint signaling. Seeking to clarify the possible involvement of HUS1 in the repair pathways required for ICL damage repair, I designed experiments to test interaction between HUS1 with players of the Fanconi Anemia (FA) pathway, canonical non-homologous end joining (C-NHEJ) and homologous recombination repair (HRR). First, we tested the role of HUS1 in responding to MMC-induced DNA damage and found that MMC treatment results in extraction-resistant nuclear retention of the 9-1-1 complex. We further observed that *Hus1*-deficiency was associated with significantly reduced viability following MMC treatment in cultured cells and mice. In addition, metaphase spread analysis revealed the formation of radial chromosomes in *Hus1*-deficient cells upon MMC treatment. These abnormal associations between non-homologous chromosomes signify error-prone DNA repair. Collectively, these phenotypes are reminiscent of FA, a heritable genomic instability disorder characterized by bone marrow depletion, increased cancer susceptibility and congenital malformations due to failure of crosslink repair. ICLs are recognized by the FA core complex which initiates a repair cascade including ubiquitination and chromatin recruitment of the heterodimer FANCD2/FANCI. I therefore tested how *Hus1* inactivation affected FA pathway signaling and found that HUS1 was required for MMC-induced FANCD2 mono-ubiquitination and recruitment to chromatin, as well as focus formation by FANCA, a core complex

factor. When testing the recruitment of DSB markers to the damage site in *Hus1*-deficient cells, I selected RAD51, an HRR key protein involved in nucleofilament formation for our assays. Immunofluorescence staining revealed a defect in RAD51 focus formation after MMC treatment but not after IR, suggesting a damage specific involved of HUS1 in HRR factor recruitment.

Taking an alternate approach to investigating the involvement of HUS1 in repair pathways I designed a mouse model that combined *Hus1* reduction with *Prkdc* deficiency. *Prkdc* codes for the PIKK family member DNA-PK, a crucial player in C-NHEJ that tethers free DSB ends in preparation for ligation. Interestingly, mice that were deficient for *Prkdc* and expressed reduced levels of *Hus1,* showed extended lifespans in aging experiments when compared to *Prkdc* single mutant controls. Dual deficient mice but not *Prkdc* single mutant mice were also exquisitely sensitive to MMC in preliminary experiments, while equally sensitive to IR in comparison to *Prkdc* single mutant mice. This suggests possible interactions of pathways in response to aging and genotoxin challenge.

In summary, my data indicate that HUS1 is essential for FA pathway activation during the response to MMC-induced ICLs, and we hypothesize that 9-1-1 may promote FA by direct scaffolding of FA proteins. 9-1-1 is involved in the repair of post-ICL DSBs in supporting the recruitment of RAD51 to the site of damage and possibly influencing NHEJ factors. Furthering the understanding of the molecular interactions in this pathway will provide important new insights into DNA damage responses, cancer prevention and therapy.

BIOGRAPHICAL SKETCH

Dr. Joanna Mleczko completed her Doctorate of Veterinary Medicine at Freie Universität Berlin, Germany in 2011. Dr. Mleczko came to Cornell after completing the Cornell Leadership Program for Veterinary Students in 2008, where she became interested in biomedical research. Her summer research within the program explored manipulation of angiogenesis in the hind brain using the quail embryo as a model. Later on during her graduate studies, she focused on deciphering the molecular interactions between canonical non-homologous end joining (C-NHEJ) and the Fanconi-Anemia pathway with the ATR pathway protein HUS1. The ultimate goal of her project is to help elucidate potential cancer drug targets, through discovery of synthetic lethal protein inactivation.

Acknowledgements

First and foremost, a huge thank you to my family Sylwia Poremska-Mleczko, Andrzej Mleczko, Krzysztof Mleczko, Aleksandra Mleczko, Marcin Mleczko and my mentor and friend Dr. vet. med. Axel Reetz. You always supported me and fostered scientific curiosity from an early age on, enduring so many questions and enabling and supporting my journey. My close friends Adrian McNairn, Parvin Shahrestani and Darshil Patel kept me sane when the going was rough. This would have not been possible without you.

I would also like to thank Dr. Weiss for his support and guidance as my mentor. Under Dr. Weiss care I have honed my critical thinking as well as bench skills, resulting in me becoming a better scientist.

I would also like to thank past and present members of the Weiss lab for their teachings and friendship. Special thanks to Dr. Amy Lyndaker, Dr. Kelly Hume, Dr. Erin Daugherty, Dr. Gabriel Balmus, Dr. Minxing Li and Dr. Pei Xin Lim, Claire Anderson and Jack Stupinski. Also thanks to current members of the lab Tim Pierpont, Yashira Negron, Darshil Patel, Catalina Pereira and Dr. Elizabeth Moore as well as to my co-author and collaborator Georgios Karras. Furthermore, I would like to thank the hard working undergraduate students in the Weiss lab, Cindy Luan, Charlton Tsang, Zanah Francis, Ellen Hong and David Karambizi.

A special ‘thank you’ to my committee members Dr. Marcus Smolka, Dr. John Schimenti and Dr. Paula Cohen for providing invaluable feedback.

Thanks for the Veterinary College at Cornell University for providing me with funding through a GRA fellowship.

TABLE OF CONTENTS

CHAPTER 1

LITERATURE REVIEW

1.1 Sources of DNA lesions

The DNA is the blueprint for RNAs and proteins which comprise all living beings. As such, it is crucial that its integrity is preserved and protected. Passing on of erroneous DNA code to the next generation threatens viability and health of organisms. The DNA suffers from constant attacks of both exogenous and endogenous origins [1] (Figure 1.1). The DNA as a biomolecule itself, while fairly stable in its hybridized form, is vulnerable and reactive in its single strand form, requiring regulation and protection at all times.

Endogenous damage

Deamination of bases is the most frequent spontaneous event resulting in DNA damage. Up to 10.000 occurrences of spontaneous deamination events per cell and day were measured by Lindahl et al. [2, 3]. The deamination of cytosine turns the base into uracil. Uracil is recognized and excised by uracil-DNA glycosylase [4] leaving an abasic site behind. The abasic site is repaired by AP endonucleases that nick the phosphodiester backbone of the DNA and cleave the abasic site. Consequently, polymerases fill up the gap. If left unrepaired, the deamination of cytosine into uracil can lead to wrong nucleotide insertion during replication. Uracil preferentially base-pairs with adenine. The DNA replication machinery therefore adds an adenine when it encounters an uracil on the template strand, instead of the originally intended guanine. It also creates a substrate for the mismatch repair system, which when encountering an unusual U-G pairing will falsely insert an A opposite of U, especially when uracil-DNA-glycosylase is impaired. GC→AT transitions at sites of cytosine methylation are largely responsible for the single site mutations that cause inherited disease in humans [5]. The GC→AT base change is frequent in mutated *p53* tumor suppressor genes found in many human cancers [6].

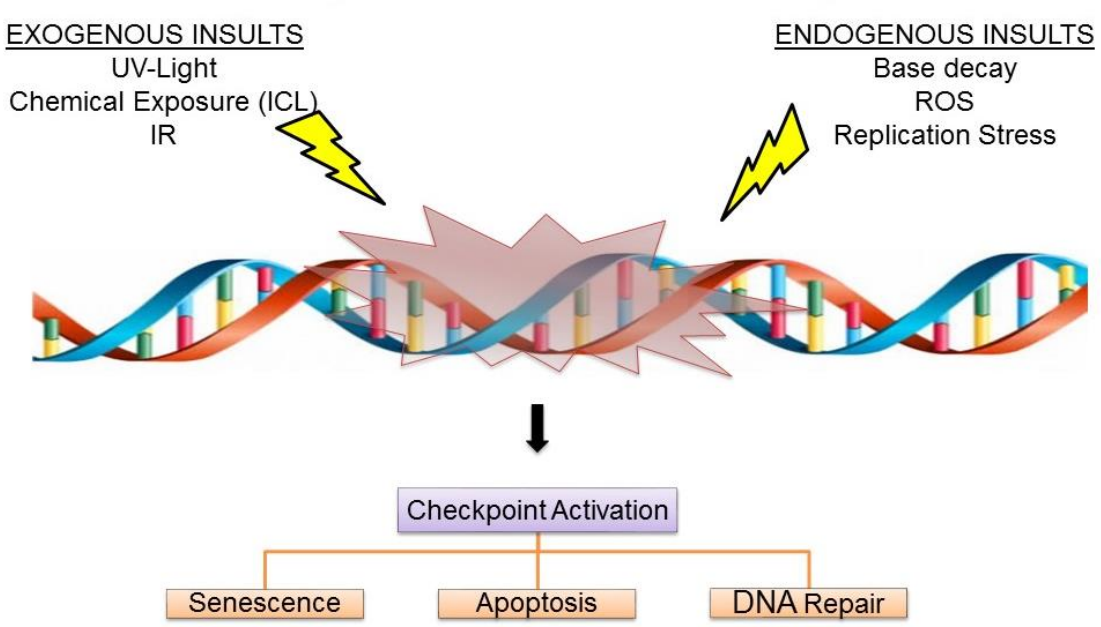

Figure 1.1. DNA endures attacks from various sources prompting a DDR response. Exogenous and endogenous insults cause lesions on the DNA. Endogenous insults can stem from spontaneous events such as base decay, from reactive oxygen species (ROS) which all result in slowed replication known as replication stress. Exogenous sources of damage include ionizing radiation (IR), UV light and chemical agents, some of which create particular toxic ICLs. The cell detects damage stemming from these insults with sensor proteins and responds with checkpoint activation. Protein-kinase-led biochemical cascades halt the cell cycle to allow for repair. When damage is too severe, cells elect apoptosis or senescence.

Endogenous damage stemming from reactive oxygen species (ROS) is another source of endogenous DNA damage encountered by cells. Attack by ROS results in oxidation of bases, single and double strand DNA breaks (DSB). One of the best studied species of oxidation-induced lesions is 8-Oxo-2'-deoxyguanosine (8-oxo-dG), an oxidized derivative of deoxyguanosine. These guanine derivatives increase the risk of base transversions (G:C to T:A), deletions and epigenetic alterations [7, 8]. Its occurrence has been measured as 2400 events per mammalian cell and day most of which are rapidly repaired in the healthy cell by the base excision repair (BER) pathway [9] (see also section 1.2.2 Repair Pathways).

There are several other chemical metabolites that also threaten the integrity of DNA (reviewed in [10]): The first to name is the process of lipid peroxidation which results in a production of highly reactive species, such as epoxides and aldehydes. Among the aldehydes 4-hydroxynonenal (HNE) and malondialdehyde (MDA) are considered most mutagenic. The bulky adducts formed by aldehydes interfere with the Watson-Crick pairing of bases, thus inviting mismatched base pairing. Other endogenous DNA damaging agents include the chemical families of base propenals, formed during DNA oxidation, by estrogens, by various alkylating and carbylating agents and lastly through DNA hydrolysis [10]. All these chemical agents can result in the formation of toxic DNA lesions.

Another source of endogenous damage encountered by cells stems from replication stress, which can be defined as the slowing or stalling of the replication machinery during DNA synthesis [11]. During replication the mini-chromosome maintenance 2–7 (MCM2–7) complex unwinds the parental strands followed by replication by the leading and lagging strand polymerases, Pol ε and Pol δ. When replication stalls at a DNA lesion, DNA synthesis can resume downstream by activation of dormant origins. Obstacles on the DNA stemming from unrepaired lesions, trinucleotide repeats [12] or collisions of the transcription machinery [13] result in fork stalling, requiring signaling for fork stabilization and restart. When not stabilized or not restarted for too long, stalled replication forks result in fork collapse, thus in failure to continue synthesis [14-16].

One of the major sources of exogenous damage is ionizing radiation (IR). IR is a form of high energy radiation. It originates from gamma-radiation, x-rays or high energy ultra violet (UV) light. When DNA encounters this type of high-energy electromagnetic waves, the absorption of energy results in DNA DSBs, i.e. severing of both strands of the DNA. On the lower energy spectrum of IR, DNA can also form single strand breaks.

The next class of exogenous damage is caused by UV light. UV light is a type of electromagnetic radiation with a wavelength between 10 and 400 nm. Its frequency lies between that of visible light and X-rays. UV-B and UV-C light exposure results in formation of covalent linkages between cytosine and an adjacent thymidine bases, known as thymidine dimers. These bulky lesions interfere with replication and confer distortion to the curvature of the DNA [17, 18]. UV-A light exposure results in occurrence of free radicals and lesions associated with them [19, 20]. In combination with photosensitive agents, such as psoralen, UVA light can cause highly toxic interstrand cross-links (ICL) [21]. A substantial variety of chemicals such as vinyl chloride and hydrogen peroxide and environmental chemicals such as polycyclic aromatic hydrocarbons found in smoke, soot and tar create a diverse range of DNA adducts, such as ethenobases, oxidized bases and alkylated phosphotriesters [2].

Various groups of chemicals contribute to a class of DNA damaging agents deserving to special recognition due to their severe toxicity: ICL-inducing agents. ICL-inducing agents such a Mitomycin C (MMC), Cisplatin, nitrogen mustard, aldehydes alkylating agents or the above mentioned psoralen create highly toxic lesions through covalently binding the guanines between two strands thus effectively blocking replication and transcription. One of the best described ICL-inducing agents is MMC. MMC is a methylazirinopyrroloindoledione antineoplastic antibiotic used to treat a variety of cancers. MMC generates oxygen radicals, alkylates DNA, and produces DNA ICLs between guanines of 5’-CG-3’ sequences, thereby inhibiting DNA synthesis [22] (Figure 1.2).

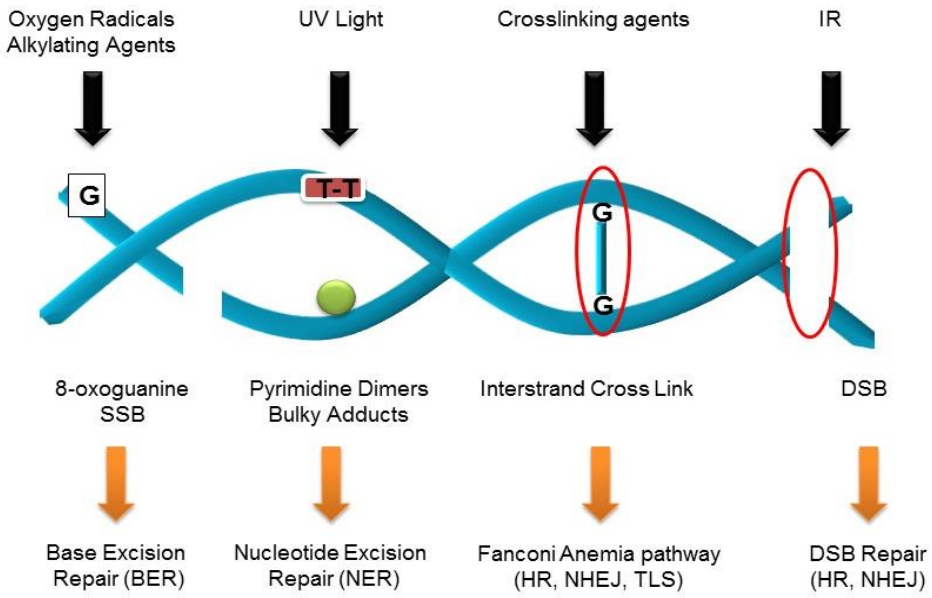

Figure 1.2. Depiction of genotoxic agents and consequent damage type.

Lesions affecting one strand caused by ROS, UV light or alkylating agents are repaired by MMR, NER or BER. ROS, free radicals and alkylating agent create lesions such as 8-oxoguanine that affect only one strand of the DNA. The repair usually involves base excision repair (BER). UV-light causes mostly bulky lesions such as thymidine dimers, requiring nucleotide excisions repair (NER) for removal. More complex lesions such as DSBs or ICLs require a combination of pathways including HR, C-NHEJ and TLS.

1.2 DNA damage response

Throughout their evolution organisms have relied on DNA as a coding molecule for biological information. In order to prevent erroneous information from being passed onto the next generation, organisms have developed mechanisms to maintain the integrity of their genomes. The DNA damage response contains a system of mechanisms, which allows cells to monitor the DNA, detect lesions, halt the cell cycle through activation of checkpoint and then commit to an appropriate fate be it repair, senescence or apoptosis (Figure 1.1).

1.2.1 DNA Damage Checkpoints

Historical overview

Since the early 1900 scientist have been observing cells undergo the process of cell division. Basic concepts of cell division were proposed already in 1832, when Barthelemy Dumortier (1797–1878) of France described "binary fission" (cell division) in plants. He observed the formation of a mid-line partition between the original cell and the new cell. These observations led him to reject the idea that new cells arise from within old ones, or that they form spontaneously from non-cellular material. The discovery of cell division is usually attributed to Hugo von Mohl (1805–1872), but Dumortier preceded him in this regard, however without insights into its mechanism of regulation, yet [23].

In the last 40 years, scientists have uncovered features of both the cell cycle and its control on a molecular level that significantly impacted the development of current models of aging, development and cancer [24]. The research on cell cycle control was spearheaded by three scientists: Leland Hartwell, Paul Nurse and Tim Hunt, who used three different model organisms to merge the formerly independent fields of genetics and cell cycle control. In 2001, they were awarded the Nobel prize in Physiology and Medicine for their achievements [25].

Fission yeast (*Saccharomyces pombe)*, a unicellular rod shaped eukaryote, grows longitudinally followed by a medial fission. It has been used as a model organism in Biology since the 1950ies. Beginning in 1976, Paul Nurse first described the gene *cdc2* [26]. He discovered that *cdc2* regulates the

transition from the cell cycle G1 phase to S-phase as well as the G2/M transition. In consequence, Nurse searched for and identified the human homolog *CDK1* in 1987, which codes for a cyclin dependent kinase [26]. Hartwell used budding yeast (*Saccharomyces cerevisiae*) to conduct his research on cell cycle control. Against the prediction of his peers, he succeeded in using yeast genetics to study the cell cycle and its control. Since budding yeast undergoes visible morphological changes as it undergoes cell division, Hartwell recognized its unique fit as a cell cycle control model. He identified various cell-division cycle (CDC) mutants that were defective in progression through specific phases of the cell cycle [27]. This collection of CDC mutants was the foundation for the major discovery in the field: The CDC genes proved to be highly conserved in eukaryotes and contained most key regulators of cell proliferation across species. Hartwell identified key events in the transition of cells through the cell cycle that slow the cycle in response to damage. This checkpoint response allows the evaluation of the damage, time for repair. Without checkpoints cells would risk passing on altered genetic information to the next generation [28].

The third scientist, Tim Hunt, used biochemical rather than genetic approaches in sea urchin (*Arbacia punctulata*) embryos to identify the key proteins important for progression of the cell cycle. Hunt and his colleagues described the protein cyclin. Cyclin level oscillation, caused by on cue expression and degradation, contributes to cell cycle regulation [29]. This demonstrated that a timing mechanism created by cytoplasmic proteins could control cell cycle progression. Hunt discovered that cyclin synthesis begins after fertilization and increases in levels during interphase. In the middle of mitosis cyclin levels rapidly declined. He also demonstrated that cyclins are conserved in vertebrates, with respectively similar functions [30].

Hunt and other scientists later showed that cyclins interact with and activate a family of protein kinases, called the cyclin-dependent kinases. A discovery fitting in with Hartwell's work on CDKs. Nurse, Hartwell and Hunt together described two groups of proteins, cyclin and cyclin dependent kinase (CDK) that control cell cycle progression. The fundamental hypothesis to be shaped by these three scientists was the notion that key cell-cycle events could be grouped into dependent, genetically definable

pathways [31]. These were to guarantee, that only after completion of specific cell cycle events, following events would occur.

Initially, the favored hypothesis was that dependent relationships of events in the cell cycle could be explained by earlier events generating products that were required for later events. Nurse, Hartwell and Hunt, however showed that these dependencies were regulated in an entirely different fashion: Through upstream to downstream signal transduction. When genes in these checkpoint pathways are mutated, then late events are permitted to unfold before the completion of early events, resulting in faulty division of cells. This was shown by Hartwell and colleagues in key checkpoint experiments in which checkpoint defective cells failed to arrest when challenged with DNA damaging agents [32]. Cell cycle checkpoints therefore monitor and preserve genomic integrity by allowing for detection and repair of problems, or rejection of cell cycle progression.

Current understanding of DNA damage checkpoints

As the cell undergoes mitosis, it has to ensure that its daughter cells will be provided with intact copies of its genome. Damage from exogenous or endogenous sources will result in cell cycle arrest through the G1/S, intra-S, or G2/M checkpoints, in order to allow time for repair. If DNA damage checkpoint pathways are defective, this can result in mutagenesis, cellular toxicity or genome instability. If cell arrest is achieved, repair pathways will be activated to remove the lesion, otherwise cells will elect apoptosis or senescence. DNA damage surveillance is active during the whole cell cycle and can therefore halt or slow the transition of the cell into the next phase when needed. Halting of the cell cycle at G1/S, intra-S, and G2/M coins the title of the respective checkpoint.

The three checkpoints have in common that they respond to DNA damage and that they share many proteins. Two DNA damage signaling pathways existent in mammalian cells are individually headed by two phosphatidylinositol 3-kinase-like (PIKK) serine/threonine protein kinases named ATM and ATR respectively. The genomic disorder Ataxia Telangiectasia was name-giving for the two PIKK kinases ATM and ATR (**A**taxia **T**elangiectasia **M**utated, respectively **A**taxia **T**elangiectasia and **R**ad3

related). The activation of the kinases results in phosphorylation of their downstream targets CHK1 and CHK2. CHK1 and CHK2, carrying phospo-kinase properties themselves, phosphorylate CDC25 marking it for degradation. The absence of CDC25 prevents activation of the cyclin E-CDK complex causing arrest in G1 [33]. Other responses follow in order to maintain the arrest: CHK1 or CHK2 also phosphorylate P53. This saves P53 from ubiquitin mediated degradation. P53 serves as a transcriptional activator for various targets. Among them is P21, another important cell cycling controlling protein. P21 inhibits cyclin E-CDK21, thus maintaining the arrest.

During S-phase, as DNA strands replicate, the forks may encounter lesions which do not allow for progression of the fork. Most typically, obstacles such as bulky lesions or ICLs cause the fork to halt. Through exposed ssDNA that becomes coated with RPA, ATRIP-ATR and activating factors are attracted to the site of damage (see also 1.5.1). In cases of DSBs, the MRN complex binds to the free ends of the DNA. It recruits ATM which in undamaged cells, dimerizes. ATM undergoes auto-phosphorylation at serine 1981 upon damage sensing. This activates ATM and releases it from its dimer bond. Activated ATM phosphorylates multiple targets. Among them is ɣH2AX, a recruiter for further modulation and recruitment of repair factors, CHK2 and P53. These events delay replication allowing for further time to carry out repair. See 1.5.1 for more details.

In addition to mechanisms similar to the ones in the G1-checkpoint which rely on the phosphorylation of CDC25, P21 and P53, the G2/M checkpoints harbors another mechanism to arrest the cell in G2 [34]. It operates through stabilization of WEE1 which inhibits CDC2, keeping the cell arrested until the damage is repaired [35].

1.2.2 Single strand DNA damage repair pathways

Depending on the type of damage, the cell will employ one or multiple repair pathways to address the damage repair task. (see sections 1.6 and 1.7 for more detail on ICL and DSB repair). Lesions affecting one of the strands are typically repaired by one of three mechanisms: BER, NER or MMR.

Base excision repair (BER) results in DNA-glycosylases based excision of sequences containing small, non-bulky lesions that do not distort the helix. The 8-oxo-dG and uracils stemming from deamination fall into this category [36].

Nucleotide excision repair (NER) operates either within context of transcription interference (transcription coupled or TC-NER) or independently of it (global genomic or GG-NER). NER addresses bulky, or helix-distorting lesions such as thymidine dimers. In TC-NER the initializing event is the stalling of the RNA polymerase during transcription. In transcriptionally silent regions, the distortion of the helix or the bulky adduct serve as recognition factors for sensing the damage and recruitment of nucleases that cut out, and polymerases that repair the damage [37].

The evolutionary conserved mismatch repair (MMR) machinery reduces the number of false insertions stemming from replication errors, thus reducing the mutation rate in cells. It typically scans the newly synthesized DNA strand for atypical base matches. When encountering base substitution mismatches and insertion-deletion mismatches, the MMR becomes activated. Repair is initiated when homologs of MutS bind to the site of damage, followed by excision and replacement of the affected region [38].

1.2.3 Apoptosis

If a cell is faced with damage too severe to repair, this can result in a permanent block of the cell cycle. The cell can choose to undergo a suicide program called apoptosis or enter a dormant state called senescence, both possible consequences of DDR through checkpoint activation.

Apoptosis involves shrinkage of the cell body, fragmentation of all cellular components and concludes with the inevitable death of the cell. It differs from necrosis in that it is a tightly controlled and contained demise rather than a traumatic destruction. Apoptosis is induced through either an intrinsic or extrinsic pathway, depending whether the cell receives the kill signal from within or from a different cell. In both cases the process involves an activation of caspases that degrade proteins [39].

1.3 Genomic instability

Genomic instability (GIN) is the tendency to acquire and accumulate genetic alterations within the genome of a cellular lineage. This includes aberrations of DNA sequences and chromosomal instability as well as aneuploidy. Genome aberrations of various kinds are commonly found in cancer and are considered one of its hallmarks [40]. High exposures to exogenous damage, increased replication rates as well as defects in DNA repair pathways have been identified as sources of GIN. Inactivation of genes that are involved in DSB repair such as BRCA1/2 [41] or its regulators such as KU, NBS1 or ATM [42, 43] have been shown to increase likelihood of cancer occurrence in patients. This connection establishes DSB repair as an important guardian of the genome integrity and a tool to understand the origin of cancer.

1.4 Significance of DNA damage repair models for cancer therapy

In cancer, a careful balance between genomic variability and limitation of GIN is crucial for the survival and progression of a malignant cells [1]. The usage of cancer drugs, which function through DNA damage infliction is affected by the cancer cell's ability to repair the damage or disable apoptosis: The more defects in DDR genes are accumulated in a tumor cell, the more it will struggle with repairing additional damage stemming from chemotherapy drugs. In traditional treatment, DNA damage infliction acted rather indiscriminately. Any rapidly replicating cell could be affected. Through increasing knowledge of DDR pathways and their function in normal, transforming and cancerous cells, novel more selective treatment approaches are emerging. These treatment approaches take advantage of specialized roles for DDR proteins during the multi-step process of tumorigenesis.

GIN in cancer is a matter of both cause and consequence. A common model postulates a mutator phenotype, a condition in which genomic alterations in caretaker genes form a prerequisite for further alterations, which subsequently lead to tumorigenesis. DDR genes form a majority of care taker genes, with the role to prevent GIN, both prior and post initiation events.

Due to imperfections in DDR, initiation events can persist in cells and be passed on to following generations. While the majority of initiation events will remain dormant, occasionally rapid cell division,

inflammation or vulnerable gene location can result in amplification of initiation effects: When initiation events enhance cellular replication rate, initiation events transfer into the next stage of tumorigenesis, promotion. In such pre-cancerous lesions, again DDR genes such as 53BP1 and BRCA1 protect the organism by inducing apoptosis or senescence in precancerous tissues [44-48]. Only cells, which escape removal through apoptosis or senescence, can undergo tumor progression. DDR poses therefore a tumorigenesis barrier; which tumor cells can only circumvent by disabling elements of DDR.

At the forefront of the tumorigenesis barrier stands the DDR which activate P53 when a hyper proliferation signal is detected. In analyses of mutated genes in 210 human cancers, ATM was the third ranked gene in frequency [49]. Mutations in CHK2, have been linked to a cancer predisposition syndrome clinically indistinguishable from Li-Fraumeni syndrome [50]. Furthermore, upstream DDR genes such 53BP1 were found silenced in a variety of melanomas, breast and lung carcinomas [51].

After pre-cancerous lesions have progressed into the cancerous stage, DDR inhibition provides a tool for radio or chemosensitization. Inhibitors such as wortmannin and LY294002 can inhibit ATM, (ATR) and DNA-PKcs which results in increased sensitivity to radiation in exposed tissues [52, 53]. Selective inhibitors of ATM (KU55933, KU60019, and CP466722) show promise as well as radiosensitizing and chemosensitizing agents do [54-56]. For DNA-PKcs, small molecules such as NU7441, IC8736 and SU11752 are promising drugs to improve radio sensitivity [57-59].

As a consequence of breaking though the tumorigenesis barrier, most tumors acquire defects in DDR genes. Through targeted synthetic lethality, DDR mutations provide a strategy for targeted cancer therapy. Synthetic lethality is understood as cell death, caused by simultaneous occurrence of two mutations [60].

An example for this approach is simultaneous targeting of two DSB repair pathways: canonical non-homologous end joining (C-NHEJ) and homologous recombination repair (HRR). In a very successful approach for treating breast and ovarian cancers, which often hold BRCA1/2 mutations, PARP1 inhibition was used [61-63]. PARP inhibitors are toxic in *BRCA*-mutant but not in normal cells, resulting in the development of several inhibitors including iniparid, olaparib, PF-01367338, veliparib,

and CEP-9722 for clinical trials [64]. A similar approach successfully targeted ATM and DNA-PK in parallel, creating a new therapy target [65].

Recently a drug based screen revealed new interactions: The sensitivity of 67 cancer cells lines to a specific inhibitor of one of the major DNA DSB repair pathways C-NHEJ was assessed resulting in the identification of a novel therapeutically actionable synthetic lethal interaction between the MMR protein MSH3 and DNA-PK [66]. By further exploring mechanisms for DSB processing and repair, new interactions between repair pathways can be revealed and the knowledge could be exploited for further establishment of treatment targeting different types of cancer. I hypothesize that simultaneous disabling of a player of the C-NHEJ pathway, DNA-PK and of the PCNA-like heterotrimeric checkpoint clamp 9-1-1, may result in a synthetic lethal interaction on a cellular or organismal level, due to cytotoxic effects of unrepaired DSB accumulation.

Alternatively, 9-1-1 and DNA-PK simultaneous disabling can lead to chemosensitization or radiosensitization. If 9-1-1 has an important role in HRR, in DSB repair and for ICL repair pathway (Mleczko et al., manuscript in preparation), targeting the disruption of the clamp could impart severe damage to cancer cells, sensitizing them to conventional cancer drugs, radiation and endogenous DNA damage repair defects. This study will elucidate the role of HUS1 in genomic instability, HRR and its potential function as a regulatory entity in the processing of DSBs (Figure 1.3).

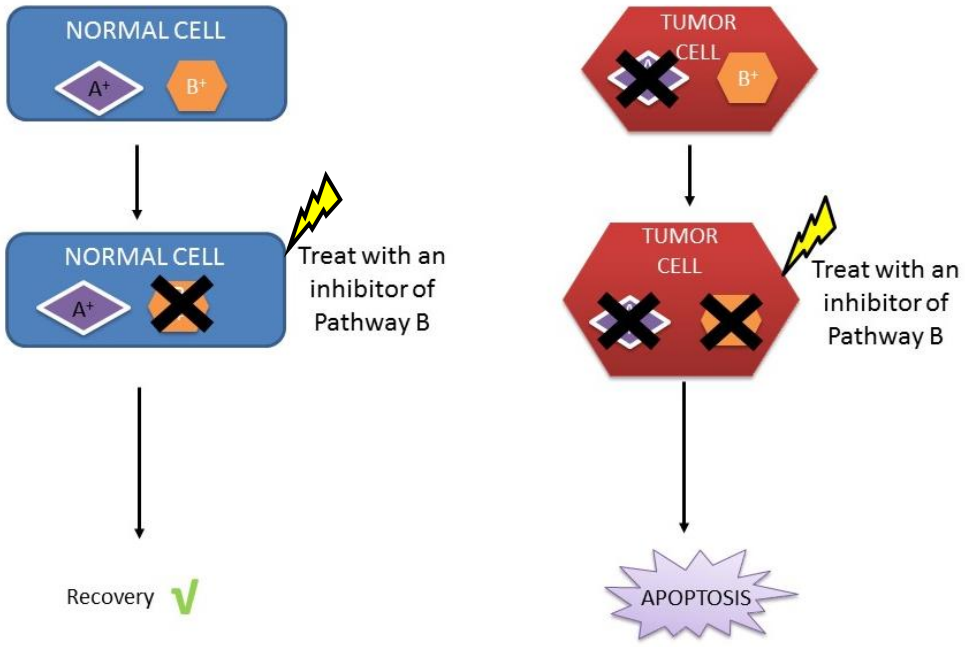

Figure 1.3. Acquired mutations sensitize tumor cells for DDR inhibitor treatment through the mechanism of synthetic lethality. Healthy cells will survive inhibition through reliance on a redundant repair pathway within DDR. Tumor cell often harbor inactivation of important DDR genes, allowing them to survive DDR based selection processes. When faced with an inhibitor of a redundant repair pathway, these cells succumb to overwhelming accumulation of genomic instability.

1.5 The role of the DNA damage checkpoint clamp 9-1-1 in DNA damage response

1.5.1 9-1-1 in checkpoint signaling

Several DNA clamps help in replication and repair of the DNA. One such clamp is the 9-1-1 DNA damage checkpoint clamp composed of three subunits, RAD9, RAD1 and HUS1. 9-1-1 does not have an enzymatic function of its own; it serves as a protein scaffold tethering various players in place. The role of the 9-1-1 complex is to bind DNA preferentially at single strand-double strand 5' junctions when RPA is present [67, 68]. The 9-1-1 complex is structurally very similar to PCNA (Proliferating Cell Nuclear Antigen), whose role in DNA replication and repair is well established. The 9-1-1 complex is known to function within the ATR-mediated DNA damage checkpoint pathway.

Upon sensing replication stress, ssDNA is coated with replication binding protein A (RPA). ATR–ATRIP is independently recruited to ssDNA–RPA stretches and RAD17/RFC2–5 loads 9-1-1 onto 5' junctions [67, 69]. 9-1-1 through interaction of RAD9 and TOPBP1 [70-72] helps activate ATR. Several ATR-dependent phosphorylation events occur, including sites on RAD17, 9–1–1 clamp components, and TOPBP1. Phosphorylated TOPBP1 can bind surfaces on ATR and ATRIP, causing ATR to become more active and to phosphorylate its downstream effectors including CHK1. The phosphorylation of CHK1 halts the cells cycle thus preventing the cell from entry into mitosis. It further allows for stabilizing the stalled replication forks. Other replication fork components such as RPA, polymerases, MCM proteins, PCNA, and Claspin are also ATR phosphorylation targets supporting the stabilization of the fork. Through phosphorylation of recombination related proteins such as BRCA1, WRN and BLM, ATR initiates repair processes [73-76].

In summary, ATR checkpoint activation allows time for and stimulates repair, or if that is not possible, launches the cell's suicide program-apoptosis (Figure 1.4).

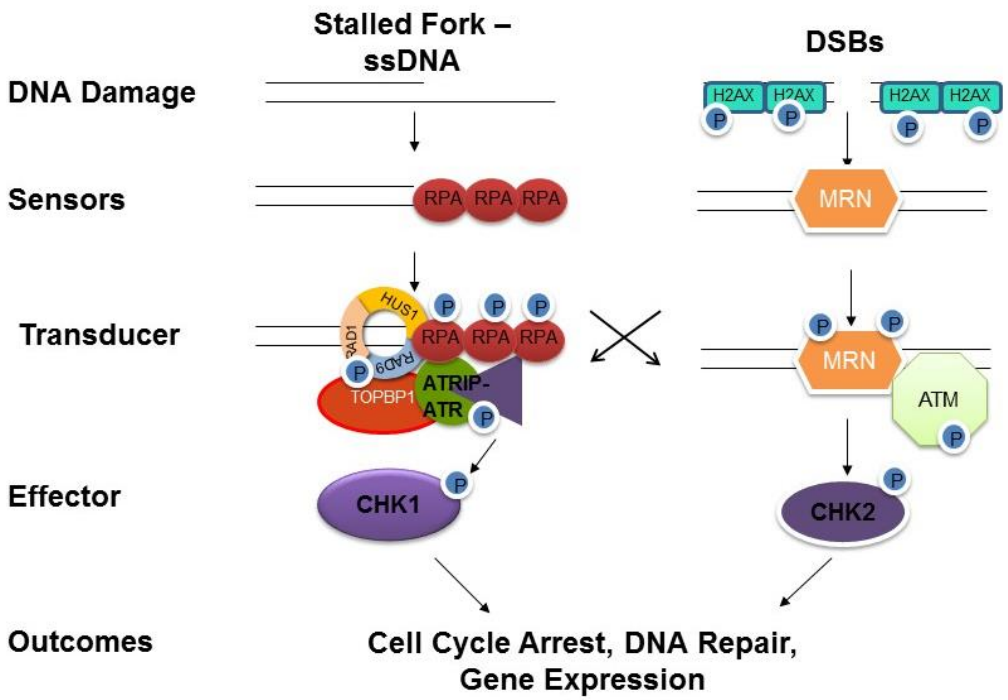

Figure 1.4. The ATM and ATR pathways work in parallel in response to DSBs and ssDNA lesions. Due to its strong affinity to exposed single stranded DNA (ssDNA) RPA coats the ssDNA. RPA attracts ATR-TRIP and the 9-1-1 loading complex RAD17/RFC2-5. TOPBP1 interacts with RAD9 and promotes activation of ATR. ATR phosphorylates downstream targets such as CHK1 resulting in cell cycle arrest. In response to DSBs the MRN complex binds free DSB ends. ATM, which exists as an inactive dimer, dissociates and autophosphorylates, thus augmenting its phosphokinase activity.

1.5.2 9-1-1 in DNA damage repair, its coordination and genomic instability

9-1-1 components were first discovered using genotoxin sensitivity screens in yeast. In fission yeast, six checkpoint genes (*hus1*$^{+}$, *rad1*$^{+}$, *rad3*$^{+}$, *rad9*$^{+}$, *rad17*$^{+}$, and *rad26*$^{+}$) were identified in close succession [77-80]. HUS1 homologs were found in humans and mice [81, 82] they also interacted with RAD1 and RAD9 [83, 84]. Molecular modeling techniques predicted a similar form and function as that of PCNA that of a DNA sliding clamp. Soon after, this was confirmed when shown that 9-1-1 forms a stable heterotrimeric clamp that in fact interacts like PCNA [84-93].

In 1999 the *Hus1* gene was first cloned in mice and placed on chromosome 11 [94]. Shortly after, Weiss et al. describe mid-gestational embryonal lethality in mice that are deficient for HUS1. MEFs obtained from *Hus1*-deficient embryos showed chromosomal instability and sensitivity to genotoxin stress [95]. The importance of HUS1 for mammalian development became apparent in 2002 when HUS1 was identified as a checkpoint protein acting upstream of CHK1 [96] with disruption of any of its components resulting in checkpoint defect phenotypes similar those to CHK1 defects [96, 97 432, 98]. In 2003, the role of HUS1 was placed in S-phase checkpoint signaling as *Hus1*-deficient cells failed to slow replication in response to replication stress inducing agents [99]. The alternative clamp loader RAD17/RCF2-5 was identified as required for 9-1-1 DNA binding in response to genotoxin induced DNA damage, in yeast frog and human models [67-69, 91, 93, 100-104].

The RAD9 tail was identified using truncation mutants to mediate checkpoint function [97, 105]. Soon, roles for 9-1-1 beyond checkpoint function emerged, first in TLS [106, 107]. Then experiments in yeast showed that RAD1 and RAD17 deletion, caused sensitivity to DSB inducing enzymes [108] and ionizing radiation [97]. The model of sliding clamp molecular tether was put forward.

Even though 9-1-1 and its component are essential for ATR activation, HUS1 has been found to function not only in checkpoint signaling but also in DNA repair. HUS1 is necessary for DSB repair following ionizing radiation through HRR but is independent of C-NHEJ. In their study the authors used an I-Sce I-induced-DNA DSBs system, which measures HRR after knockdown of HUS1. Their results

show that HRR is impaired in *Hus1*-deficient cells while C-NHEJ efficiency as measured through asymmetric field inversion gel electrophoresis remains unaffected [109].

To study the consequences of partial *Hus1* inactivation in mice, Levitt et al. developed the *Hus1* allelic series. In this approach, a partial expression allele of *Hus1*, coded by $Hus1^{neo}$ was combined with either a null allele or a wild type allele, to achieve a gradual protein level reduction of HUS1. This model, also explored in chapter three, established a role for HUS1 in genome maintenance *in vivo* as *Hus1*-deficiency increased micronucleus formation in peripheral blood in mice. Cells derived from $Hus1^{neo/\Delta 1}$ mice displayed spontaneous chromosomal instability and underwent premature senescence [110].

Using the same cells, Meyerkord et al. revealed that apoptosis in response to epotoside treatment in *Hus1*-deficient cells is mediated through the BH3 proteins PUMA and BIM. [111]. To study a role of HUS1 protein in tissue morphology homeostasis and tumor suppression, Yazinski et al. employed a mammary specific CRE-mediated *Hus1* deletion in a P53-deficient background. The authors observed accumulation of defective cells with morphological and functional changes to the mammary tissue [112]. A 2012 study by Balmus et al. analyzed the role of HUS1 in the context of ATR signaling and its effect of ATM function in mice. HUS1 reduction using hypomorphic mice resulted in embryonal lethality in the background of *Atm* deletion. A dose increase of HUS1 in the same ATM-deficient background yielded viable mice, with severe developmental defects reminiscent of human AT patients. This study underlined findings of crosstalk between ATM and ATR pathways as well as strengthened a role of HUS1 as modulator of DNA damage response [113]. Lyndaker et al. studied a role of HUS1 in meiosis in mammals, to extend on knowledge of HUS1 function in yeast worm and flies. The author utilized germ-line specific *Hus1* inactivation and discovered a crucial role for HUS1 protein in meiotic prophase I. Such as in somatic cells, HUS1 contributes to the 9-1-1 clamp formation and acts in DSB repair, thus enabling germ cell maturation and therefore fertility [114]. Balmus et al. showed that HUS1 is required for resistance of genotoxin sensitivity *in vivo*. Mice that where hypomorphic for *Hus1*, showed increased sensitivity to the replication stress inducers MMC and HU, but not the DSB inducer ionizing radiation.

These findings support the hypothesis of ATR and ATM responding in specialized manner to different types of DNA damage, *in vivo* [115].

In 2015 Lim et al. published a comprehensive site directed mutagenesis study confirming roles for HUS1 in protein-protein interactions between the 9-1-1 clamp and DNA repair players. Furthermore, the authors described functional residues responsible for clamp assembly and DNA-interactions. Firstly, Lim et al. identified the HUS1 residue arginine 128 at the RAD9A surface to be crucial for clamp formation and DNA binding. The mutation of arginine 128 to glutamine resulted in loss of clamp formation and DNA association. Next, the authors localized positively charged residues Lys-25, Lys-93, Lys-173, Arg-175, Lys-236, and Lys-237 at the inner ring surface of HUS1 that were cooperatively responsible for DNA association and genotoxin survival.

Lastly, HUS1 was found to harbor one surface area resembling interaction pockets on PCNA and one novel pocket, that when mutated, resulted in increased sensitivity to genotoxin-induced DNA damage. Interestingly, these pockets were dispensable for DNA interaction and ATR- checkpoint activation. Direct interaction between HUS1 via outer surface pockets and MYH, supports the model of HUS1 harboring several separable functions: HUS1 plays a role in ATR checkpoint activation as well as one in DNA repair [116].

Cells taken from patients of the rare genomic instability disorder Fanconi Anemia (FA) patients [117], show characteristic formation of radial shaped chromosomes upon treatment with crosslink inducing agent such as MMC. These radial chromosomes have been linked to erratic repair of DSBs. *Hus1*-deficient cells have been shown to present similar structures upon treatment with DNA damaging agents, which is suggestive of HUS1 involvement in the repair of MMC-induced DNA crosslinks (chapter two). Newly emerging studies place the 9-1-1 clamp into a context of ATR independent repair functions: BER proteins interact with 9-1-1 both physically and functionally suggesting a role for the 9-1-1 clamp as a coordinating scaffold in BER [118-121]. Furthermore, 9-1-1 has been implied in mismatch repair (MMR) [122], in regulation of DSBs [110, 123] and finally, emerged in a proteomic screening study, which examined targeted proteins needed for ICL repair [124]. HUS1 is suggested to be involved in

nucleotide excision repair (NER), base excision repair (BER), translesion synthesis (TLS) and DNA damage tolerance (DDT) pathways [121, 125-127] (Table 1). 9-1-1 is involved in end resection through stimulation of EXO1, SGS1 and DNA2 as well as ligase stimulation [128] (Figure 1.5). All these studies suggest a role for HUS1 which is likely not limited to checkpoint signaling. Two paralogs of RAD9 (also called RAD9A) and HUS1 have been identified in 2002 and 2003 respectively. RAD9B and HUS1B are highly expressed in testes and were found to interact with other elements of 9-1-1 as well as each other [129, 130]. Lyndaker et al. has put forward the idea of a non-canonical clamp consisting of RAD9B, HUS1B and RAD1 to function during meiosis [114].

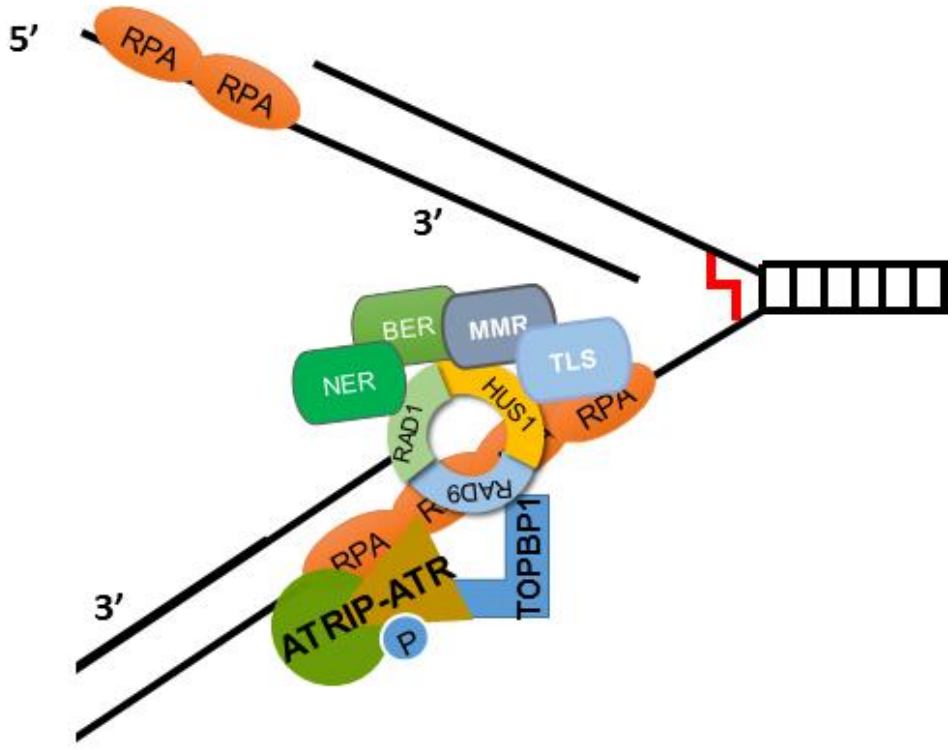

Figure 1.5. Model of 9-1-1 dual roles in ATR checkpoint activation and DNA repair. Beyond its canonical role in ATR checkpoint activation, 9-1-1 has proposed roles in DNA repair. It associates with members of the NER, BER, TLS and MMR pathways and works thus as a molecular scaffold.

Table 1. DDR proteins that interact with elements of the 9-1-1 complex.

Model system	Method	DNA repair component	Repair pathway	Interacting partner(s)	Reference
S. pombe	In vitro pulldown, crystal structure	SpMYH	BER	SpRad9, SpHus1, SpRad1	[131]
H. sapiens	In vitro pulldown	FEN1	BER	Rad9, Hus1, Rad1	[119]
H. sapiens	In vitro pulldown	Pol β	BER	Rad9, Hus1, Rad1	[118]
H. sapiens	In vitro pulldown	DNA Lig I	BER	Rad9, Hus1, Rad1	[121]
H. sapiens	In vitro pulldown	APE1	BER	Rad9, Hus1, Rad1	[132]
H. sapiens	In vitro pulldown	NEIL1 glyc.	BER	Rad9, Hus1, Rad1	[122]
H. sapiens	In vitro pulldown	TDG glyc.	BER	Rad9, Hus1, Rad1	[122]
H. sapiens	In vitro pulldown	hOGG1 glyc.	BER	Rad9, Hus1, Rad1	[133]
H. sapiens	In vitro pulldown	MSH2	MMR	Rad9, Hus1, Rad1	[122]
H. sapiens	In vitro pulldown	MSH3	MMR	Rad9, Hus1, Rad1	[122]
H. sapiens	In vitro pulldown	MSH6	MMR	Rad9, Hus1, Rad1	[122]
H. sapiens M. musculus	In vitro pulldown	MLH1	MMR	Rad9	[134]
S. cerevisiae	Y2H screen and in vivo studies	Rev17	TLS	Mec3 (Hus1) Ddc1 (Rad9)	[135]
S. pombe	In vitro pulldown	DinB	TLS	SpHus1, SpRad1	[107]
S. cerevisiae	In vitro pulldown	Rad14 (XPA?)	NER	Ddc1 (Rad9)	[136]
H. sapiens	In vitro pulldown	Metnase	NHEJ	Rad9	[137]
M. musculus	In vitro pulldown	Rad51	HR	Rad9	[138]

1.6 The Fanconi Anemia pathway and the repair of interstrand cross-links

Sensitivity to genotoxin-induced DNA damage has been exploited in cancer treatment, as highly replicative transformed cells have an increased sensitivity to DNA damage. Thus, our understanding of DNA damage repair pathways helps advance treatment of cancers through inducing targeted damage in neoplastic growths [139].

One type of exogenous damage applied in cancer chemotherapeutic treatment is by utilization of ICLs generating agents. ICLs are covalent linkages between the complementary strands of the DNA helix. They are particularly toxic to cells as they interfere with the unwinding of the DNA, thus blocking transcription, replication and recombination. Among the many classes of ICL-inducing genotoxins, Mitomycin C (MMC) is one frequently used in chemotherapeutic treatment.

1.6.1 DNA ICL crosslink creation and recognition

Repair of ICLs can happen inside or outside of replication, still in both cases similar steps are required for repair [140]: Recognition during S-phase is induced through the collision of replication forks into an ICL, signaling and recruitment of downstream effectors, followed by excision through nucleases at 3'and 5' of the lesion. If carried out during S-phase this results in a DSB intermediate, eventually repaired by RAD51 mediated (HRR) [141]. In both cases, unhinging of the lesion is followed by trans lesion synthesis (TLS) repair and the remaining bulky lesion is removed by nucleotide excision repair (NER) [142].

1.6.2 FA signaling cascade

The proteins involved in the repair of ICL have been traditionally grouped into a family of proteins coined the Fanconi Anemia (FA) Pathway. The pathway is named after the Swiss pediatrician Guido Fanconi who originally described the related FA syndrome in 1927 [143]. FA is a rare genetic disorder characterized by cancer susceptibility, bone marrow failure and congenital abnormalities believed to occur as a result of failure to repair ICLs. Mutations of one of at least 17 genes coding for the FA protein

family have been demonstrated to result in characteristic genomic and chromosomal abnormalities in humans and various model systems. Cells obtained from patients display extreme sensitivity to ICL-inducing agents such as MMC or Cisplatin. The mechanistic details of the role of FA proteins, especially for the core complex, largely remain unresolved. Due to its low abundance, complex structure and the lack of orthologues in lower class eukaryotic systems the purification of the core complex components has proven to be a challenge, only recently resolved in an avian model [144].

While in mammalian cells ICL repair begins with the recruitment of sensor proteins to the site of damage, the detailed molecular interactions of this process remain unresolved. The FA core complex protein FANCM, a DNA translocase and its helper proteins FAAP24, MHF1 and MHF2 are the sensors of ICLs [145, 146]. The phosphorylation of FANCM by ATR [147] and the assembly of the remaining core complex proteins follows [148]. The core complex is activated after phosphorylation of FANCI [149-151] by ATR, phosphorylation of core complex components [152-154] and the following ubiquitination of the FANCI/ FANCD2 (ID) heterodimer which then localizes to the site(s) of damage [116, 155].

The ubiquitination of the ID heterodimer is a crucial step in activation of the FA pathway after which the heterodimer must localize to the chromatin for normal FA signaling. The RING domain-containing E3 ligase FANCL carries out the monoubiquitination of ID. Along with FANCL, the presence of FANCB and FAAP100 is required for ubiquitination in vitro [156] while disease associated mutations in crucial components of the complex disrupt ubiquitination of FANCD2 [155, 157, 158]. Isolated FANCL is capable of ubiquitinating FANCD2 by itself in vitro, however its activity and specificity greatly increases in presence of the remaining core complex components [156] (Figure 1.6).

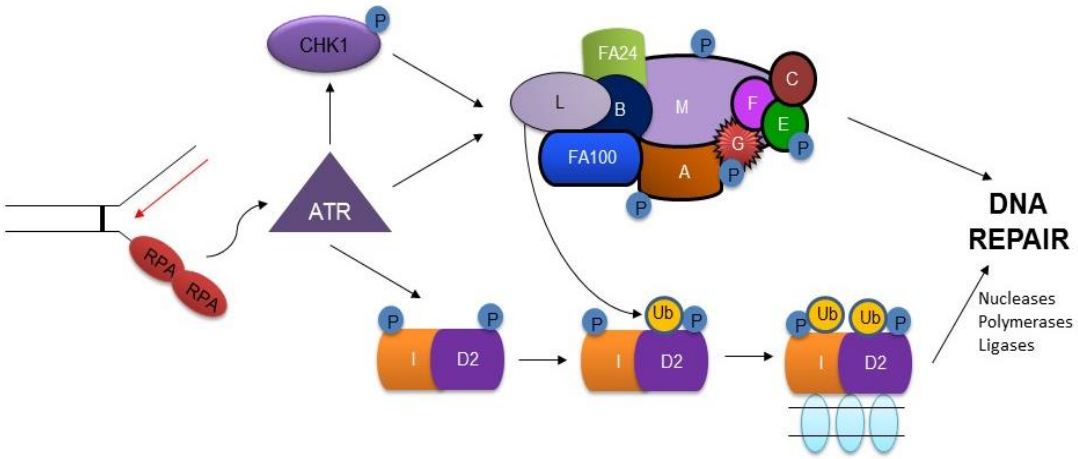

Figure 1.6. The Fanconi Anemia pathway combats ICL-induced DNA damage.

When replication forks stall at ICL, exposed ssDNA associated with RPA. ATR-ATRIP binds RPA and activates the phospho-kinase activity of ATR. ATR phosphorylates FANCI and elements of the core complex, after which, the core complex ubiquitinates FANCD2. The phosphorylated and ubiquitinated FANCD2/FANCI dimer localizes to DNA and serves as a recruiting platform for downstream repair steps involving, nucleases, polymerases and ligases.

1.6.3 Interstrand cross-link resolution

The binding of the ID heterodimer to chromatin signals for recruitment of downstream players, such as SLX4, XPF-ERCC1, FAN1, SLX1 and MUS81-EME [159, 160]. FAN1 and XPF-ERCC1 nucleases perform incisions at 3'and 5' of the lesion allowing for further processing [161-164]. During S-phase, the strands are separate as they undergo replication. The incision on one strand therefore results in creation of DSBs, which requires HRR for error free repair [165]. The DSBs if unprocessed or repaired erroneously, pose a major threat to chromosomal integrity.

One of the consequences of FA protein dysfunction, as seen in clinical cases, is the formation of cross-like chromosomal structures. These are called radial chromosomes and have been used as a diagnostic feature for more than 30 years [166], long before the responsible protein mutations were identified. They are believed to be remnants of a failed HR attempt and subsequent C-NHEJ substitution. While multiple FA and non- FA protein defects lead to observation of radials chromosomes, a DSB intermediate seems to be a common denominator, thus linking the FA pathway once again to DSB pathways [167].

1.7 Mechanisms of DNA double strand break resolution

DNA DSBs are lesions in which both strands of the DNA are severed. Common pathological sources of DSBs are ionizing radiation, or fork collapse stemming from collisions of the fork with obstacles during replication. A number of DNA alterations can cause these obstacles, starting with simple base detoriation, bulky lesions, intercalating agents to highly toxic ICLs, preventing separation of strands. Unrepaired DNA DSBs pose a danger to the maintenance of genome integrity as reviewed in [168]. Thus, the cell employs multiple repair mechanisms to respond to DSBs reviewed in [169] (Figure 1.1). One of them, HRR is active during S-phase as it requires an intact sister chromatid to be used as a template. C-NHEJ on the other hand is responsible for the majority of repairs outside of S-phase with some overlap of the

pathways during S-phase and G2 phase [170]. C-NHEJ (reviewed in [171]) is the more error prone pathway as it does not employ an intact template, but instead ligates ends together. If applied to imperfect or structurally damaged ends, the C-NHEJ proteins will resect sequences resulting in loss of information. Alternative End Joining, (A-EJ) is a backup pathway that relies on micro homology sequences. It steps in in absence of functional HRR and C-NHEJ with a tendency to incorporate errors as it has no proofing mechanism [172] (Figure 1.7). A-EJ has been proposed to be responsible for chromosome radial formation, which are products of error prone repair. I hypothesize that the 9-1-1 clamp suppresses both end joining pathways to favor HRR, or suppress C-NHEJ but not A-EJ.

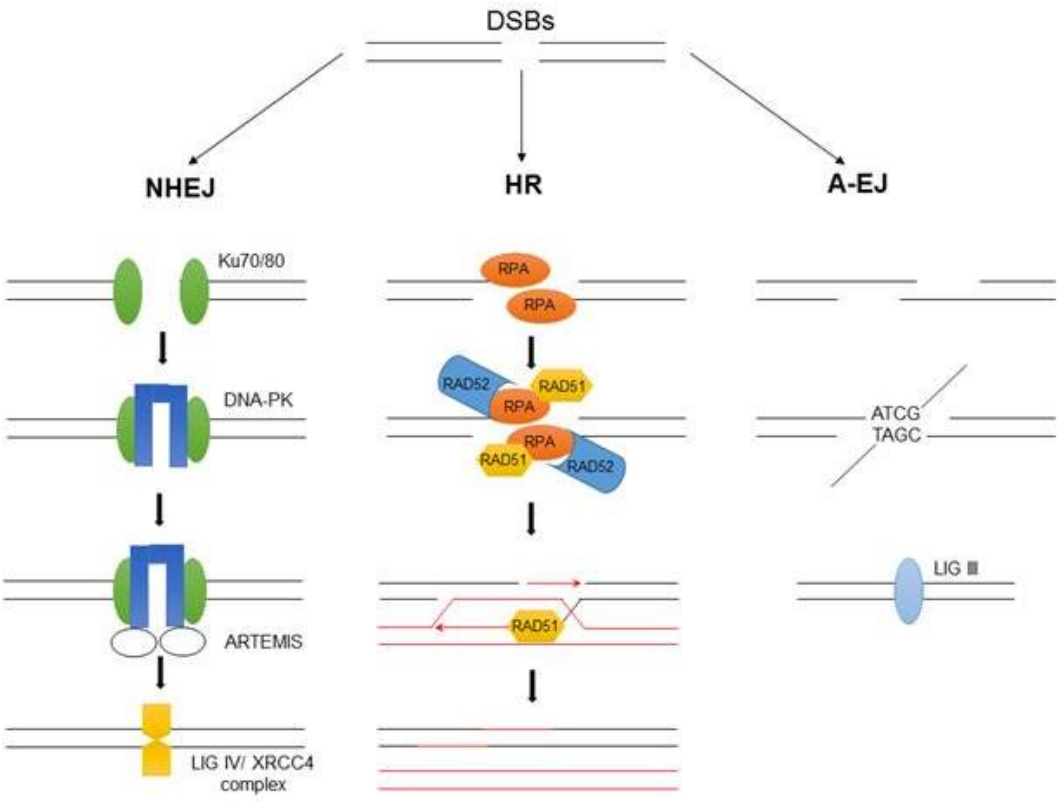

Figure 1.7. C-NHEJ, HRR and A-EJ compete for access to DSBs.

When cells repair DSBs, multiple repair systems compete for access to free DSB ends. During S-phase HRR, a mostly error-free template based repair pathway, wins priority. Outside of S-phase C-NHEJ or A-EJ repair the lesions, with regulating mechanisms still remaining unclear.

1.7.1 Homologous Recombination Repair

HRR begins with the binding of the MRN complex to free ends during S-phase. The MRN complex harbors nuclease activity that begins the resection of DSB ends in cooperation with CTIP. MRN also recruits DNA2, SGS1 and EXO1 to follow up with prolonging the resection until a free 3'overhang ssDNA end is created [173]. RPA coats the exposed single strand DNA. With the help of BRCA2, and following phosphorylation events on RPA, RAD51 loads onto the single strand end and begins the strand invasion. The invading RAD51 strand finds a donor strand with the help of RAD54 resulting in displacement of the complimentary strand of the donor DNA, a D-loop forms. Polymerases now using the donor DNA template fill in the missing elements.

Post synapsis, the HRR pathways separates into multiple sub pathways. When a second free end is available, synthesis-dependent strand annealing SDSA will attempt to reverse the D-loop, leading to annealing with the newly synthesized strand. Outside of meiosis the HRR pathways avoids crossovers which could lead to genomic rearrangement. During meiosis, HRR undergoes double Holliday junction formation and their resolution. This process serves primarily accurate chromosome segregation and secondly, rearrangement of genetic information to guarantee generation of diverse offspring [174].

1.7.2 Canonical-Non-Homologous End Joining

C-NHEJ is one of three DSB repair mechanisms. It allows the cells to join any type of DSB regardless of sequence at any time during the cell cycle. Thus, together with A-EJ, it carries out the majority of cellular DSB repair events [175-177]. C-NHEJ can be divided into a five step process: After recognition and binding of the free ends (I), the alignment and bridging of the free ends follows (II); the ends are processed to generate congruent elements (III), next ligation of the free ends occurs (IV) and finally resolution of the repair complex concludes the successful repair (V).

The initializing step (I) is the binding of free DSB ends by the protein subunits KU70 and KU80, which form the heterodimer KU [178]. KU is a highly conserved and abundant protein. It has an essential

role in C-NHEJ as it initiates the binding of free DSB ends [179-183]. The subunits form a ring which cover the sugar backbone of the DNA, making it inaccessible for other competing binding proteins and providing protection against nucleolytic processes [184]. The high abundance and DNA affinity of KU guarantees rapid DNA binding to the free ends [185]. Without KU cells experience dramatic disruptions of DSB rejoining resulting in chromosomal aberrations through error prone break repair, increased sensitivity to ionizing radiation, aneuploidy, and mutagenesis [183, 186-190]

Next (II), the DNA-PK catalytic subunit (DNA-PKcs) a member of the phosphoinositide 3-kinase-related kinase (PIKK) family [191] joins KU to form an enzymatically active complex named DNA-PK. DNA-PK promotes juxtaposition and tethering of the ends. The combined DNA-PK and KU holoenzyme also serves as a binding platform for following repair factors. DNA-PK undergoes 15 auto-phosphorylation events [192-196] and phosphorylates KU. The deletion of *Prkdc*, which codes for the DNA-PKcs, results in decreased C-NHEJ function. This defect manifests in IR sensitivity in certain cell types and disrupted Variable-Diversity-Segment (V(D)J) recombination, a process which rearranges genetic information in maturating lymphocytes [197]. The following step (III) which eventually results in ligation is flexible. The order and participation of processing factors such as nucleases and polymerases depends on the presentation and quality of the free ends, which the system encounters. Non-ligatable residues are processed by a number of kinases/phosphatases, nucleases (WRN, MRE11, ARTEMIS, EXO1), polymerases, helicases (RECQ1) to produce compatible DNA ends [198]. For the following step, again KU presence is required to recruit the ligation complex comprising of DNA ligase IV, XRCC4/CERNUNNOS, XLF and PAXX [185, 199-202]. The exact sequence in which the processing steps take place remains uncertain. However, it has been proposed that in cases of low complexity of the DSB surrounding DNA damage, the processing steps can be omitted allowing for a simple ligation following KU binding. Accordingly, highly complex structures rely more heavily on the catalytic activity of DNA-PK and the processing factors [203, 204]. The remaining step, the removal of KU, leaves many questions open. Due to its high affinity to DNA and the fact that in the process of ligation KU translocates proximally and away from the free ends, it could become trapped after the repair is concluded. Various

DNA repair models have been applied to date, suggesting that either proteasomal degradation or nicking of the DNA allows KU to be removed from the site [205-208]. A recent study from the Jackson lab suggests the neddylation pathways as the responsible mechanism to release KU from the site of former damage [209].

1.7.3 Alternative End Joining

The A-EJ is considered an intermediate between HRR and C-NHEJ as it shares certain characteristics of each pathway. The molecular interactions in A-EJ are not yet fully characterized, however it is considered the most error prone of the three pathways due to sequence deletions [210]. The A-EJ employs micro homology sequences of 5-25 bp flanking the break to prepare for DSB repair, which represents its foremost distinguishing property. The application of homology sequences that are distant from the DSB results in extended resection and therefore loss of genetic information. It is the source of the mutagenic properties of A-EJ [172, 210-212]. In stark contrast to HRR, there is no requirement for a homolog to be used as a template, therefore A-EJ is theoretically active throughout the cell cycle but secondary to C-NHEJ [211, 213, 214]. C-NHEJ repair attempts can result in the employment of A-EJ as the cell rarely encounters perfectly compatible DSB ends. In absence of functional C-NHEJ, such as in KU and XRCC4/CERNUNNOS knockout cells, reporter plasmid assays revealed an elevated rate of deletions during residual ligation events [215, 216]. This resulted in the recognition of A-EJ as a related but partly distinct pathway from C-NHEJ, frequently defined as an end joining event that is KU and LIGIV independent. In contrast to C-NHEJ mechanism, the A-EJ can be summarized in at least three main steps. First, the two DNA ends must be recognized and held together, associated with PARP1 and MRN. Several end processing steps follow, including the operation of factors such as PNK, FEN1, XPF-ERRC1, CTIP and POL δ, λ and ɵ [217]. While all above mentioned factors function in other repair pathways, the third and final step that is the ligation being carried out by LIGIII or LIGI define the distinction of A-EJ [210].

1.7.4 Regulation of DNA double strand break resolution and the competition of pathways

Among the three repair pathways, HRR is considered the least error prone. However, it is only available during S-phase and G2 when a suitable homologue is available in close proximity. It appears therefore intuitive that cellular decision-making processes would take a cue from the cell cycle, which provides the information that a homologous template is available. The choice of the pathways is linked to cyclin dependent proteins [218], which regulate end resection and therefore the competition of proteins such as MRN complex and KU for DNA DSB end binding [173]. Resection is defined as the generation of ssDNA from a DSB. It requires nucleolytic degradation of the 5'-terminated strands to generate 3'-ssDNA tails. It is the deciding step in preventing the binding of KU, thus committing the cell to HRR.

In the absence of resection stimulating signals from CDK proteins, KU binds DSB ends therefore preventing resection promoting enzymes such as MRN and CTIP and nucleases from accessing and resecting the ends [184]. In absence of KU, HRR is promoted [219]. On a more upstream level, BRCA1 is known to promote resection [220], whereas 53BP1 counteracts it [221]. While exact mechanisms are yet to be understood, the 9-1-1 complex is proposed to have an enhancing role in regulating resection, and thus regulating the pathway choice for the repair of the break [128]. Other than in C-NHEJ, KU and DNA-PK are dispensable for the ligation. Studies in cell lines deficient for elements of C-NHEJ show an increased use of A-EJ both in combatting IR induced damage as well as in V(D)J recombination (Figure 1.7).

1.8 Epistatic effects in DDR genes predict molecular interactions

ATM and HUS1

Any member of the ATR pathway is essential, thus null mutants cannot be viable. The sister pathway led by the ATM kinase, responds to DSB breaks, with *Atm* inactivation yielding viable mice, with some features of Ataxia Telangiectasia, the genome instability disorder coining the name for the ATM kinase. Even though ATR and ATM pathways respond to different types of DNA damage, cross-talk between

pathways has been proposed early on [222]. In order to dissect the molecular relationship between the ATR and ATM pathways, an *ATM*$^{-/-}$*Hus1*$^{neo/\Delta 1}$ mutant mouse was created by our lab [113]. A hypomorph mutant of HUS1 that is viable although suffering from genome maintained defects, proved to be synthetic lethal in *Atm*$^{-/-}$ background. With partial HUS1 inactivation through combination of two *Hus1*^{neo} alleles in *Atm*$^{-/-}$ background a viable model emerged. *Atm*$^{-/-}$ *Hus1*$^{neo/neo}$ mice were born at reduced Mendelian ratios and suffered from a dwarfism phenotype combined with cranio-facial abnormalities. This study confirmed a cooperative relationship between the ATR and ATM pathways, in which simultaneous disabling of *Hus1* and *Atm* resulted in a synthetic lethal phenotype or increased genomic instability phenotype with a HUS1 dose dependent regulation of severity.

RAD54 and HUS1

Cells with *Hus1* deficiency show defects in HRR and spontaneous genomic instability. RAD54 is an auxiliary protein in HRR. Simultaneous disabling of *Rad54* and *Hus1* was predicted to aggravate HRR defects as well as overall genomic instability through a synthetic sick interaction as is currently under investigation in a parallel study in the Weiss lab. Mice that are defective for both *Rad54*$^{-/-}$*Hus1*$^{neo/\Delta 1}$ showed signs of early aging and mild skeletal abnormalities. Furthermore, the mice showed elevated rates of genomic instability in peripheral blood, infertility and genotoxin sensitivity. Preliminary results suggest that MEFs defective for both *Rad54* and *Hus1* have increased genotoxin sensitivity. In survival assays MEFs defective for both *Rad54* and *Hus1* showed increased chromosomal instability as seen in metaphase chromosome analyses (Lim et al. unpublished data). Taken together, this model of dual inactivation of genes acting in related pathways shows promise of deepening the understanding of the interplay between the pathways as well as revealing novel function of its individual proteins of interest.

PRKDC and ATM

Another example of how dual deactivation of related pathways can become a powerful tool of synthetic lethality was revealed by Gurley et al. As observed in similar examples where single mutants displayed mild phenotypes but showed epistatic exacerbation when combined, they bred *Prkdc* with *Atm* mutant mice. While causing phenotypes of genomic instability and IR sensitivity when inactivated in mice, neither the DNA-PK nor ATM kinase are essential for embryogenesis. The combined defect was embryonic lethal, displaying dramatic effects of synthetic interaction when combining inactivation of DDR genes [223].

LIGIV and RAD54

In order to elucidate the interaction between HRR and C-NHEJ, Mills et al. generated mice that harbor a dual deficiency for RAD54 and LIGIV [224]. LIGIV null mice show a sever phenotype involving embryonic lethality, likely mediated through P53 mediated neuronal apoptosis. Additional P53 inactivation rescues viability, however the mutants suffer from proliferation defects, substantial IR sensitivity, and genomic instability as well as neuronal defects and a Severe Combined Immuno-deficiency (SCID) phenotype [225, 226]. RAD54 mice on the other hand, appear mostly normal [227] with only subtle sensitivity to HRR challenges. In order to study RAD54 function in absence of C-NHEJ activity, RAD54 null mice were bred in LIGIV null background. The authors observed that dual impairment in addition to RAD54 resulted in severe DSB repair and proliferation defects in cells, although the mice were viable. This revealed a cooperation of LIGV and RAD54 in repair of DSBs, maintenance of chromosomal and genomic integrity.

With a similar rationale, Couëdel et al. generated crosses between **RAD54 and KU80**: Double mutant mice had decreased survival rates, severe IR sensitivity and displayed fertility defects, again uncovering a novel interaction between C-NHEJ and HRR pathways [228].

1.9 Summary

The DNA damage response system provides the tool kit that allows cells to maintain and repair their genome. At the hub of the DDR stand two serine/threonine- phosphor kinases, ATM (Ataxia Telangiectasia mutated) and ATR (Ataxia telangiectasia Rad3-related) driving checkpoint and repair regulation. Proteins featured in checkpoints and repair pathways such as P53, RB, P21, BRCA1 and BRCA2 were increasingly found mutated in human and animal tumors, prompting the interest for further research. Other DDR proteins when mutated conferred complex syndromes such as in the cases of the FA Syndrome, Li-Fraumeni-Syndrome, Seckel-Syndrome or Xeroderma Pigmentosum.

These syndromes shared features such as tumor proneness, sensitivity to DNA damaging agents as well as proliferation and repair defects. Deepening analyses in the molecular interaction of these and other syndromes revealed crucial roles for DDR proteins in protecting the genome, controlling the cell cycle and protecting development. With the identification of tumor suppressor and oncogenes, the therapeutic potential that manipulating the DDR system held, crystallized. Scientists understood that cancer cells benefit from genetic alteration, but they do so in a controlled manner. Selection for advantageous mutations allows tumor to adapt to their changing environment and toxic challenges. However, if the subtle balance in mutations spirals out of control, genomic instability can harm tumor cells. Furthermore, while disabled DNA repair elements can allow tumor cells to thrive, they also bear the risk of leaving a tumor cell defenseless in the face of medically inflicted damage in the form of chemotherapy drugs.

The concept of synthetic lethality exploits this fragile balance: With increasing knowledge on an individual tumors genome and the weaknesses it is bearing; a targeted approach is increasingly applicable. Multiple synthetic lethality drugs are already in clinical trials. BS1-201, a PARP1 inhibitor has progressed into phase 3 of clinical trials, with multiple inhibitors of MGTM, CHK1 and P53 in phase one or two in the pipelines. However, as recurrences and metastatic disease prove, cancer is capable of changing its genome to grow resistant.

9-1-1 is a DNA sliding clamp with growing importance in the field of DDR. Its role in ATR checkpoint activation and genome maintenance is well described. However, as a regulatory hub for multiple repair pathways it is an important candidate in the search for new cancer drug targets that are capable in exploiting non-oncogene addictions in tumors. The purpose of molecular interactions between 9-1-1 and various binding partners is yet to be explored.

In chapter two I analyze implications for HUS1 in ICL repair. I base this study on prior findings discovered in the lab that showed phenotypes for HUS1 that resembled those found in FA and HRR defective cells. I employ interaction screens to identify potential binding partners and *Hus1*-deficient cells to test possible roles for HUS1 in ICL resolution.

In analyzing the role of HUS1 I will gain insight in the decision making process between HRR and C-NHEJ. Both pathways are specialized in the repair of DSBs. During S-Phase, they compete for the right of way at DSB ends. In light of the redundancy of pathways, it is important to monitor 9-1-1 function in a C-NHEJ defective background. The generation of a $Prkdc^{-/-}$ $Hus1^{neo/\Delta 1}$ double mutant mouse will allow insights into DSB repair regulatory mechanisms that have been proposed for HUS1. Furthermore, possible synergistic interactions, applicable for future drug discovery can be revealed through this study.

CHAPTER 2

THE 9-1-1 DNA DAMAGE RESPONSE COMPLEX IS REQUIRED FOR FANCD2 AND RAD51 FUNCTION DURING DNA INTERSTRAND CROSS-LINK REPAIR

[1]

Joanna M Mleczko[1], Darshil Patel[1], Georgios Karras[2], Catalina Pereira[1], Pei Xin Lim[1] and Robert S. Weiss[1*]

The 9-1-1 DNA damage response complex is required for FANCD2 and RAD51 function during DNA interstrand cross-link repair

Joanna M Mleczko[1], Darshil Patel[1], Georgios Karras[2], Catalina Pereira[1], Pei Xin Lim[1] and Robert S. Weiss[1*]

Manuscript in preparation

2.1 Abstract

DNA interstrand cross-links (ICLs) induced by chemotherapeutics such as Mitomycin C (MMC) are highly toxic to cells as they block replication and transcription. To combat the negative impact of ICLs, mammalian cells launch a multifaceted repair response that includes the FA pathway. Here, we establish a requirement for the RAD9A-RAD1-HUS1 (9-1-1) checkpoint clamp, for activation of the FA pathway and proper resolution of ICLs. *Hus1*-deficiency disrupted MMC-induced chromatin loading of the FA signaling protein FANCD2, resulting in radial chromosome formation and significantly increased cellular sensitivity to MMC. In addition to physically associating with several FA proteins, the 9-1-1 complex also was necessary for loading of the critical repair protein RAD51 onto DNA at MMC-induced ICLs but not at DNA breaks caused by ionizing radiation. Taken together, the results suggest a model in which the scaffolding activity of the 9-1-1 complex coordinates multiple signaling and repair proteins required for efficient and accurate ICL repair.

2.2 Introduction

DNA is constantly exposed to endogenous and exogenous insults, resulting in DNA lesions which if left unrepaired disrupt replication and transcription, and can cause genomic instability and cancer. On the other hand, sensitivity to genotoxin-induced damage has been exploited in cancer treatment, as highly replicative transformed cells have an increased sensitivity to DNA damage. Among the chemotherapeutics used clinically are agents that induce ICLs, covalent linkages between the complementary DNA strands. ICLs prevent DNA unwinding and thus interfere with transcription, replication and recombination. Mitomycin C (MMC) is a prototypical ICL inducer used in the treatment of certain cancers.

ICL repair is carried out in most part by the members of the FA pathway. FA is a rare genetic

disorder characterized by cancer susceptibility, bone marrow failure, and congenital abnormalities hypothesized to occur due to defective ICL triggered repair responses. FA pathway activation begins with the sensing of ICLs by the FA core complex protein FANCM and associated proteins [146], followed by the assembly of the remaining core complex proteins at the ICL. The FANCL component of the core complex serves as a ubiquitin ligase that targets the FANCI/FANCD2 (ID) heterodimer, enabling its localization to damage sites [155]. The ID heterodimer coordinates the actions of a number of downstream players, including XPF1-ERRC1 and FAN1 in collaboration with SLX4 [160, 162-164] which carry out the unhooking of the lesion. After translesion synthesis (TLS) restores the template [229], HRR synthesizes the missing information [141].

One consequence of FA pathway dysfunction, as seen in clinical cases, is the formation of aberrant chromosomal structures known as radial chromosomes. Radial chromosomes are believed to reflect failure of HRR in DSB repair and use of error-prone mechanisms such as the C-NHEJ pathway [167]. During HRR, DSBs are resected to create 3' ssDNA overhangs that give rise to RAD51 nucleofilaments which invade an intact template duplex (reviewed in [230]). The observation that cells deficient in FA core proteins are proficient in repairing ionizing radiation (IR) but not ICL- induced DSBs [231], highlights the distinct nature of ICL lesions and the requirement for specialized repair processes.

Another element of the cellular response to DNA lesions such as ICLs are the DNA damage checkpoint signaling pathways that regulate cell cycle progression, coordinate DNA repair, and mediate other responses that protect genomic integrity. Of particular relevance during ICL responses is the checkpoint pathway headed by the kinase ATR. When exposed single strand DNA (ssDNA) accumulates at ICLs or other lesions, it becomes coated by RPA facilitating the recruitment of ATR and its binding partner ATRIP, as well as the heterotrimeric RAD9A-HUS-RAD1 (9-1-1) complex. The 9-1-1 complex is structurally similar to the sliding clamp PCNA and like PCNA is loaded onto recessed DNA ends by a clamp loader, where it serves as molecular scaffold [232]. One binding partner of 9-1-1 is TOPBP1, which interacts with the C-terminal tail of RAD9A and then stimulates the ATR kinase through its ATR activating domain [70]. Activated ATR phosphorylates downstream effectors including the kinase CHK1,

which further transduces the DNA damage signal [233], resulting in cell cycle arrest and initiation of DNA repair, or apoptosis in case of severe damage. The phosphorylation of core complex proteins by ATR and the FA pathway is activated through phosphorylation of FANCI [119] by ATR, and the phosphorylation of core complex components [150] which is followed by monoubiquitination of the ID dimer, marking the activation of the FA pathway.

In addition to promoting ATR activation and checkpoint signaling, the 9-1-1 complex also executes ATR-independent repair functions through direct interactions with a variety of effectors. 9-1-1 subunits have been reported to interact with protein from BER, NER, TLS, HRR repair pathways [110, 118-122, 128]. Notably, disruption of putative effector binding sites on the exterior surface of the HUS1 subunit causes genotoxin hypersensitivity without affecting TOPBP1 binding or ATR activation [101].

The 9-1-1 complex was previously shown to be essential for resistance to ICL inducing agents, both in cultured cells and in mice [115, 116, 234]. Moreover, a recent proteomic analysis established 9-1-1 complex recruitment to ICL containing chromatin, which preceded both FANCD2 and RAD51 loading [124]. Here we build on these findings by showing that the 9-1-1 complex acts at multiple steps during the cellular response to ICLs. Consistent with observations that *Hus1*-deficiency causes hallmark features of a FA defect, including MMC hypersensitivity and susceptibility to radial chromosome formation, we found that the 9-1-1 complex physically interacts with several FA proteins and is required for FANCD2 focus formation after MMC exposure. Furthermore, 9-1-1 is necessary for RAD51 recruitment to DNA following MMC treatment, indicating a central role for the checkpoint clamp at multiple steps during ICL repair.

2.3 Materials and Methods

Cell culture and treatments

MEFs of *Hus1*$^{-/-}$*p21*$^{-/-}$ and *Hus1*$^{+/+}$*p21*$^{-/-}$, *Hus1*$^{-/-}$*p53*$^{-/-}$ and *Hus1*$^{+/-}$ *p53*$^{-/-}$, cells were described before [95]. MEFs were grown in DMEM with 10% BCS cells and 1% Penicillin-Streptomycin, 1% NEA and 1% L-

Glutamine. Transfected or infected cells were maintained in 1.83μg/ml puromycin selection medium.

MEFs from FANCD2 [235] and FANCA [236] null mice (129 background) and controls were generated from 13.5 days old embryos, immortalized with large T antigen virus [237]. Cells were grown in DMEM with 10% BCS cells and 1% Penicillin-Streptomycin, 1% NEA and 1% L-Glutamine. In brief, MEFs were seeded in 60 mm dishes and after 24 hours were treated with 2.5ml of Phoenix medium containing 2.5 μl Polybrene (Sigma-Aldrich) per dish and 250 μl of large T virus. Cells were puromycin (Fisher Scientific) selected by feeding cells with 10% BCS 1% Penicillin-Streptomycin, 1% NEA and 1% L-Glutamine medium containing 1.5ug/ml puromycin. Cells were maintained in 1.83 μg/ml puromycin selection medium. Plasmids, vectors and transfection and infection methods are described in Co-Immunoprecipitation, Immunoblotting and Constructs. All plasmids contained mouse DNA with the exception of Co-IP experiments which used human DNA. FANCI-HA plasmids were a generous gift from Dr. Tony Huang.

Survival assays

Short term viability assays with MMC (Abcam) were carried out by seeding 20,000 cells in triplicate in 6-well plates 24 hour prior to treatment with and without genotoxin. Control cells were treated with either DMSO, 0.25μg, 0.50μg, or 1.00μg for 1 hour. Cells were counted 72 hours post-treatment using a hemocytometer. For trioxsalen treatment, 5,000 cells were seeded in triplicate in 6-well plates 48 hours prior to treatment. Cells were treated for 20 minutes with either DMOS, 100μM, 1μM, or 0.1μM of trioxsalen and then activated with 2.5 J/cm^2 of UVA by exposing cells in 6- well dishes to UVA light for 10 seconds. 72 hours post treatment cells were counted using a hemocytometer. Percent survival was calculated by dividing the average of cells treated with genotoxin by cells untreated. Error bars ± SD. Statistical analysis was carried out by Student's T-test, and p-values of <0.05 were considered significant.

Immunofluorescence Staining

For IF staining cells were seeded on 0.01 % gelatin coated glass coverslips in 6 well dishes and allowed to attach for 24 hours. Then cells were treated with 5 μM Hydroxyurea, 2 μg/ml of MMC or 10 Gy of IR at indicated time points. When staining for FANCD2, cells were pre-extracted with 0.5 % Triton-X 100 for 1 min before fixation with 4% PFA for 20 min at RT. Following fixation cells were washed in 1X PBS, then permeabilized with 0.5 % NP40 for 20 min. Cells were then blocked in PBG (0.2% cold water fish gelatin (Sigma G-7765) and 0.5% BSA (Sigma A-2153) for 20 minutes and incubated in primary antibody solution at a concentration of 1:500 (FANCD2 Abcam ab2187) overnight. The next day, cells were triple rinsed in 1X PBS and incubated in a 1:1000 dilution of secondary antibody (Alexafluor 488 A11034 anti-rabbit) for two hours in the dark. Cells were mounted in DAPI containing 0.05% DAPI mounting medium and imaged the same day using a Leica DMRE fluorescence microscope. For γH2AX immunofluorescence staining cells were grown and treated as above but fixed with methanol, triple rinsed in 1X PBS and permeablized in 3% BSA (Sigma). Next, cells were incubated with anti-γH2AX (Millipore) primary antibody and goat anti-mouse Alexa Fluor 488 secondary antibody. Immunofluorescence co-staining was performed on *Hus1*$^{-/-}$*p21*$^{-/-}$ MEFs stably expressing WT or mutant mHUS1-3XFLAG proteins. Cell were grown and treated as described above, then immunostained with mouse α-FLAG (Sigma-Aldrich) and rabbit α-FANCD2 (Novus Biologicals) primary antibodies overnight one antibody at a time. Alexa Fluor 488 goat α -mouse and 555 goat α-rabbit secondary antibodies (Life Technologies X) were used for IF detection according to antibody manufacturer's instruction.

For RPA staining, cells were pre-extracted with 0.1% Triton X-100 for 1 minute then fixed in 10% phosphate buffered formalin following 10% goat serum block and rat anti-RPA antibody (Cell Signaling). For RAD51 staining, cells were fixed in 4% PFA followed by 15 min of permeabilization in 0.5% Triton X-100 and 3% BSA block. The antibody used was purchased from Calbiochem. Cells were mounted in DAPI containing 0.05% DAPI mounting medium and imaged the same day using a Leica DMRE fluorescence microscope.

For BrdU staining, cells were pre-treated with 0.03 mg/ml BrdU for 48 hours to allow for incorporation into the DNA. Then, cells were treated with 2 μg of MMC for 16 hours. After MMC treatment, one HCL control was denatured with 2 M HCL solution for 30 minutes. The remaining conditions, were fixed in 4% PFA followed by 15 min of permeabilization in 0.5% Triton X-100 and 3% BSA block. The antibody used was purchased from Cell signaling (Bu20a) Mouse mAb #5292. Cells were mounted in 0.05% DAPI containing mounting medium and imaged the same day using a Leica DMRE fluorescence microscope.

Metaphase spread preparation

MEFs were seeded in 10 cm dishes and grown until 70% confluence was reached. Then, cells were treated with 0.10 μg/ml, 0.20 μg/ml, 0.30 μg/ml or 0.40 μg/ml of MMC for 24 hours. Cells were then incubated in 0.10 μg/ml Colcemid for 1 h. Cells were then harvested by trypsinization, incubated for 7 min at 37°C in hypotonic buffer (0.034M KCl, 0.017M $Na_3C_6H_5O_7$), and fixed for at least 20 min at 4°C in 75% methanol-25% acetic acid three times. Cells in fixative were then spotted onto microscope slides and stained with 2.0% Giemsa in Gurr buffer (pH 6.8). Chromosomal abnormalities were scored based on standard guidelines [238].

Co-Immunoprecipitation, Immunoblotting and Constructs

To analyze the interaction of HUS1 with FANCD2, FANCG and FANCI protein, HEK293T cells transiently transfected with human pCMV-*Hus1*-3xFLAG, or pCMV- *Hus1*-HA and *FancI*-HA or *FancG*-3xFLAG constructs were treated with 0.5 μg/ml of MMC or DMSO as control. After 24 hours of treatment, the cells were fractionated to isolate nuclear fraction and subsequently protein lysates are prepared for co-IP analysis. Lysates were incubated with Anti-Flag M2 resin (Sigma) or Anti-HA antibody (Covance) overnight before immunoblotting. For analysis of HUS1 mutants' interaction with FANCI and FANCD2, HEK293T cells were transiently transfected with pCMV-3XFLAG construct containing either wildtype human *Hus1*, pCMV- *Hus1*-R4D (PM1), pCMV- *Hus1*-V151Y (PM3) or pCMV- *Hus1*-R4D+V151Y (PM4). Cells were treated with 0.5 μg/ml of MMC, before fractionation and

cell lysate preparation described above. Lysates were incubated with Anti-FLAG resin. Immunoprecipitates and total cell lysates (input) were resolved by SDS-PAGE. Standard immunoblotting procedures were performed using antibodies specific for FLAG M2 (Sigma-Aldrich), HA (Covance), and, FANCD2 (Novus Biologicals). Analysis on γH2AX was assessed by immunoblotting using antibodies against γH2Ax (S139) (Millipore), RPA70 (Santa Cruz) and Actin (Sigma-Aldrich).

Chromatin fractionation *Hus1*$^{-/-}$*p21*$^{-/-}$ MEFs stably expressing mouse WT, PM4 or A6 HUS1 protein were treated with 0.5 μg/ml of MMC overnight before fractionating the cells as described in [239] with a few modifications. Cells were hypotenized using Buffer 1 (10 mM HEPES, pH 7.9; 10 mM KCl; 1.5 mM $MgCl_2$; 0.34 M sucrose; 10% glycerol; 1mM DTT; 0.3 mM PMSF) for 5 minutes, before centrifuging them at 5000g for 5 minutes to separate the cytoplasmic (supernatant) and nuclear fraction (pellet). The pellet (nuclear fraction) was lysed using Buffer 2 (3 mM EDTA, 0.2 mM EGTA, 1 mM DTT, 0.3 mM PMSF) and incubated for 30 minutes on ice. After centrifugation at 5000g for 5 minutes, the supernatant (soluble nuclear fraction) was collected and the pellet (chromatin fraction) was resuspended with Buffer 3 (10 mM Tris-HCl pH 8.0, 5 mM KCl, and 1 mM $CaCl_2$) along with 1 unit of Micrococcus nuclease. The solution was incubated at 37^{o}C for 10 minutes before centrifuging at 14000 rpm for 10 minutes to produce the chromatin fraction in the supernatant. 0.5 μg of the chromatin fraction were used for immunoblotting. Immunoblotting was performed using specific antibodies against FANCD2 (Novus biologicals), Phospho-RPA32 (Bethyl), RA51 (CalBioChem), GAPDH (ImmunoAffinity), and histone 3 (Abcam).

LUMIER with BACON

Lumier with bait control (BACON) was performed as described before [240]. 3xFLAG-tagged constructs were transfected in 96-well format in duplicates into HEK293T-derived reporter cell lines using polyethylenimine (Polysciences 24765). To avoid spatial gradients in transfection efficiency, plates were incubated at room temperature for 30 minutes before transfer to 37°C (5% CO_2). Two days after

transfection, cells were washed in 1xPBS using an automated plate washer (Biotek ELx406) and lysed in 50mM HEPES [pH 7.9]/150mM NaCl/10mM $MgCl_2$/20mM Na_2MoO_4 (stabilizes metastable chaperone-mediated protein interactions)/0.7% TritonX-100/5% glycerol, protease and phosphatase inhibitors, benzonase and RNAseA. The lysates were transferred with an automated liquid handler (Tecan) into 384-well plates that had been coated with monoclonal anti-FLAG M2 antibody (Sigma-Aldrich, F1804) and blocked with 3% BSA/5% sucrose/0.5% Tween 20. Plates were incubated at 4°C for 3 h, after which plates were washed with HENG buffer [241] using an automated plate washer. Luminescence was measured with a plate reader (Perkin-Elmer Envision) using Gaussia Flex luciferase kit (New England Biolabs, E3308). To determine FLAG bait protein expression levels, after luminescence measurement, HRP-conjugated anti-FLAG antibody in ELISA buffer (1x PBS, 2% goat serum, 5% Tween 20) was added to wells. Plates were incubated for 90 minutes at room temperature and were subsequently washed in 1xPBS/0.05% Tween 20 with an automated plate washer. ELISA signal was detected using a chemiluminescent substrate (Thermo Scientific, 37069) and used for LUMIER Interaction Scoring. To avoid normalization artifacts due to the low expression of bait proteins, ELISA signal was used only qualitatively to determine which proteins were expressed. To correct for variability in cell number across wells, LUMIER signal was normalized against the luminescence of the total cell extract (5%). Background ratios fit a log-normal distribution, and thus we calculated z-scores for each protein-protein interaction. Three independent experiments were performed and average z-scores and standard deviations were plotted.

2.4 Results

2.4.1 9-1-1 complex dysfunction causes cellular hypersensitivity to DNA crosslinking agents and leads to ICL-induced radial chromosome formation.

Previous findings indicated that *Hus1*-deficient cells are hypersensitive to ICL-inducing agents [115, 116, 234]. To compare the degree of MMC sensitivity in *Hus1*-null cells to that of cells lacking *Fanca* or

Fancd2, we performed short term survival assays in MMC-treated and untreated control mouse embryonic fibroblasts (MEFs). Direct comparison among the cell lines revealed *Hus1*-null cells to be comparably sensitive to MMC as *Fanca* or *Fancd2*-null cells (Fig. 2.1A and B). To further characterize the response of *Hus1*-null cells to crosslinking agents, we used UVA-activated Trioxsalen, which induces a higher frequency of ICLs than monoadducts or intrastrand crosslinks [242]. Similar to the results with MMC, *Hus1*-null MEFs showed hypersensitivity to UVA-activated Trioxsalen (Fig. 2.1C).

The sensitivity of *Hus1*-null cells to MMC and Trioxsalen/UVA was suggestive of failure to repair ICLs. We therefore directly monitored chromosomal integrity in these cells. Upon low dose MMC treatment, multiple independent *Hus1*-null MEF lines showed increased chromosomal damage relative to matched control cultures (Fig. 2.1D, 2.1E, 2.2A, and 2.2B), including chromosome breaks, fusion events and formation of radial chromosomes (Table 2). Radial chromosomes are thought to stem from error prone DSB repair and used as a pathognomonic tool in diagnosis of FA syndrome in human patients [243]. Together with the observations of MMC hypersensitivity in *Hus1*-null cells, these findings suggested a possible connection between 9-1-1 and the FA pathway. We previously determined that epitope tagged HUS1 localizes to nuclear foci following MMC treatment [116] and therefore tested whether the 9-1-1 clamp and the FA protein FANCD2 co-localized at damage sites. Indeed, FANCD2 and HUS1-FLAG co-localized in large punctate structures consisting of 5-10 smaller foci in a subset of MMC-treated cells. (Fig 2.1F). Thus, not only does 9-1-1 dysfunction cause cellular phenotypes characteristic of FA, but 9-1-1 and FA proteins co-localize after MMC treating, hinting at a possible role for the 9-1-1 complex in the FA pathway in response to ICL formation.

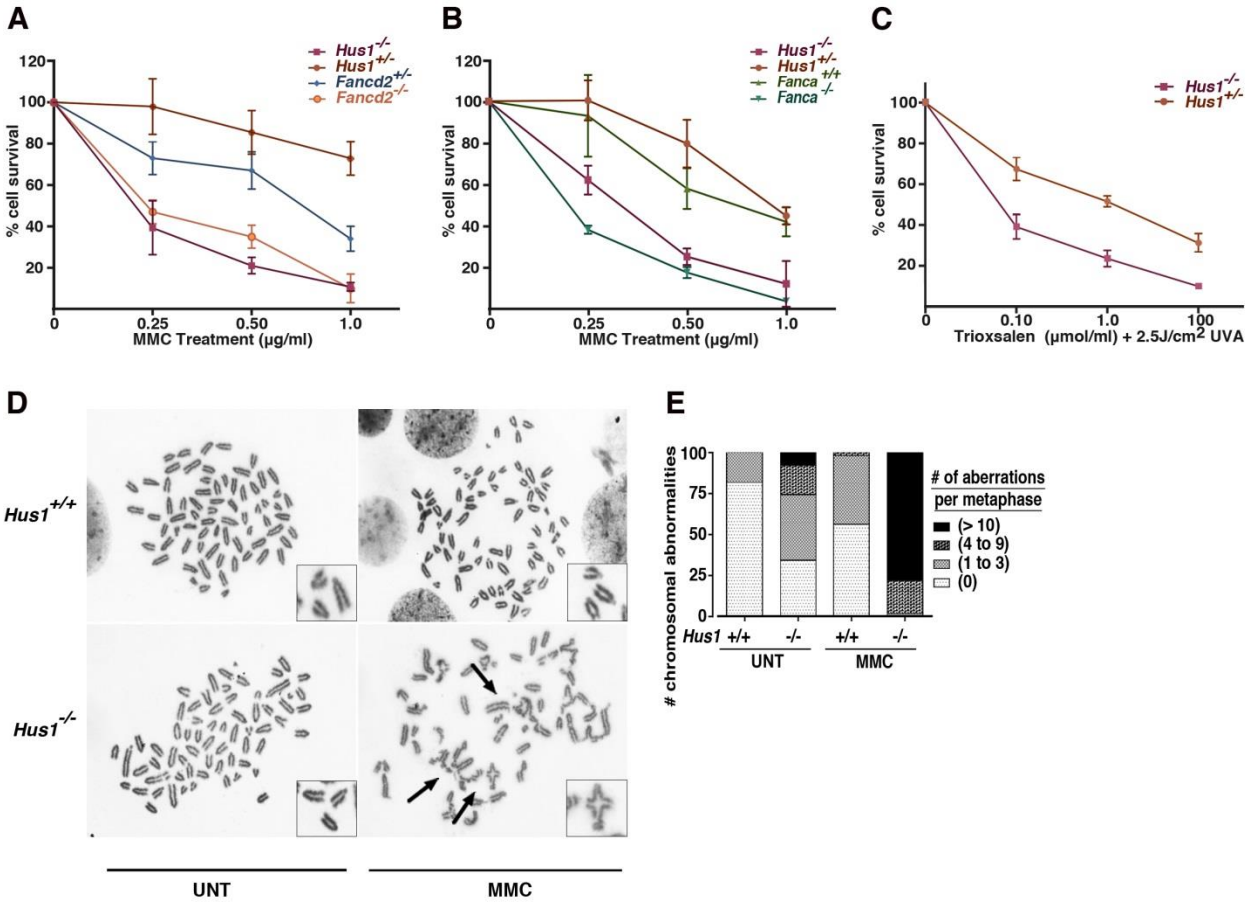
A
B
C
% cell survival
MMC Treatment (μg/ml)
Trioxsalen (μmol/ml) + 2.5J/cm2 UVA
Hus1-/-
Hus1+/-
Fancd2+/-
Fancd2-/-
Fanca+/+
Fanca-/-
D
Hus1+/+
Hus1-/-
UNT
MMC
E
chromosomal abnormalities
of aberrations per metaphase
(> 10)
(4 to 9)
(1 to 3)
(0)
Hus1 +/+ -/- +/+ -/-
UNT
MMC
F
Hus1-/- +HUS1 3xFLAG
FLAG
FANCD2
DAPI
MERGE
UNT
MMC

Figure 2.1. The 9-1-1 complex is required for proper DNA damage responses to MMC-induced lesions in mouse fibroblasts.

A, B and C. Short term viability assay. **A and B.** *Hus1*$^{-/-}$ (*Hus1*$^{-/-}$*p21*$^{-/-}$), control (*Hus1*$^{+/+}$*p21*$^{-/-}$) *FancD2*$^{-/-}$, *FancA*$^{-/-}$ and their respective controls (*Hus1*$^{+/+}$*p21*$^{-/-}$, *Fancd2*$^{+/+}$, *Fanca*$^{+/+}$) were treated with either DMSO or MMC doses of 0.25μg, 0.50μg, or 1.00μg for 1 hour and counted 72 h post treatment. The proportion of viable cells relates to the untreated control as shown. **C**. *Hus1*$^{-/-}$ (*Hus1*$^{-/-}$*p21*$^{-/-}$) and control (*Hus1*$^{+/+}$*p21*$^{-/-}$) cells were treated with Trioxsalen for 20 minutes with doses of either 100μM, 1.0μM, or 0.1μM and then activated with 2.5 J/cm^2 of UVA. Cells were counted 72 h post treatment. The proportion of viable cells relates to the untreated control as shown. The experiments in A, B and C were performed by Catalina Perreira. **D and E.** Metaphase chromosome analysis of *Hus1*$^{-/-}$ (*Hus1*$^{-/-}$*p21*$^{-/-}$) and control (*Hus1*$^{+/+}$*p21*$^{-/-}$) cells following mock treatment or treatment with 0.06 μg/ml MMC for *Hus1*. **F.** Immunofluorescence co-staining for FANCD2 and FLAG in *Hus1*-3xFLAG complemented *Hus1*$^{-/-}$ (*Hus1*$^{-/-}$*p21*$^{-/-}$) cells following treatment with 2 μg/ml MMC for 24h. Cells were counterstained with 0.05% DAPI.

Table 2. Chromosomal aberrations in *Hus1*$^{-/-}$ *p21*$^{-/-}$ and *Hus1*$^{+/+}$ *p21*$^{-/-}$ control cells following MMC treatment [a].

Genotype	Breaks/Gaps	Fusions	Acentrics	Radials
Hus1$^{+/+}$ *p21*$^{-/-}$ (UNT)	3	5	4	0
Hus1$^{-/-}$ *p21*$^{-/-}$ (UNT)	8	27	72	0
Hus1$^{+/+}$ *p21*$^{-/-}$ (MMC)	6	6	15	0
Hus1$^{-/-}$ *p21*$^{-/-}$ (MMC)	139	143	303	24

[a] *Hus1*-deficient and control cells were treated with Mitomycin C (MMC) at 0.06 μg/ml for 24 hours or mock treated (UNT). Then chromosome spreads were prepared and 50 spread per condition were counted.

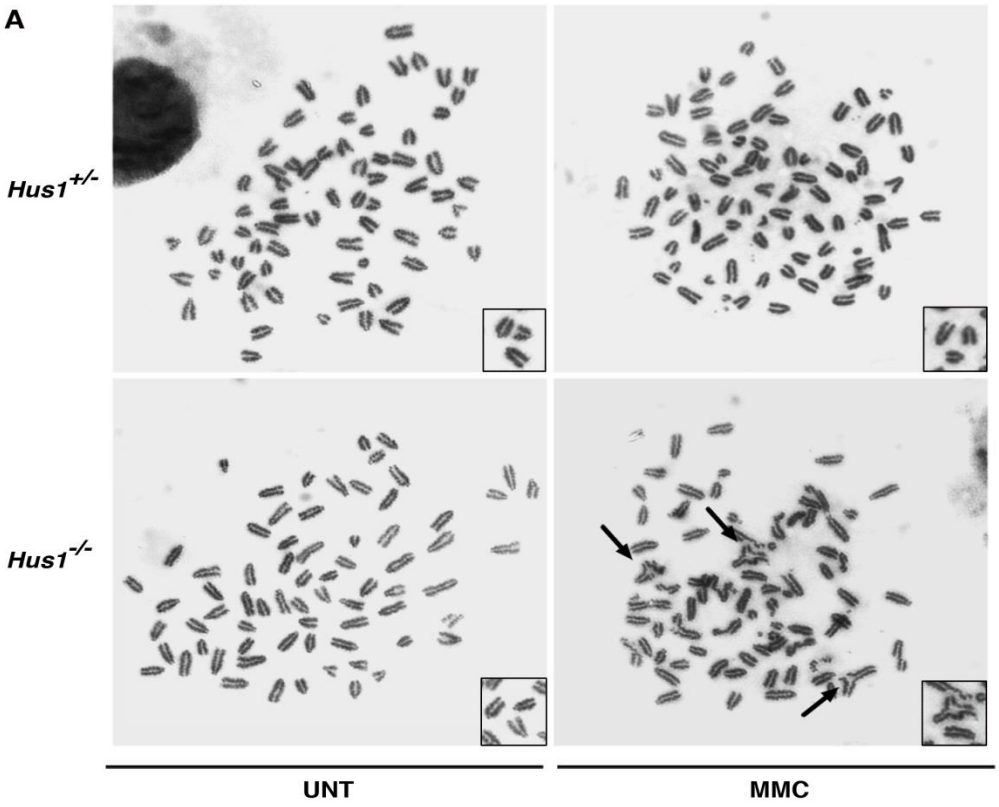
A
Hus1+/-
Hus1-/-
UNT
MMC

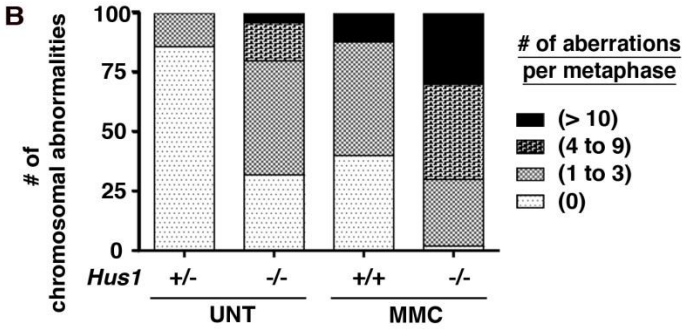
B
# of chromosomal abnormalities
100
75
50
25
0
Hus1 +/- -/- +/+ -/-
UNT
MMC
# of aberrations per metaphase
(> 10)
(4 to 9)
(1 to 3)
(0)

Figure 2.2. The 9-1-1 complex is required for proper DNA damage responses to MMC-induced lesions in mouse fibroblasts. A and B. Metaphase chromosome analysis and quantification of *Hus1*-deficient (*Hus1*$^{-/-}$*p53*$^{-/-}$*)* and control (*Hus*$^{+/-}$ *p53*$^{-/-}$*)* cells following mock treatment or treatment with 0.06 μg/ml MMC for 24 h shown in independent cell line. Spreads categorized based on number of aberrations per spread.

2.4.2 HUS1 is required for FANCD2 focus formation and chromatin loading in response to ICLs.

The formation of FANCD2 foci in MMC treated cells is a traditional readout of FA pathway activation. We therefore tested whether the 9-1-1 complex was necessary for FANCD2 focus formation. Whereas FANCD2 foci readily formed in *Hus1*-proficient cells after MMC treatment, they failed to form in multiple independent *Hus1*-null cell lines (Fig. 2.3A, 2.4A, 2.4B and 2.4C and 2.4D). Importantly, this phenotype could be rescued by complementing the *Hus1*-null cells with a retroviral *Hus1* expression construct, which restored nearly wild-type levels of FANCD2 formation (Fig. 2.3B and C), suggesting that the 9-1-1 complex is indeed required for FA pathway activation. To rule out the possibility that the FANCD2 defect was due to a reduced amount of DNA damage in *Hus1*-null cells, we performed staining for the histone variant γH2AX (Fig. 2.3D, and 2.4E). As early as 2 hours after treatment γH2AX focus formation occurred to a similar extent in *Hus1*-null and control cells, indicating that cells lacking *Hus1* failed to form FANCD2 foci despite experiencing MMC-induced damage. To confirm these findings in an independent assay, we performed chromatin fractionation on MMC-treated and control cells followed by immunoblotting. MMC-treated *Hus1*-proficient cells showed the expected significant increase in presence of FANCD2 on chromatin but this failed to occur in *Hus1*-null cells (Fig. 2.3E), further implicating the 9-1-1 complex in FA pathway signaling.

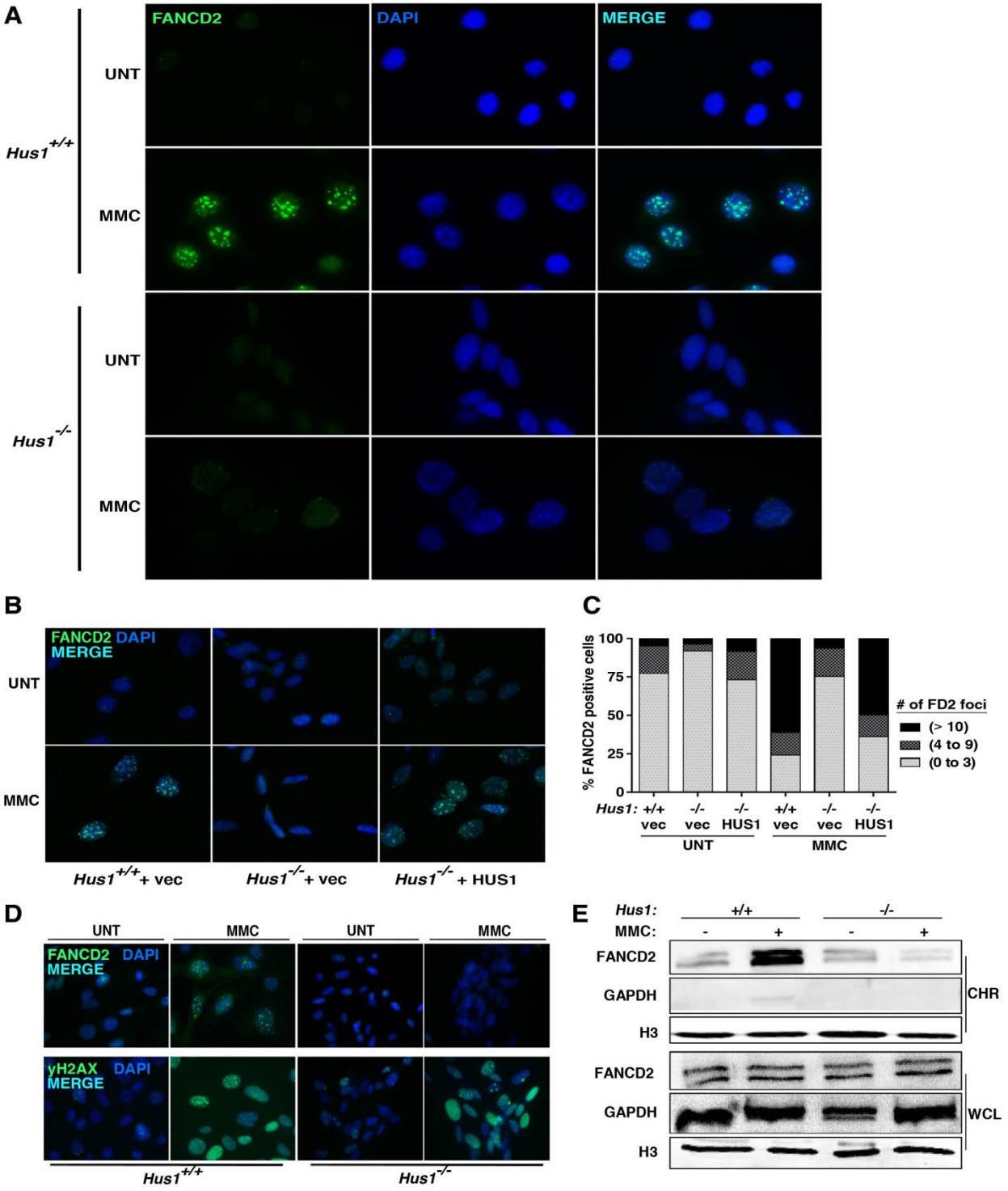
A
FANCD2
DAPI
MERGE
UNT
MMC
Hus1+/+
Hus1-/-
B
FANCD2 DAPI
MERGE
Hus1+/+ + vec
Hus1-/- + vec
Hus1-/- + HUS1
C
% FANCD2 positive cells
100
75
50
25
0
# of FD2 foci
(> 10)
(4 to 9)
(0 to 3)
Hus1: +/+ -/- -/- +/+ -/- -/-
vec vec HUS1 vec vec HUS1
UNT
MMC
D
UNT
MMC
FANCD2 DAPI
MERGE
γH2AX DAPI
MERGE
Hus1+/+
Hus1-/-
E
Hus1:
MMC:
FANCD2
GAPDH
H3
CHR
WCL

Figure 2.3. DNA crosslink-induced FANCD2 focus formation and chromatin binding are defective in *Hus1*$^{-/-}$ cells and can be rescued by *Hus1* complementation. A, B. Immunofluorescence staining for FANCD2. **A.** *Hus1*$^{-/-}$ (*Hus1*$^{-/-}$ *p21*$^{-/-}$) and control (*Hus1*$^{+/+}$*p21*$^{-/-}$) cells were treated with 1 μg/ml MMC for 24h. Nuclei were counterstained with 0.05% DAPI. **B.** *Hus1*$^{-/-}$ (*Hus1*$^{-/-}$*p21*$^{-/-}$) and control (*Hus1*$^{+/+}$*p21*$^{-/-}$) cells complemented with *Hus1*, or GFP as a control, were treated and stained as in A. **C.** Quantification of the FANCD2 staining data shown in B. The number of FANCD2 foci per cell was counted in 50 cells per condition. **D.** Immunofluorescence staining for FANCD2 side by side with γH2AX. **E.** Immunoblot analysis of chromatin fractionating and whole cell lysate: Cells were treated with 0.5 μg/ml of MMC and were fractionated to obtain the chromatin-bound proteins to perform immunoblotting with antibodies specific to FANCD2, phospho-RPA32 (S4/S8), RAD51, GAPDH and histone 3. GAPDH and histone 3 served as fractionation controls. The experiment in E was performed by Darshil Patel.

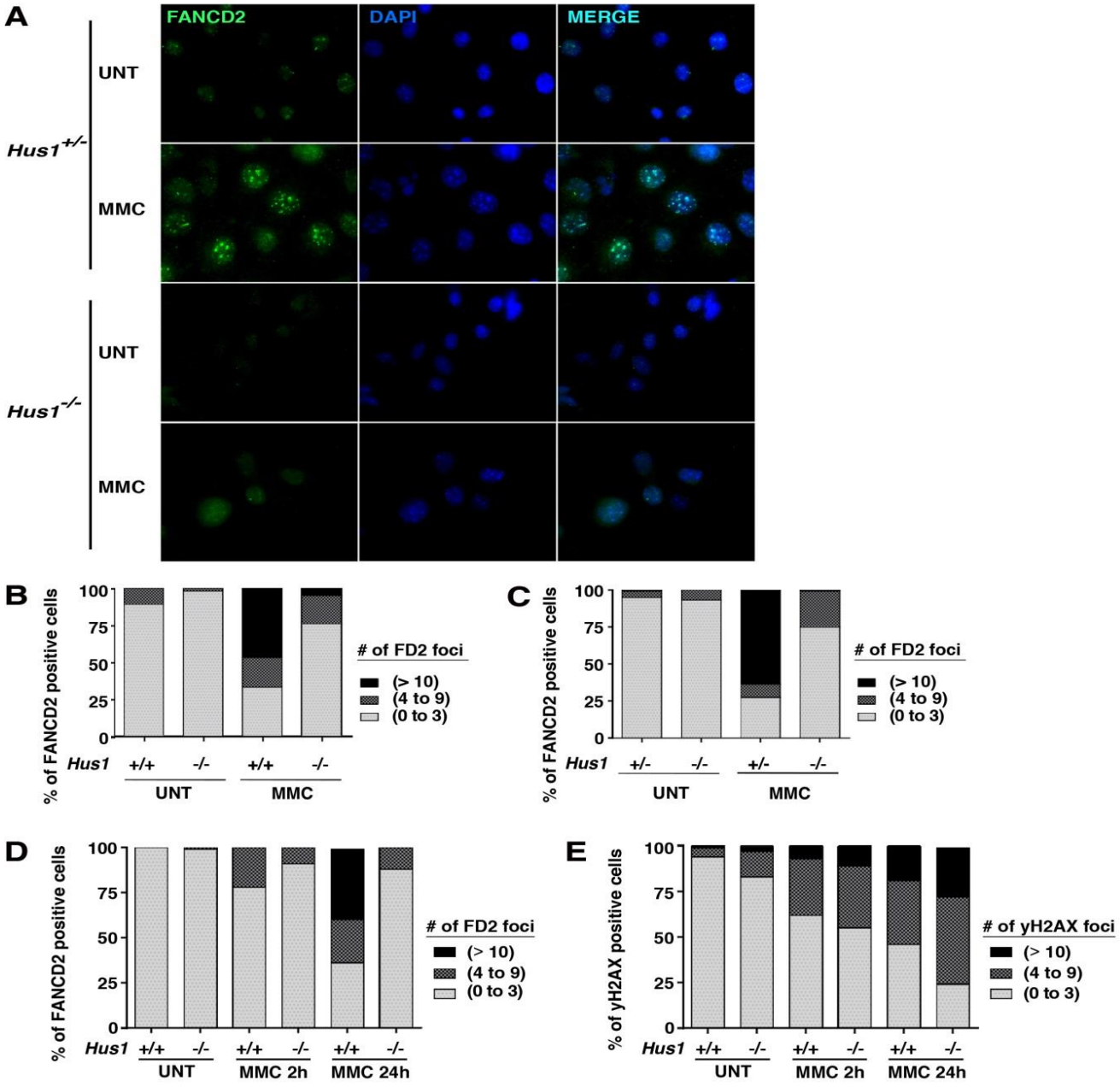
A
FANCD2
DAPI
MERGE
UNT
Hus1+/-
MMC
UNT
Hus1-/-
MMC
B
% of FANCD2 positive cells
100
75
50
25
0
Hus1 +/+ -/- +/+ -/-
UNT
MMC
# of FD2 foci
(> 10)
(4 to 9)
(0 to 3)
C
% of FANCD2 positive cells
100
75
50
25
0
Hus1 +/- -/- +/- -/-
UNT
MMC
# of FD2 foci
(> 10)
(4 to 9)
(0 to 3)
D
% of FANCD2 positive cells
100
75
50
25
0
Hus1 +/+ -/- +/+ -/- +/+ -/-
UNT
MMC 2h
MMC 24h
# of FD2 foci
(> 10)
(4 to 9)
(0 to 3)
E
% of yH2AX positive cells
100
75
50
25
0
Hus1 +/+ -/- +/+ -/- +/+ -/-
UNT
MMC 2h
MMC 24h
# of yH2AX foci
(> 10)
(4 to 9)
(0 to 3)

Figure 2.4. DNA crosslink-induced FANCD2 but not yH2AX focus formation and chromatin binding are defective in *Hus1*$^{-/-}$ cells. A and C Immunofluorescence staining and quantification for FANCD2 in independent cell line. *Hus1*-deficient (*Hus1*$^{-/-}$*p53*$^{-/-}$*)* and control (*Hus1*$^{+/-}$*p53*$^{-/-}$*)* cells were treated with 1 μg/ml MMC for 24h. Nuclei were counterstained with 0.05% DAPI. **B.** Quantification of the FANCD2 staining data shown in Figure 2.3. **D and E** Quantification of the FANCD2 and yH2AX staining data as shown in Figure 2.3D. The number of FANCD2 and yH2AX foci per cell was counted in 50 cells per condition.

2.4.3 The 9-1-1 complex physically associates with multiple Fanconi Anemia pathway components.

As a PCNA-like DNA clamp, the 9-1-1 complex directly interacts with a variety of effectors involved in DNA damage signaling and repair. The defective cellular and molecular responses to crosslinking agents in *Hus1*-null cells suggested possible association between 9-1-1 and FA proteins. To test for co-localization between 9-1-1 and FA core complex proteins we performed Immunofluorescence experiments in presence and absence of HUS1 in MEFs1 (Fig. 2.5A, 2.6A, B, C). FANCA foci readily formed after MMC treatment in *Hus1* wildtype cells, however reduced numbers of foci were seen when *Hus1*-deficient cells were used. To exclude off target effects from long term *Hus1*-deficiency we reintroduced functional copies of *Hus1* into *Hus1*-deficient cells and observed a rescue of FANCA foci formation in response to MMC treatment (Fig. 2.5B and C) Taken together, 9-1-1 displayed both physical and functional interaction with FA core complex proteins when challenged with ICL-induced MMC.

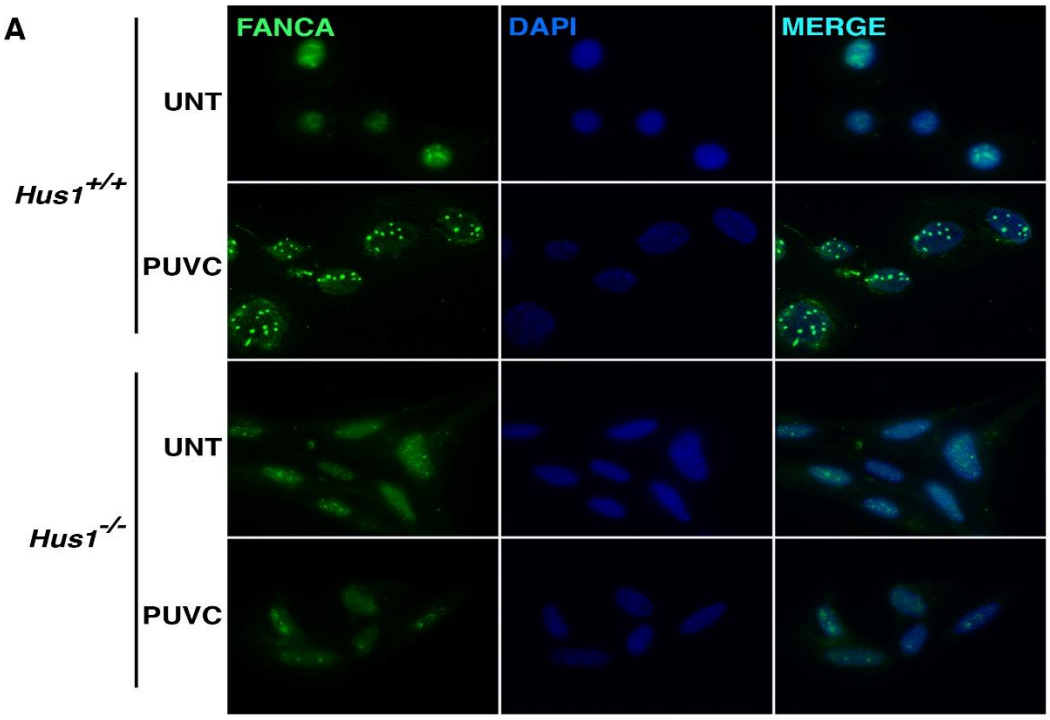
A
FANCA
DAPI
MERGE
UNT
PUVC
Hus1+/+
Hus1-/-

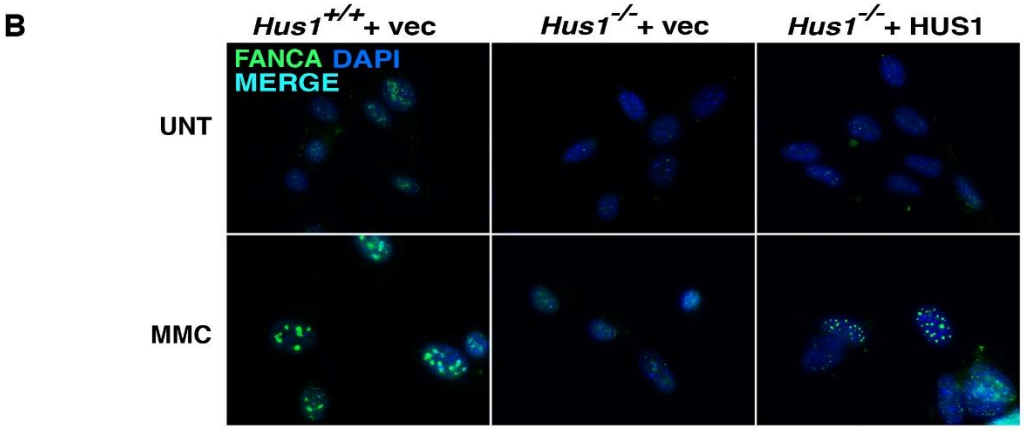
B
Hus1+/+ + vec
Hus1-/- + vec
Hus1-/- + HUS1
FANCA DAPI
MERGE
UNT
MMC

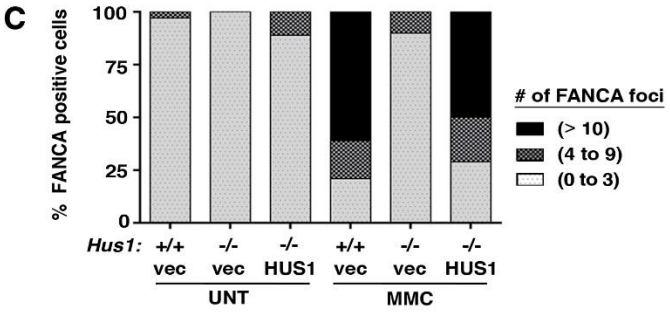
C
% FANCA positive cells
100
75
50
25
0
Hus1: +/+ -/- -/- +/+ -/- -/-
vec vec HUS1 vec vec HUS1
UNT
MMC
# of FANCA foci
(> 10)
(4 to 9)
(0 to 3)

Figure 2.5. DNA crosslink-induced FANCA focus formation is defective in *Hus1*$^{-/-}$ cells and can be rescued by *Hus1* complementation. A, B. Immunofluorescence staining for FANCA. **A.** HUS1$^{-/-}$ (*Hus1*$^{-/-}$*p21*$^{-/-}$) and control (*Hus1*$^{+/+}$*p21*$^{-/-}$) cells were treated with 1 μg/ml MMC for 24h. Nuclei were counterstained with 0.05% DAPI. **B.** *Hus1*$^{-/-}$ (*Hus1*$^{-/-}$*p21*$^{-/-}$) and control (*Hus1*$^{+/+}$*p21*$^{-/-}$) cells complemented with *Hus1*, or GFP as a control, were treated and stained as in A. **C.** Quantification of the FANCA staining data shown in B. The number of FANCA foci per cell was counted in 50 cells per condition.

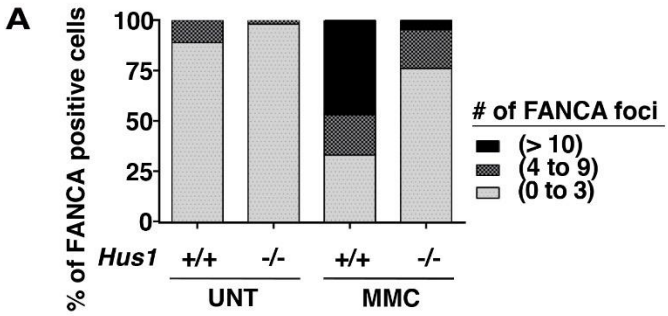
A
% of FANCA positive cells
100
75
50
25
0
Hus1 +/+ -/- +/+ -/-
UNT
MMC
# of FANCA foci
(> 10)
(4 to 9)
(0 to 3)

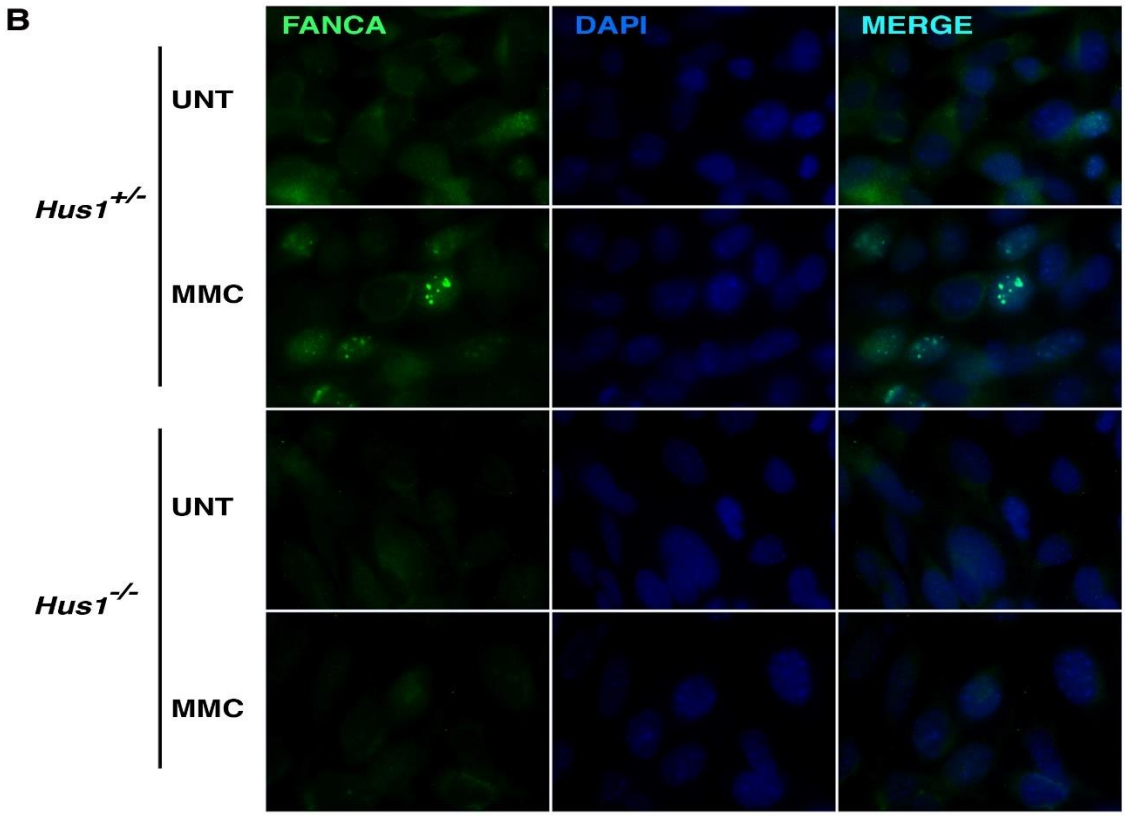
B
FANCA
DAPI
MERGE
Hus1+/-
UNT
MMC
Hus1-/-
UNT
MMC

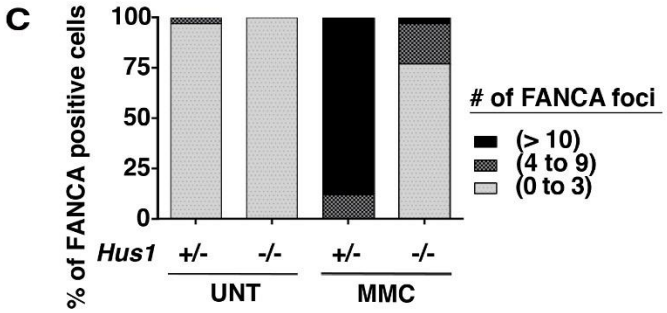
C
% of FANCA positive cells
100
75
50
25
0
Hus1 +/- -/- +/- -/-
UNT
MMC
# of FANCA foci
(> 10)
(4 to 9)
(0 to 3)

Figure 2.6. DNA crosslink-induced FANCA focus formation is defective in *Hus1*$^{-/-}$ cells and can be rescued by *Hus1* complementation. A, B and C Immunofluorescence staining for FANCA. **A.** Quantification of the FANCA staining data shown in Figure 2.5. The number of FANCA foci per cell was counted in 50 cells per condition. **B** *Hus1*$^{-/-}$ (*Hus1*$^{-/-}$*p53*$^{-/-}$) and control (*Hus1*$^{+/+}$*p53*$^{-/-}$) cells were treated with 1 µg/ml MMC for 24h. Nuclei were counterstained with 0.05% DAPI. **C**. Quantification of the FANCA staining data shown in B. The number of FANCA foci per cell was counted in 50 cells per condition.

To screen for potential physical interactions, we next performed (luminescence-based mammalian interactome mapping (LUMIER) assays [241]. In LUMIER, FLAG-tagged bait and Renilla luciferase-tagged prey proteins are co-expressed in mammalian cells and their ability to interact is quantified by luciferase assay following FLAG IP, allowing for high throughput screening of potential protein-protein interactions. In this study, luciferase-tagged 9-1-1 subunits were individually expressed in 293T cells and then tested for interaction with FLAG tagged FA proteins, with luciferase-tagged PCNA serving as the negative control bait. Notably, LUMIER assays revealed that luciferase-tagged HUS1 or RAD9A-C (lacking the C-terminal tail of RAD9A) interacted with several FA proteins (Fig. 2.7A). RAD9A showed the most robust interactions with FA proteins, including FANCG, FANCL, FANCM, PALB2, SLX4 and FANCF (listed in decreasing score for strength of interaction). HUS1 on the other hand showed significant interaction with PALB2, FANCG, FANCL, FANCA, FANCF, SLX4 and FANCD2. Other pathway components fell just below our rigorous threshold for significance (z-score of 2) but nevertheless could be legitimate interactors, particularly since the LUMIER assay was done without genotoxin treatment. FANCC and FANCI were found to interact with luciferase alone and therefore were excluded from further analysis. Interestingly, RAD1 displayed only weak interactions with FA proteins but strongly associated with HUS1 as expected, suggesting that the assay reads out direct interactions rather than indirect contacts via associated 9-1-1 subunits. Overall, the findings from LUMIER assays suggest that the 9-1-1 complex may promote FA signaling by scaffolding several pathway components.

We next validated the potential physical interactions by performing co-immunoprecipitation (co-IP) experiments using FLAG-tagged HUS1 to detect either endogenous FANCD2 or HA-FANCI.

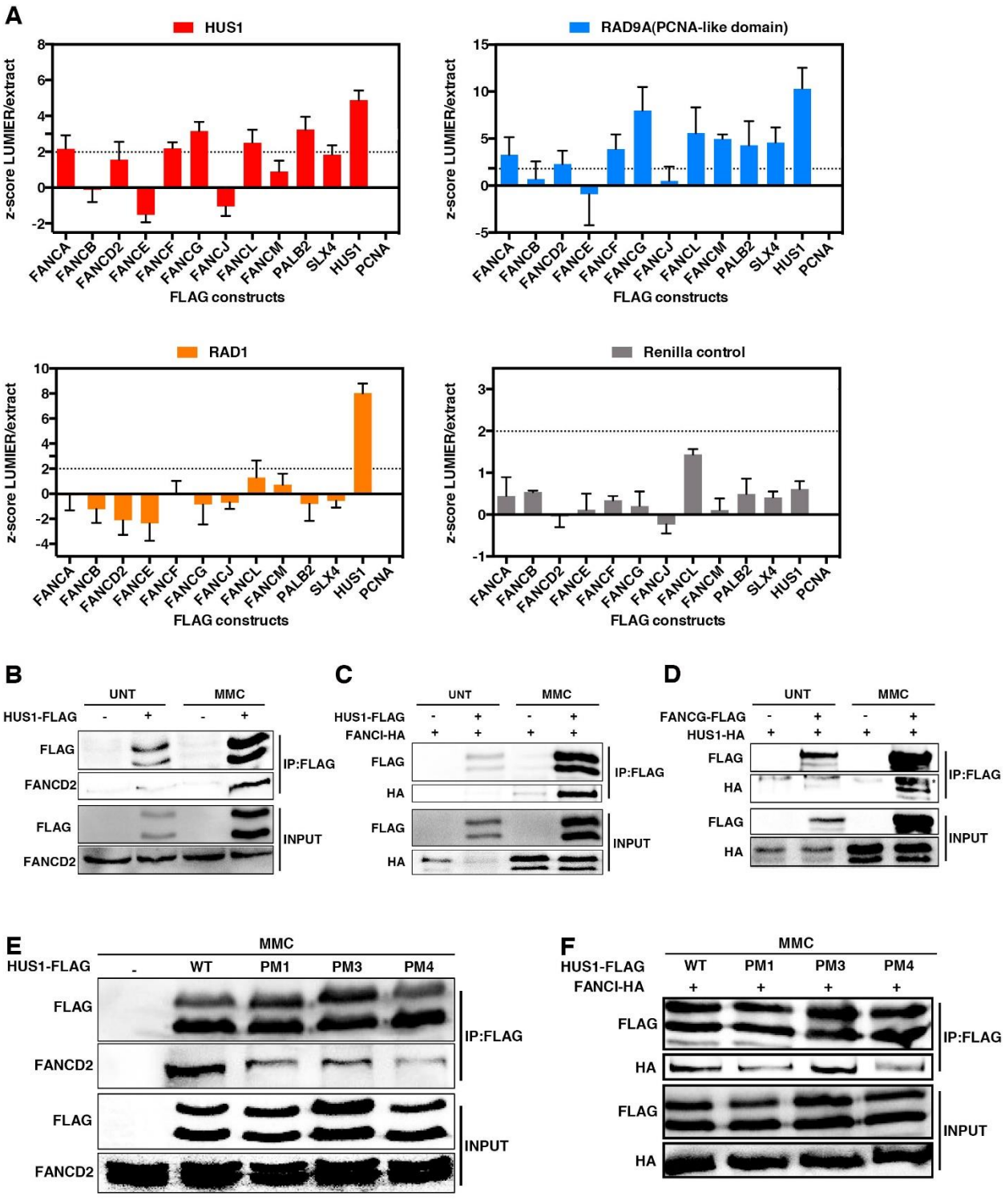
A
HUS1
RAD9A(PCNA-like domain)
RAD1
Renilla control
z-score LUMIER/extract
FANCA FANCB FANCD2 FANCE FANCF FANCG FANCJ FANCL FANCM PALB2 SLX4 HUS1 PCNA
FLAG constructs
B
UNT
MMC
HUS1-FLAG
FLAG
FANCD2
IP:FLAG
INPUT
C
FANCI-HA
HA
D
FANCG-FLAG
HUS1-HA
E
WT
PM1
PM3
PM4
F

Figure 2.7. 9-1-1 subunits directly interact with multiple Fanconi Anemia pathway components. A. Mammalian yeast-two hybrid screen. LUMIER-BACON assay showing interactions for RAD9/RAD1/HUS1 and FA proteins. The experiment and analysis was performed by Dr. Gorgios Karras. **B, C and D.** Co-IP interaction between FANCD2, FANCI-HA and FANCG-3XFLAG with HUS1 was assessed by co-IP. Cells were treated with 0.5 μg/ml of MMC or DMSO before preparing nuclear fractionation. Nuclear lysates were used to perform the IP using Anti-FLAG M2 resin and subsequently immunoblotting was performed with antibodies specific to FLAG M2, HA, and FANCD2. The experiment was performed by Darshil Patel. **E and F**. Co-IP with interactions between FANCD2 and FANCI-HA with HUS1-3xFLAG and HUS1 mutants. Nuclear proteins were isolated after treating the cells with 0.5 μg/ml MMC overnight. Nuclear lysates were used to perform the IP using Anti-FLAG M2 resin and subsequently immunoblotting was performed with antibodies specific to FLAG M2, HA, and FANCD2. The experiment was performed by Darshil Patel.

Both subunits of the ID dimer weakly interacted with FLAG-tagged HUS1 in absence of damage inducing agents. MMC-induced damage caused a significant increase in the levels of HUS1 in the nucleus and triggered much greater co-IP of FANCD2 and HA-FANCI (Fig. 2.7B and C). To test interactions between 9-1-1 and an FA core complex component, we co-expressed HA-HUS1 and FLAG-FANCG and found that HUS1 and FANCG specifically interacted, again to a much greater extent in MMC-treated cells (Fig. 2.7D).

9-1-1 complex subunits are believed to associate with binding partners via the outer surface of the clamp, paralleling the mechanism utilized by PCNA. We recently established that the outer surface of the HUS1 subunit features two functionally important hydrophobic pockets. The first is positioned similarly to the PIP box binding pocket of PCNA, and we disrupted this pocket by introducing the V151Y substitution mutation (termed PM3). A second distinct hydrophobic pocket is positioned closer to the subunit interface with RAD9A and could be disrupted with the R4D mutation (PM1). Cells expressing either PM1 or PM3 showed increased MMC sensitivity. The double mutant, R4D+V151Y (PM4) was associated with greater MMC sensitivity than either single mutant and was found to be greatly impaired for interactions with a known HUS1 binding partner, MYH1. Importantly PM4 and the other HUS1 out surface mutants were fully functional for clamp formation, chromatin loading, and activation of ATR checkpoint signaling, which is mediated by the RAD9A c-terminal tail. These mutants therefore provide a useful separate of function for distinguishing between the checkpoint signaling and signaling-independent roles of the 9-1-1 complex during a DNA damage response. When tested in the co-IP we saw a modest reduction in FANCD2 binding with PM3, a more substantial defect in both FANCD2 and FANCI binding with PM1, and the greatest disruption of binding in the PM4 double mutant (Figs. 2.7E and F). These results suggest that the both HUS1 outer surface hydrophobic pockets contribute to interactions between HUS1 and the ID dimer.

We next tested the impact of the HUS1 outer surface mutations on FA signaling. MMC-induced FANCD2 focus formation was analyzed in *Hus1*-null cells complemented with wild-type *Hus1*, the *Hus1* mutants, or the empty vector. While wild-type *Hus1* was able to rescue the defect in FANCD2 formation,

cells expressing the PM4 *Hus1* mutant remained defective for FANCD2 focus formation, to the same extent as cells with the empty vector. (Fig. 2.8A). Since the PM4 mutant is competent for MMC-induced CHK1 phosphorylation by ATR, these results identify a checkpoint signaling-independent function mediated by the HUS1 outer surface in the formation of MMC-induced FANCD2 foci on chromatin. We also tested the ability of the *Hus1* mutants to suppress chromosomal aberrations following MMC treatment (Fig 2.8B and C). As compared to cells complemented with wild-type *Hus1*, which eliminated MMC-induced radial chromosome formation, cells expressing the PM4 mutant showed an intermediate but modest increase in MMC-induced radial chromosomes (6 radials in 50 metaphases), suggesting that the HUS1 outer surface does contribute to this role although other factors also seem to be involved. As expected, cells expressing the empty vector showed elevated MMC-induced radial chromosome formation (23 radials in 50 metaphases).

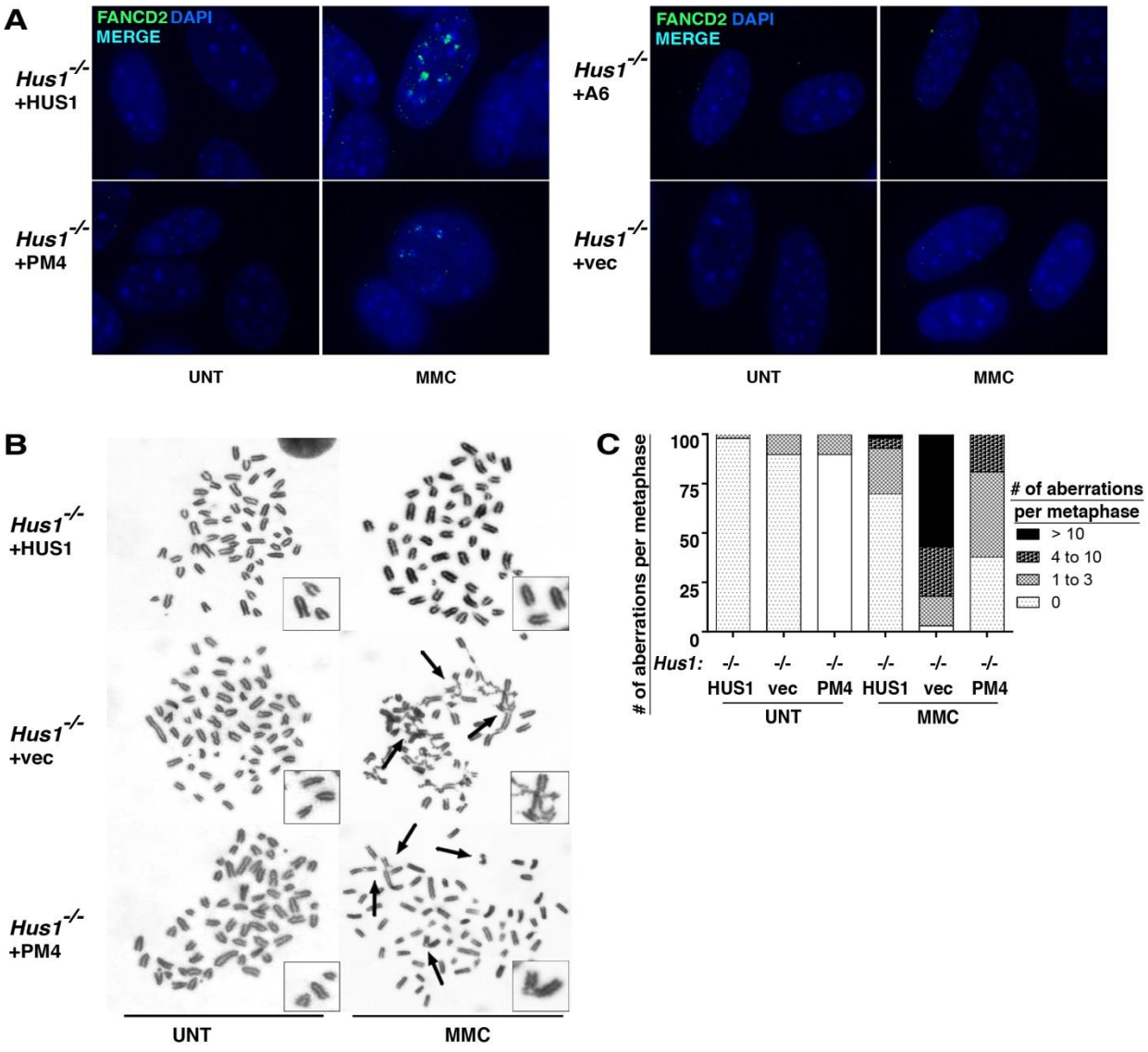
A
FANCD2 DAPI
MERGE
Hus1-/-
+HUS1
Hus1-/-
+PM4
Hus1-/-
+A6
Hus1-/-
+vec
UNT
MMC
B
Hus1-/-
+HUS1
Hus1-/-
+vec
Hus1-/-
+PM4
UNT
MMC
C
# of aberrations per metaphase
100
75
50
25
0
Hus1: -/- -/- -/- -/- -/- -/-
HUS1 vec PM4 HUS1 vec PM4
UNT
MMC
# of aberrations per metaphase
> 10
4 to 10
1 to 3
0

Figure 2.8. The 9-1-1 complex is required for proper DNA damage responses to MMC-induced lesions in mouse fibroblasts and cannot be rescued by *Hus1* surface mutant expression. A. Immunofluorescence staining for FANCD2 in *Hus1*-deficient (*Hus1*$^{-/-}$*p21*$^{-/-}$) cells complemented with PM4, A6 or empty vector. Cells were treated with 1 μg/ml MMC for 24h. Nuclei were counterstained with 0.05% DAPI. **B and C.** Metaphase chromosome analysis and quantification of *Hus1*-deficient (*Hus1*$^{-/-}$*p21*$^{-/-}$) cells complemented with PM4, A6 or empty vector following mock treatment or treatment with 0.06 μg/ml MMC for 24h. Spreads were categorized based on the number of aberrations per spread.

2.4.4 9-1-1 promotes ICL resolution by promoting HRR repair

When replication forks converge at an ICL during S-phase, the subsequent processing steps create a DSB that normally is repaired by HRR. The severe chromosomal aberrations observed in *Hus1*-null cells after MMC treatment (Fig. 2.1C, 2.1D, 2.2A, 2.2B, 2.8B and 2.8C) raised the possibility that the 9-1-1 complex also might act later during ICL repair to promote accurate resolution events. After ICL unhooking creates a DSB, end processing allows the strand exchange protein RAD51 to form the nucleoprotein filament necessary for template strand invasion and error free repair. To assess these steps of HRR repair we first examined RAD51 focus formation. Remarkably, MMC-treated *Hus1*-null cells showed a complete absence of RAD51 foci at all investigated time points (Fig. 2.9A and C). Similar results were observed with another replication stress inducing agent, hydroxyurea (HU), but following IR both *Hus1*- null and –proficient cells formed RAD51 foci (Fig. 2.9B and D). Further time course analyses revealed that the number of RAD51 foci after IR was slightly decreased in *Hus1*-null cells, unlike the fully defective response to MMC or HU (Fig. 2.9D, 2.10A). γH2AX phosphorylation was comparable in *Hus1*- null and –proficient cells following MMC, HU, or IR (Fig 2.11A), establishing a lesion-specific requirement for HUS1 for RAD51 loading.

Several potential molecular defects could account for the observed failure of RAD51 loading. RAD51 nucleoprotein filament formation requires ssDNA reviewed in [244], and 9-1-1 has previously been implicated in end resection [123]. RAD51 focus formation also requires RPA coating of the ssDNA [244]. Although a defect in RPA coating might have explained the failure of RAD51 loading, IF confirmed the presence of RPA on chromatin in *Hus1*- null cells following IR, HU or MMC (Fig. 2.9F, 2.11A and 2.12C). We proceeded to confirm these results in an independent assay using chromatin fractionation.

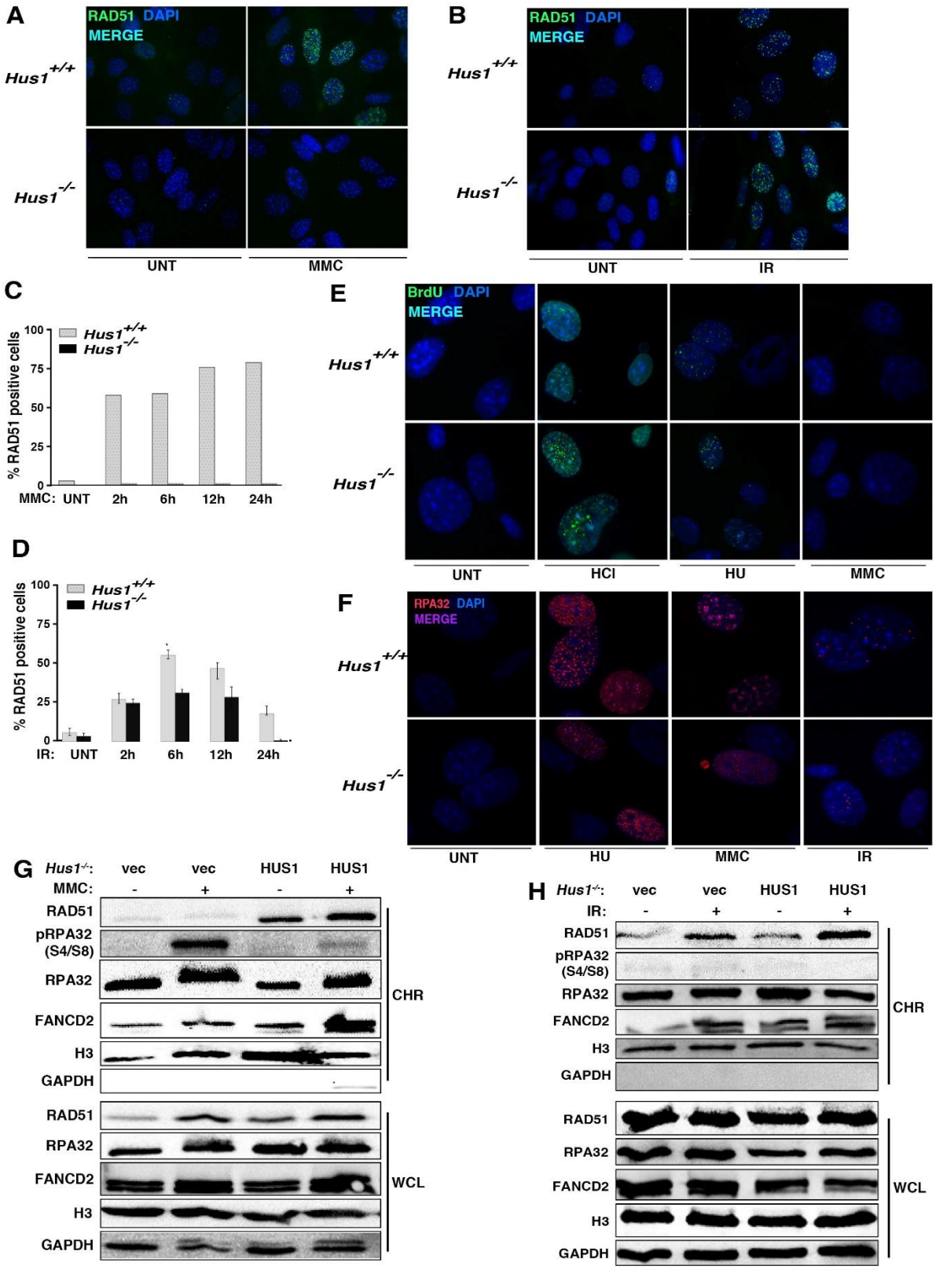
A
RAD51 DAPI
MERGE
Hus1+/+
Hus1-/-
UNT
MMC
B
RAD51 DAPI
MERGE
Hus1+/+
Hus1-/-
UNT
IR
C
% RAD51 positive cells
Hus1+/+
Hus1-/-
MMC: UNT 2h 6h 12h 24h
D
% RAD51 positive cells
Hus1+/+
Hus1-/-
IR: UNT 2h 6h 12h 24h
E
BrdU DAPI
MERGE
Hus1+/+
Hus1-/-
UNT
HCl
HU
MMC
F
RPA32 DAPI
MERGE
Hus1+/+
Hus1-/-
UNT
HU
MMC
IR
G
Hus1-/-: vec vec HUS1 HUS1
MMC: - + - +
RAD51
pRPA32 (S4/S8)
RPA32
FANCD2
H3
GAPDH
CHR
RAD51
RPA32
FANCD2
H3
GAPDH
WCL
H
Hus1-/-: vec vec HUS1 HUS1
IR: - + - +
RAD51
pRPA32 (S4/S8)
RPA32
FANCD2
H3
GAPDH
CHR
RAD51
RPA32
FANCD2
H3
GAPDH
WCL

Figure 2.9. 9-1-1 governs post-MMC DSB resolution through promotion of HRR repair. A and B. Immunofluorescence staining for RAD51 in *Hus1*$^{-/-}$ (*Hus1*$^{-/-}$*p21*$^{-/-}$) following treatment with 2μg/ml MMC or 10Gy of IR over a time course. Cells were counterstained with 0.05% DAPI. **C and D**. Quantification of A and B. Time course experiment was carried out once, with individual time points repeated in other experiments. Means are shown. Error bars in **D** are SEM, obtained using 5 optical field values in one experiment. **E**. Immunofluorescence staining for BRDU in *Hus1*$^{-/-}$ (*Hus1*$^{-/-}$*p21*$^{-/-}$) following treatment with 2 μg/ml MMC or 6mmol HU. HCL treatment as positive control. Cells were counterstained with 0.05% DAPI. **F**. Immunofluorescence staining for RPA in *Hus1*$^{-/-}$ (*Hus1*$^{-/-}$*p21*$^{-/-}$) following treatment with 2 μg/ml MMC, 6mmol HU or 10 Gy IR. Cells were counterstained with 0.05% DAPI. **G and H**. Immunoblotting analysis of chromatin fractionation and whole cell lysate. Cells were treated with 0.5 μg/ml of MMC. Fractions and WCL were immunoblotted with antibodies specific to FANCD2, phospho-RPA32 (S4/S8), RAD51, GAPDH and histone 3. GAPDH and histone 3 served as fractionation controls. The experiments in E,F,G and H were performed by Darshil Patel.

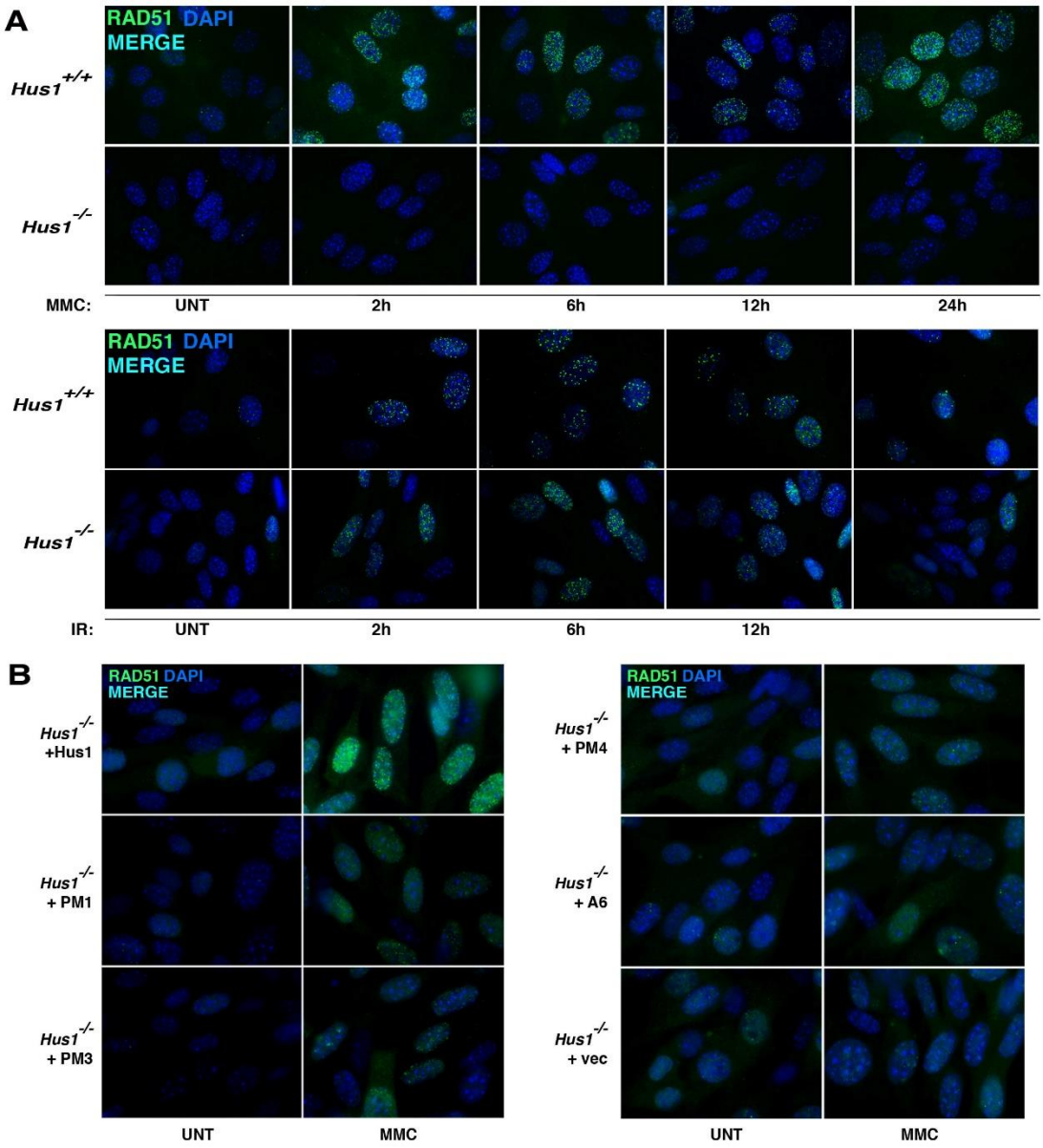
A
RAD51 DAPI
MERGE
Hus1+/+
Hus1-/-
MMC:
UNT
2h
6h
12h
24h
RAD51 DAPI
MERGE
Hus1+/+
Hus1-/-
IR:
UNT
2h
6h
12h
B
RAD51 DAPI
MERGE
Hus1-/-
+Hus1
Hus1-/-
+ PM1
Hus1-/-
+ PM3
UNT
MMC
RAD51 DAPI
MERGE
Hus1-/-
+ PM4
Hus1-/-
+ A6
Hus1-/-
+ vec
UNT
MMC

Figure 2.10. HUS1 is required for RAD51 function in response to interstrand cross-links. A. Immunofluorescence staining for RAD51 in *Hus1*-deficient (*Hus1*$^{-/-}$*p21*$^{-/-}$*)* and control (*Hus1*$^{+/+}$ *p21*$^{-/-}$*)* cells were treated with 1 µg/ml MMC or 10Gy of IR for a time course from 2 to 24h. Nuclei were counterstained with 0.05% DAPI. **B.** Immunofluorescence staining for RAD51 in *Hus1*-deficient (*Hus1*$^{-/-}$ *p21*$^{-/-}$*)* cells complemented with PM1, PM3, PM4, A6 or empty vector. Cells were treated with 1 µg/ml MMC for 24h. Nuclei were counterstained with 0.05% DAPI.

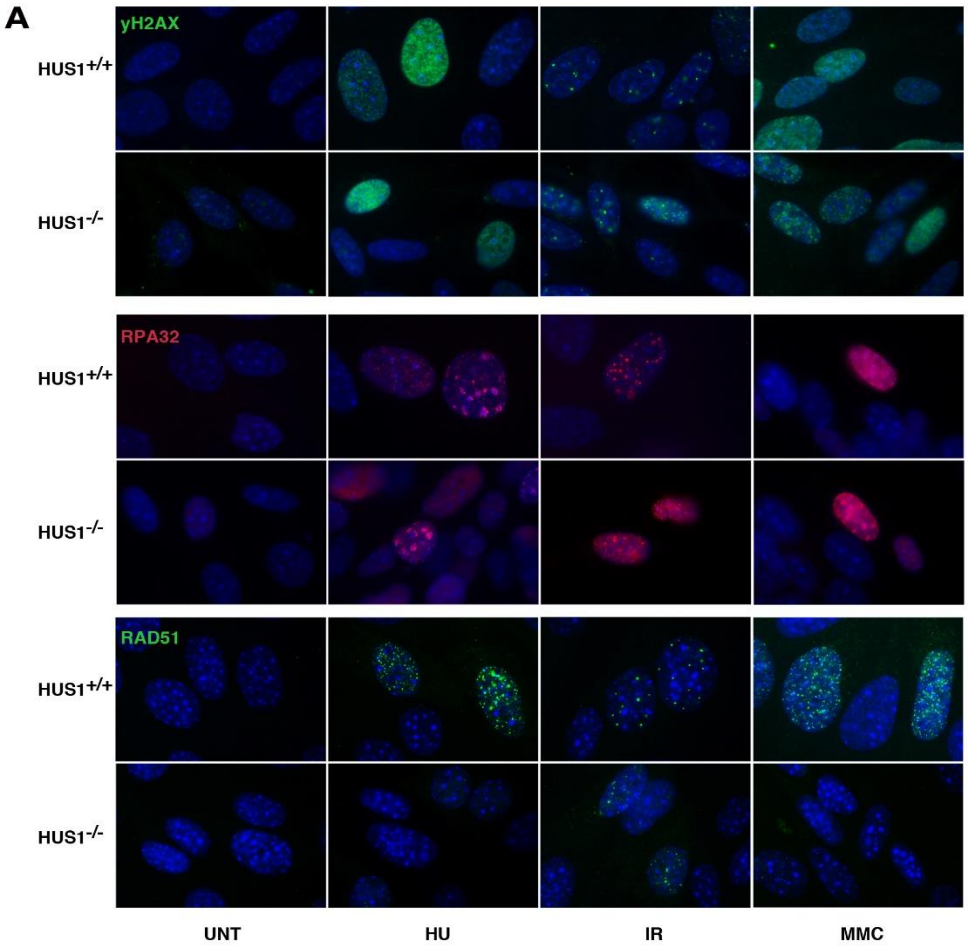
A
γH2AX
HUS1+/+
HUS1-/-
RPA32
HUS1+/+
HUS1-/-
RAD51
HUS1+/+
HUS1-/-
UNT
HU
IR
MMC

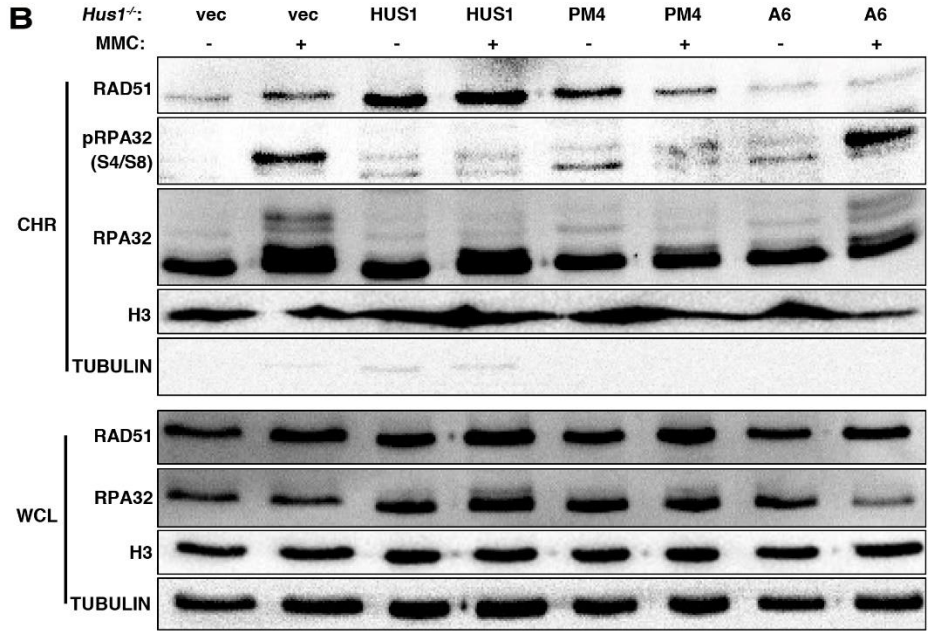
B
Hus1-/-: vec vec HUS1 HUS1 PM4 PM4 A6 A6
MMC: - + - + - + - +
CHR
RAD51
pRPA32 (S4/S8)
RPA32
H3
TUBULIN
WCL
RAD51
RPA32
H3
TUBULIN

Figure 2.11. RAD51 defect in chromatin binding is ICL specific.

A. Immunofluorescence staining for yH2AX, RPA and RAD51 carried out side by side, in *Hus1*-deficient (*Hus1*$^{-/-}$*p21*$^{-/-}$) and control (*Hus1*$^{+/+}$ *p21*$^{-/-}$) cells. Cells were treated with 1 μg/ml MMC, 10 Gy of IR or 0.5 mmol of HU for a time course from 2 to 24h. Nuclei were counterstained with 0.05% DAPI. **B**. Immunoblotting analysis of chromatin fractionation and whole cell lysate in *Hus1*-deficient (*Hus1*$^{-/-}$*p21*$^{-/-}$) cells complemented with PM1, PM3, PM4, A6 or empty vector. Cells were treated with 0.5 μg/ml of MMC. Fractions and WCL were immunoblotted with antibodies specific to FANCD2, phospho-RPA32 (S4/S8), RAD51, GAPDH and histone 3. GAPDH and histone 3 served as fractionation controls.

Consistent with the IF results, RAD51 accumulation on chromatin was severely impaired in MMC treated *Hus1*-null cells containing the empty vector as compared to those complemented with wild-type HUS1 (Fig. 2.9F). Also in line with our earlier findings, MMC-induced chromatin loading of FANCD2 was only observed in the presence of HUS1. On the other hand, RPA accumulation on chromatin following MMC in both *Hus1*- null and *Hus1* proficient cells. However, the RPA immunoblots revealed a mobility shift in lysates from MMC-treated *Hus1*- null cells, suggestive of RPA hyper-phosphorylation. Because RPA hyper-phosphorylation at S4/S8 by ATM and/or DNA-PKcs has been suggested to suppress RAD51 loading [245] we monitored phosphorylation of this site and observed a dramatic increase in phospho (S4/S8)- RPA in MMC-treated *Hus1*- null cells. To test whether RPA hyper-phosphorylation was responsible for the RAD51 loading defect, we attempted to block RPA hyper-phosphorylation by treating cells with the DNA-PK inhibitor NU7441 and the ATM inhibitor KU55933. Kinase inhibitor treatment failed to restore RAD51 loading in MMC-treated *Hus1*-null cells. However, while the kinase inhibitors reduced the total level of RPA hyper-phosphorylation in MMC-treated *Hus1*-null cells but they did not reduce the phosphorylation of chromatin-bound RPA, leaving a possible role for RPA phosphorylation in the RAD51 loading defect (Fig. 2.12A).

To further understand the HUS1 functions that modulate RPA and RAD51 dynamics, we tested the same parameters in cells expressing the separation of function or loss of function of HUS1 mutants. In IF assays, both the outer surface (PM4) and inner surface (A6) *Hus1* mutants were defective for supporting RAD51 focus formation, yielding results similar to those in *Hus1*-null cells containing the empty vector (Fig. 2.11B). In chromatin fractionation assays, the A6 mutant was unable to support RAD51 localization to chromatin, similar to the results from the IF assay. However, the outer surface PM4 mutant showed only a partial defect in RAD51 loading functions suggesting that checkpoint signaling cannot be ruled out. These findings establish that the HUS1 outer surface plays an important role in promoting DSB resolution at ICLs.

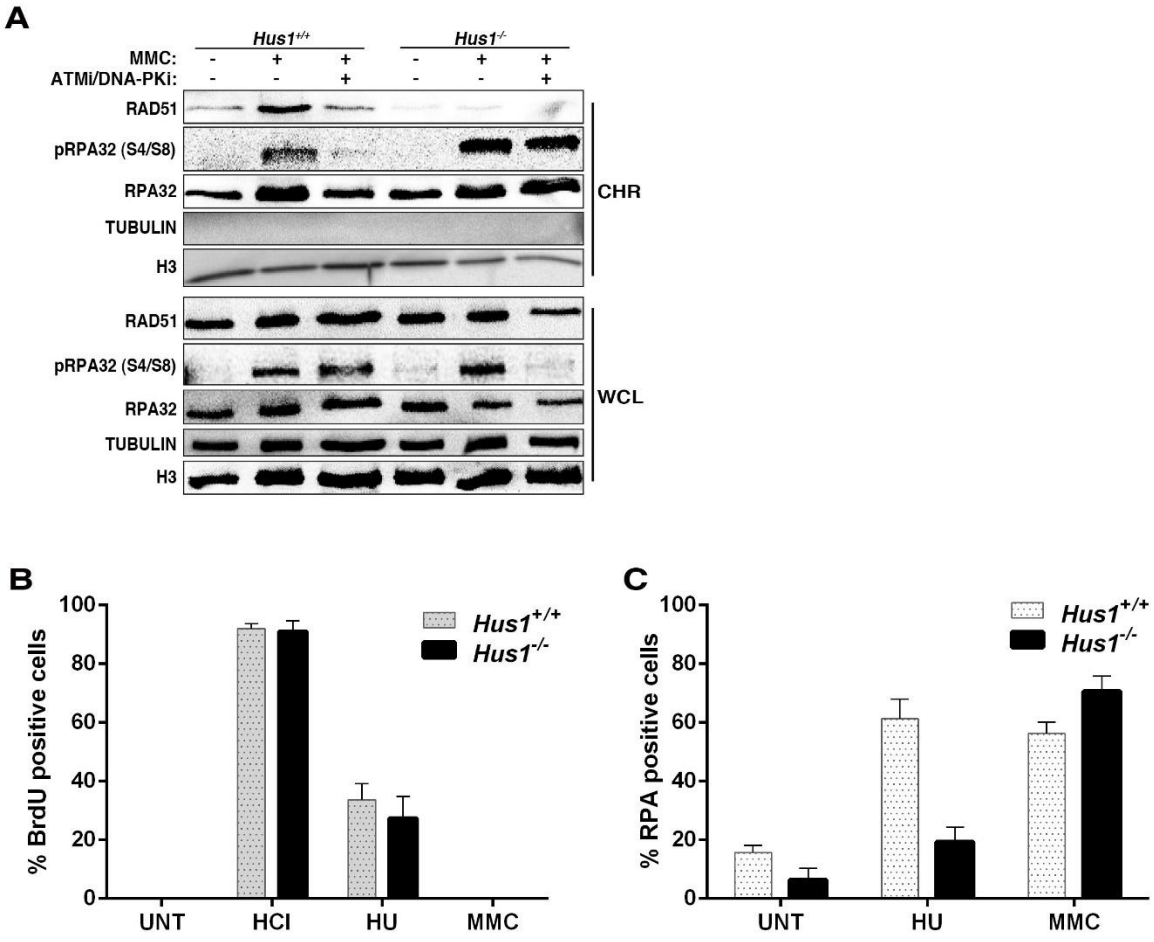

Figure 2.12. HUS1 regulates the loading of RPA and RAD51 as well a ssDNA generation at the chromatin in context of ICL repair.

A. Immunoblotting analysis of chromatin fractionation and whole cell lysate. Treatment with the addition of ATM and DNA-PK inhibitor and MMC as indicated. **B**. Quantification of BRDU staining from figure 2.9. **C**. Quantification of RPA staining from figure 2.9.

although this level of loading was not sufficient to drive detectable RAD51 focus formation in IF assays (Fig. 2.10B). Similar results were obtained for FANCD2 and phospho-RPA (S4/S8) chromatin association, with cells expressing HUS1-A6 yielding results similar to those with empty vector, while cells expressing HUS1-PM4 showed intermediate phenotypes.

2.5 Discussion

As previously reported by our group [115] *Hus1*-deficiency significantly reduces viability following MMC treatment in *Hus1* hypomorph mice. Here we showed that cultured cells that are deficient for HUS1 have severe sensitivity to MMC and Trioxsalen/UVA, suggesting functional interaction of 9-1-1 and ICL repair pathways. Cells failing to repair ICL DSB intermediates will display increased chromosomal damage. Here we demonstrate increased chromosomal aberrations as well as the formation of radial chromosomes in *Hus1*$^{-/-}$ cells post MMC exposure, which likely is a consequence of failed DSBs repair attempts. Radial chromosomes are pathognomonic for the FA disorder, which origins from defects in ICL repair pathways. This provided the rationale to investigate the link between *Hus1* and ICL repair pathways.

Formation of FANCD2 foci is a hallmark of the activation of the FA pathway in competent cells. Strikingly, our *Hus1*-deficient cells lines displayed a defect in FANCD2 focus formation as well as disruption of FANCD2 in binding to chromatin. Failure to form foci in absence of HUS1 revealed a possible function of the clamp in activation of the pathway. Previous reports suggested that inactivation of ATR results in a similar loss of FANCD2 foci [246]. HUS1 is essential for checkpoint function; therefore, the question arose: Is the loss of foci a consequence of ATR impairment or does HUS1 play a direct role in FA pathway function? The results of our study suggest a checkpoint independent function for HUS1, likely through direct modulation of interacting repair proteins.

Ubiquitination of the ID dimer is important for their localization to the site of damage and is

maintained by the FA core complex. In the absence of 9-1-1, residual mono-ubiquitination of FANCD2 is still measureable. *Hus1*$^{-/-}$ cell lines showed elevated levels of ubiquitination in untreated conditions, likely due to increased replication stress in those cells. However, we observed no augmentation in the ubiquitination of FANCD2 post MMC treatment [115]. This indicates that the core complex retains a level of activity but is impaired in localization to the DNA or its target FANCD2. These results support the claim that 9-1-1 works as a scaffold allowing the interaction of the key proteins with each other at the damage site. We suggest the following: HUS1 allows for recruitment of the ID dimer to the chromatin, in its absence the likelihood of interaction between the ID dimer and the core complex is reduced. FANCL ubiquitin ligase monoubiquitinates FANCD2 at low levels, though the subsequent tethering to the chromatin is HUS1 dependent and lost in absence of HUS1. This separation of FANCD2 ubiquitination and chromatin localization is reminiscent of events observed in BRCA1 and FANCJ as well [155 , 247]. They suggest that ubiquitination and localization could be separately regulated events, with the potential for new regulatory elements to be identified. FAND2 foci formation cannot occur without prior ubiquitination. Ubiquitination of the ID dimer can occur as a residual function even if members of the FA protein family are disrupted. IF, as suggested, the evens of chromatin binding, protein recruitment, complex formation, and complex stabilization are independently regulated, 9-1-1 could play a role in regulation of these key events.

Given the PCNA-like behavior of 9-1-1 as a scaffolding protein, functional defects in *Hus1*$^{-/-}$ cells in response to MMC, I predicted molecular interactions between 9-1-1 and FA pathway components. In LUMIER the RAD9A and HUS1 subunits showed reliable interactions with various FA proteins, with strong representation of FANCG, FANCA and FANCD2 suggesting that both the ID heterodimer and the core complex potentially coalesce around 9-1-1. The co-IP experiments showed a strong interaction of FANCD2, FANCG and FANCI with HUS1.

The direct interactions as shown in the LUMIER assay and co-IP suggest molecular interaction between 9-1-1 and FA proteins, suggested an independent role for HUS1 in ICL repair. However, whether the phenotypes seen in *Hus1*$^{-/-}$ cells reflect the role of 9-1-1 in ATR activation or are independent of ATR

function remained unclear. In order to answer this question, we utilized three of the *Hus1* mutants generated in our laboratory, *Hus1*-PM1, PM3 and PM4. These mutants of *Hus1* harbor one of two or both mutations at important residues on the outer surface of the clamp. One mutation, R4D (PM1) exchanges the positively charged residue of arginine for the negatively charged aspartic acid in a conserved pocket near the RAD9A interface, the other, I152Y (PM3), obstructs the PCNA like hydrophobic pocket. Both residues are mutated simultaneously in PM4. Those mutations leave the clamp integrity unaltered, therefore maintaining the checkpoint [116]. The HUS1 outer surface double mutant PM4 that was generated in our lab failed at rescuing FANCD2 foci formation, despite being proficient for ATR checkpoint activation, suggesting a role for HUS1 surface residues in facilitating FANCD2 chromatin loading. *Hus1*$^{-/-}$ cells complemented with the HUS1 outer surface mutant have decreased cell survivability in response to MMC when compared to the wild type cells [116]. Moreover, HUS1-PM4 disrupts 9-1-1 interaction with both FANCI and FACND2.

Growing evidence suggests a role for 9-1-1 in coordination of the base excision repair (BER) pathway. The clamp is shown to interact with multiple components of LP-BER [121, 131, 132]. In a similar fashion, 9-1-1 helps govern in mismatch repair (MMR) [122]. HUS1 helps regulate the repair of DSBs [110, 123] and finally, emerged in a proteomic screening study, which examined targeted protein needed for ICL repair [124]. Overall, a protein scaffold function for 9-1-1 in complex repair processes seems increasingly likely. To further understand the role of HUS1 in DSBs and HRR especially, we looked into RAD51, an important HRR protein that sets up the stage for HRR repair. Our IF results show presence of RAD51 foci in *Hus1*-proficient cells and complete absence in *Hus1*$^{-/-}$ cells suggesting a critical role of HUS1 in mediation of HRR.

The role of RAD51 and its paralogs has been established as essential for HRR (reviewed in [244]), in fork protection [248, 249] and in ICL repair [141]. Loss of RAD51 or its paralogs results in embryonic lethality and fertility defects [250-256] thus proving its importance in maintained of genome integrity and DSB repair.

Multiple factors guide and govern the loading of RAD51 onto DNA in its role in replication fork

protection. FANCD2, BRCA1 CHK1, PARP1 all collaborate with RAD51 in fork stabilization [248, 257]. In HRR, BRCA2 is crucial as it sequesters RAD51 away from DNA and releases it upon DNA damage signaling (reviewed in [258]).

The role of FANCD2 in loading of RAD51 is controversial. Various groups have published contradicting evidence. It's been shown that absence of FANCD2 results in a reduction of RAD51 and BRCA2 focus formation, along with HRR defects [119, 259-261]. Contradicting reports suggest association of RAD51 with chromatin in a FANCD2 independent manner, in which *Fancd2*-deficient cells still load RAD51 onto chromatin [262]. Others observed that presence of RAD51 was required for FANCD2 loading. [124, 141]. These contradicting reports are difficult to reconcile. In a model in which RAD51 recruitment is regulated differentially depending on the DNA damage context and extent, the question still remains how to achieve a separation of function during a number of processes: In fork protection, due to MCM-helicase and replication polymerase uncoupling, in ICL fork stalling, in post ICL DSBs, in IR-induced end resection RAD51 may require, may be helped by or could be independent of FANCD2. In our studies, the 9-1-1 complex which is known to work as a molecular scaffold, seems to be following a similar dynamic. In processing of MMC-induced ICLs, HUS1 is essential for the formation of RAD51 foci, however in response to IR, there is only a moderate decrease in foci positive cells, when comparing $HUS^{-/-}$ to wild type cells. HUS1 directly interacts with FANCD2 suggesting that it could carry a role in regulating and recruiting known DNA damage repair factors to the site of damages as needed.

We were able to eliminate the idea of lacking ssDNA through resection defects in $Hus1^{-/-}$ cells, as our ssDNA binding assay showed presence of ssDNA in both $Hus1^{-/-}$ and wild type cells (Figure 2.9E and 2.12B). This result begged the question what is inhibiting the RAD51 loading of the DNA in $Hus1^{-/-}$ cells.

During the DDR, such as after exposure to ionizing radiation, RPA get hyper-phosphorylated on residues S23 and S29 by CDK. Mutations of these residues to alanine reduced the hyper-phosphorylation and had consequences for the DDR: S23/29A cells had reduced RAD51 chromatin binding after DSB induction, suggesting that phosphorylation of RPA32 may regulates HR repair pathway [263]. Another mutant of RPA32, S33A/T21A was impaired in DNA synthesis and delayed RPA displacement [264].

S23/29A and S33A/T21A mutants were also shown to be defective in proper recruitment to the site of DNA damage for the HRR proteins PALB2 and BRCA2 [265]. Cells expressing an RPA32 mutant lacking seven phosphorylation sites (RPA32 Ala7: S4A, S8A, S11A, S12A, S13A, T21A and S33A) displayed reduced RAD51 chromatin loading after HU challenge but not after IR [266]. Together, these findings suggest that the phosphorylation of different sites of RPA32 may affect HRR differently, and these effects may be context specific. Recent studies suggested that hyper-phosphorylation of RPA32 at sites of damage S4/S8 delays RAD51 loading and HRR-mediated DSB repair [245]. Further investigation in the role of RPA phosphorylation in HUS1$^{-/-}$ cells revealed a state of hyper-phosphorylation of RPA32 at sites S4/S8 in HUS1$^{-/-}$ cells corresponding to Liaw et al [245]. RPA is known to undergo hyper-phosphorylation upon experiencing UV or IR-induced DNA damage [267]. The hyper-phosphorylation of the RPA32 is proposed to be carried out by the members of the PIKK family – ATM, ATR and DNA-PK [268]. As *Hus1*$^{-/-}$ cells are impaired in DNA repair, the cells experience heightened stress post MMC treatment. This results in continuous phosphorylation of RPA conferring the hyper-phosphorylation state of RPA32 in *Hus1*$^{-/-}$ cells. This could provide a possible explanation for the loss of RAD51 loading onto the chromatin in *Hus1*$^{-/-}$ cells The phosphatase responsible for dephosphorylating RPA32 is PP4C [269]. Both knockdown of the PP4C and overexpression of phosphor-mimetic RPA32 mutant results in disruption of the RAD51 nuclear foci after DNA damage [269]. Hence, our data converge with previous reports suggesting that a hyper phosphorylated state of RPA32 inhibits RAD51 loading to the chromatin in *Hus1*$^{-/-}$ cells. Alternatively, in a possible, albeit yet to be tested explanation, widespread RPA phosphorylation after MMC treatment in *Hus1*-deficient cells could result from cellular catastrophe following unrepaired extensive DNA damage.

The Taniguchi group with Tomida et al set out to test the relationship between ATR function and the activation of the FA pathway. Canonically, ATR activates checkpoint signaling through phosphorylation of one of its targets, CHK1. The authors propose that ATR has a second independent path of activation which is specific to the FA pathway and targets FANCI, the important molecular switch FA protein. They propose a manner of FANCI phosphorylation that is independent of canonical,

RAD17/9-1-1 mediated ATR checkpoint function, providing a niche for possible, ATR-independent 9-1-1 scaffolding [270]. Other groups show that loss of RAD9A and RAD17 results not only in decreased survival in response to ICL inducing agents but also in impaired monoubiquitination of FANCD2 [271]. In their 2008 study, Meier et al found that *mrt-1*and the 9-1-1 complex may function in a common pathway to promote ICL repair, in concordance with our results.

Based on our data that show interaction with various FA core complex proteins and the ID heterodimer, we propose that the 9-1-1 has a PCNA-like regulatory function in governing the FA pathway (Figure 2.13). Chromatin loading of the core complex and the ID dimer is impaired in absence of 9-1-1 suggesting a functional role of the clamp in recruiting the respective complexes to chromatin. HUS1 contains hydrophobic pockets on its outer surface, which are important for interaction with repair proteins. While the *Hus1*-PM4 mutant rescues CHK1 activation, it fails to restore the focus formation of the ID complex, indicating ATR independent function. Co-immunoprecipitation data and LUMIER screening show physical interaction between 9-1-1 and FA proteins. Lastly, HUS1 shows a role in MMC-induced DSB repair through promoting HRR. Taken together, the evidence collected in this and related studies, confirms a role for the 9-1-1 clamp in checkpoint independent repair through mediation of repair proteins, specifically for coordinating events in the FA pathway.

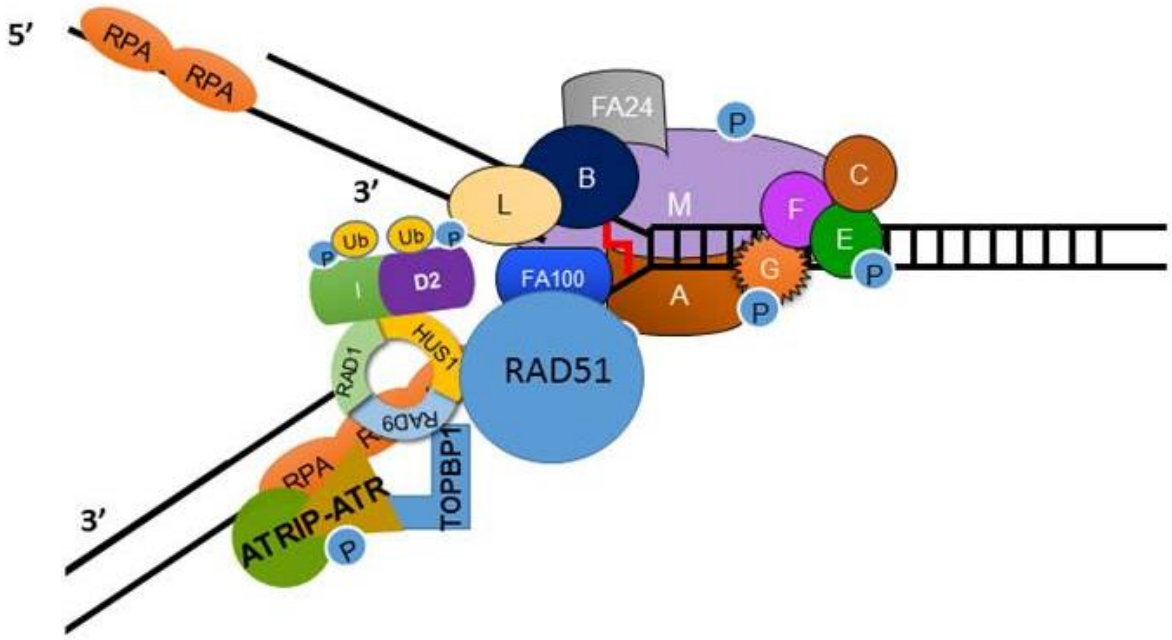

Figure 2.13. Model of how HUS1 coordinates Fanconi Anemia and Homologous Recombination factors in response to ICL-induced DNA damage.

As a scaffolding clamp, 9-1-1 tethers various players in plays allowing interaction and therefore activation of ATR, the core complex, and the localization of HRR protein RAD51.

2.6 Acknowledgement

The Lumier assay in this chapter has been performed by Dr. Georgios Karras. The western blotting assays were carried out by Darshil Patel. The survival assays were performed by Catalina Pereira. The author furthermore thanks Drs. Markus Grompe, John Schimenti, Marcus Smolka, Paula Cohen and Adrian McNairn for reagents and helpful discussions, and members of the Weiss lab for feedback and technical assistance. The Weiss lab extends special appreciation to Dr. Warren Zipfel's laboratory for assistance with UVA/Trioxsalen experiments. This work was supported by NIH grant R01 CA108773 to RSW; funding for DP from NIH training grant T32 GM07273; a NSF predoctoral fellowship to CP; and a National Center for Research Resources grant (S10RR023781) for instrumentation.

CHAPTER 3

HUS1-DEFICIENCY MODIFIES GENOMIC INSTABILITY, GENOTOXIN SENSITIVITY AND LYMPHOCYTE MATURITY IN NHEJ-DEFICIENT MOUSE MODEL

3.1 Abstract

HUS1, a member of the DNA sliding clamp 9-1-1, has a well-established role in canonical activation of the ATR checkpoint, which supports safeguarding of the genome. Growing evidence suggests that HUS1 has a role not only in checkpoint activation, but in DNA damage repair as well. HUS1-deficient cells showed no decreased y-H2AX or 53BP1 signal upon MMC treatment, however BRCA1 focus formation was reduced. This is suggestive of a potential regulatory role for HUS1 in HRR. HUS1 has been suggested by others to promote HRR. HRR which is considered the most error free DSB repair pathway, is backed up by the partially redundant C-NHEJ pathway and its subtype A-EJ. Roughly 70% of DSB events are believed to be repaired through the template free ligation process of C-NHEJ, exclusively so outside of S-Phase [272]. In S-Phase however, when a sister chromatid template is available for HRR, both pathways compete with each other for first access to free DSB ends. In order to investigate the role of HUS1 in protection of genome integrity through a putative function in HRR, I generated a mouse model with parallel impairment in HUS1 and C-NHEJ. I hypothesized that synthetic lethal defects in the dual inactivation mouse would affect frequency in birth ratio, survival, health and genotoxin sensitivity; however, the *Prkdc*$^{-/-}$*Hus1*$^{neo/\Delta1}$ was viable. As expected, the *Prkdc*$^{-/-}$*Hus1*$^{neo/\Delta1}$ double mutant mouse had elevated genomic instability measured by micronuclei assay. The double mutant mouse was exquisitely sensitive to MMC compared to wild type and single mutants but when exposed to IR, the *Prkdc*$^{-/-}$ *Hus1*$^{neo/\Delta1}$double mutant and *Prkdc*$^{-/-}$ single mutant mice were similarly sensitive. This is suggestive of a supportive role for HUS1 in HRR. Surprisingly, the *Prkdc*$^{-/-}$*Hus1*$^{neo/\Delta1}$ mice had a prolonged live span in comparison to their *Prkdc*$^{-/-}$ single mutant littermates, suggesting an unexpected rescue of the reduced viability phenotype seen in *Prkdc*$^{-/-}$. Lymphocyte maturity analysis suggested a partial rescue of T-lymphocytes in *Prkdc*$^{-/-}$*Hus1*$^{neo/\Delta1}$ mice and a potential novel role for HUS1 in lymphocyte maturation.

3.2 Introduction

Maintenance of genomic integrity is crucial for survival of all cells. In order to preserve the genome, most cells have an array of defense mechanisms at their disposal, referred to as the DDR. Among the tasks

tackled by the DDR is the sensing and repairing of DNA lesions as well as the regulation of DNA damage checkpoints.

DNA lesions such as DSBs jeopardize the integrity of the genome. If left unrepaired, chromosomal integrity is compromised. If repaired erroneously, the information coded in the DNA can be altered or lost [1]. The cell has various options to repair DSBs, the most common and best understood being two mechanisms: The first is the error-free HRR, in which the sister chromatid is used as a template during S-phase. The second one is the error-prone C-NHEJ pathway in which the broken ends are directly ligated back together, potentially resulting in mutagenesis due to digestion of ill-fitting DSB ends [273]. Individual and simultaneous deactivation of C-NHEJ and HRR disturbs DSB repair and promotes chromosomal aberrations [167]. Unrepaired damage contributes to genomic instability which is the underlying reason for premature aging, cancer and degenerative diseases as reviewed in [1]. To assure correct repair of a DSB, the cells needs to commit to either HRR or NHEJ. The regulation of this process is tightly linked to the cell cycle, which provides the signal of sister chromatid template availability [174]. BRCA1, a tumor suppressor gene has been linked to promotion of HRR as cells deficient for BRCA1 show decreased rates of HRR [274]. 53BP1 is the counter player which protects DSB ends from resection, thus positively regulating C-NHEJ [221]. The phosphorylation of H2AX by PIKKs is one of the first steps in DSB repair, serving as a surrogate marker for DSB detection through immunofluorescence staining [275].

HUS1, alongside of RAD9 and RAD1, is an imperative member of the DNA sliding clamp 9-1-1 [84, 88, 89, 91]. When the cell senses DNA damage, the hetero-trimetric sliding clamp is loaded onto the DNA at the site of damage by its clamp loader RAD17-RFC which consists of RAD17 and four small subunits of the PCNA-loading RFC complex (RFC2-5) [69, 101, 276]. Once loaded, its function in part is to enhance ATR checkpoint activation through interaction with TOPBP1 [70, 71, 277]. Furthermore, 9-1-1 participation has been observed in DNA repair pathways [232, 278], particularly in HRR [109], in NER [121], BER [279], and MMR [122]. In concordance with the described functions of the clamp,

inactivation of *Hus1* results in increased genomic instability and genotoxin sensitivity [95]. *Hus1*-deficiency disrupts the S-phase checkpoint [99].

Loss of components of HRR or C-NHEJ leads to varying degrees of sensitivity to DNA ICL-inducing agents such as MMC [280]. ICLs are toxic lesions which prevent the separation of strands during replication and transcription. In the process of their excision, a DSB forms and requires repair [229]. In absence of proper repair mechanisms, scientists observed the occurrence of radial chromosomes [281]. These cross-shaped structures are believed to be a consequence of improper fusion of broken chromosome arms. Whether they are intermediate arrested stages of proper repair or irresolvable errors as well as the exact mechanisms of ICL repair remain unresolved. Careful dissection of molecular interactions is required, as the DSB pathways HRR and C-NHEJ act partially redundant.

With the rationale of further elucidating the role of HUS1 in HRR and the decision making process between C-NHEJ and HRR, I have designed a dual inactivation mutant in a mouse model, with the goal of reducing the activity of both pathways in parallel. Inactivation of HUS1 in a C-NHEJ-deficient background holds promise to reveal unknown accessory roles of HUS1 in HRR, as well as potential epistatic effects between the pathways. As there is functional overlap of the C-NHEJ and HRR pathways during S-phase the involvement of yet unknown proteins in the pathways could be masked, as one pathway stands in for the other, thus possibly hiding importance and contribution of individual players in simple single mutant assays. I hypothesized that HUS1 is a player in HRR which is masked by the partial pathway redundancy with C-NHEJ.

With *Hus1* being an essential gene, complete inactivation is lethal [95]. To circumvent mid-gestational death as seen in *Hus1* null mice, a hypomorphic (*Hus1*$^{neo/\Delta 1}$) mouse was created for *in vivo* studies. This mouse combines a null allele, containing an excised first exon, with a partial expression allele, containing a neo cassette. The mouse is grossly normal, but displays increased genomic instability [110] and increased sensitivity to MMC treatment [115].

To explore the role of HUS1 in the repair of DSBs, I combined the *Hus1* defect with defects in C-NHEJ in mice. The C-NHEJ pathway consists of a number of proteins, beginning with KU70 and KU80, which

form the KU complex. KU, after detecting and binding free DSB ends [282], proceeds to bind DNA-PKcs to form the kinase active DNA-PK complex [283]. In selecting the candidate for impairment from the C-NHEJ pathway, I was considering upstream players to achieve sufficient inactivation of C-NHEJ. However, KU70 and KU80 have roles that are independent of DSB repair such as in regulation of expression [284]. Selecting one of the KU proteins as an inactivation partner for HUS1 could therefore result in additional phenotypes, which could be unrelated to DSB repair. Knocking out DNA-PKcs (*Prkdc*) on the other hand has no known roles outside of DSB repair and its deletion sufficiently disables the C-NHEJ pathway. Deficiency or reduction of DNA-PK in mice results in increased IR sensitivity and impaired V(D)J, the latter manifesting in severe immunodeficiency [197, 285, 286]. An important read out of C-NHEJ proficiency is provided by analyzing V(D)J recombination in lymphocytes. As lymphocytes mature, they undergo a tightly controlled process that involves rearrangement as well as initiation of expression of antigen receptor genes (Fig. 3.1). Absence of CD4 and CD8 surface markers (double negative (DN) cells), marks an early stage of T-cell development in which rearrangement at the TCRβ locus begins. Only cells that successfully rearrange the TCRβ locus, proceed to the CD4+ and CD8+ or double positive (DP) intermediate stage or pre-T stage. Next, the TCRα chain is assembled. With expression of successfully rearranged TCRα chains as well, thymocytes progress into either CD4+ or CD8+ single positive (SP) stage, thus becoming fully mature and ready for migration into peripheral lymphoid organs [287] (Fig. 3.2).

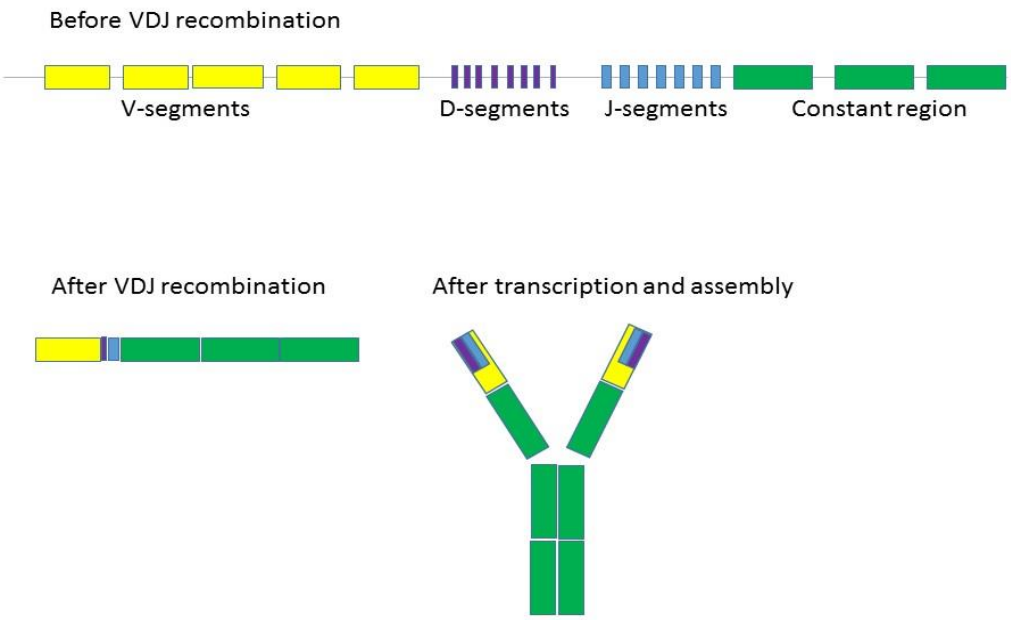

Figure 3.1. Somatic V(D)J recombination accounts for antigen variability in T-Cell receptors. Gene segments are cut and rearranged at the junction of two distinct segments, then ligated using C-NHEJ. Newly arranged segments code for T-cell receptors expressed on the surface of the cell.

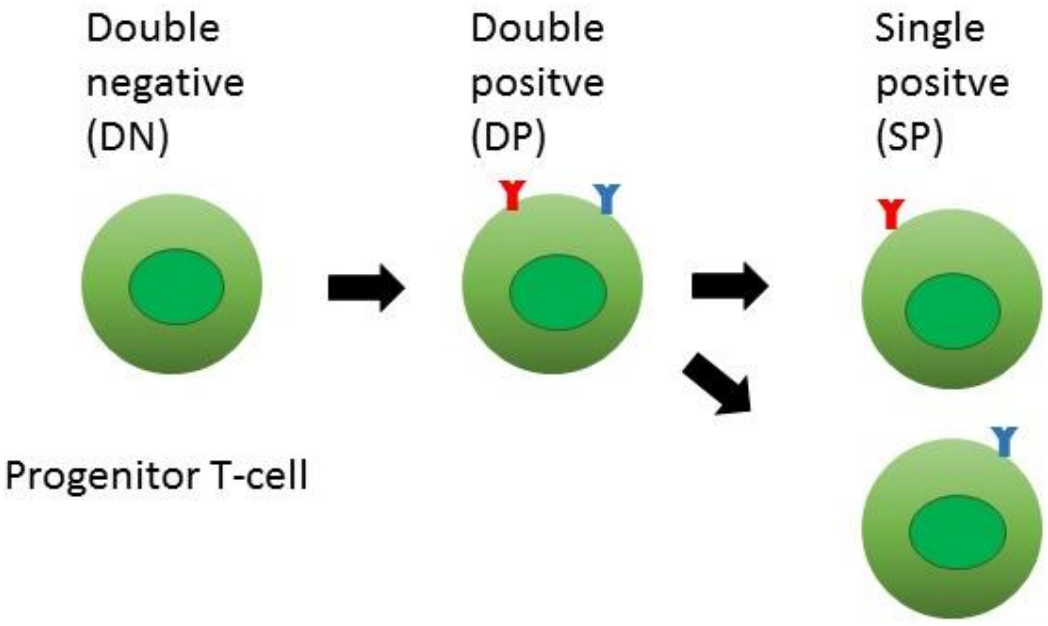

Figure 3.2. Maturation stages of T-Cells.

T-cells acquire CD4 and CD8 receptors in the intermediate stage of maturation. After successfully recombining TCR, cells commit to either CD4+ or CD8+ lineage.

After selection of the candidate proteins for dual inactivation I proceeded with creating a mouse which is null for *Prkdc* and partially deficient for *Hus1* (*Hus1*$^{neo/\Delta 1}$). I proposed that this mouse is sufficiently impaired for C-NHEJ, as well as impaired for HUS1. Since HUS1 has been proposed to act in DSB repair via HRR [109], simultaneous disabling of the alternative repair mechanism C-NHEJ is likely to result in synthetic effects stemming from defects in overlapping functions of DSB repair. Accumulating damage from unrepaired DSBs can result in catastrophic cellular events and consequently apoptosis. The synthetic effects of cellular or organismal death could possibly manifesting in early aging, tumor proneness, genomic instability or genotoxin sensitivity. The *Rad54*$^{-/-}$*LigIV*$^{-/-}$ dual inactivation conducted by Mills et al. is an example of dual impairment of HRR and C-NHEJ resulting in unmasking of new functions of HRR accessory proteins in C-NHEJ-deficient background as well as demonstrating a partial overlap in function DSB repair function of the pathways [224].

In a similar fashion, dual impairment of DNA-PK and HUS1 as proposed in this thesis will uncover new roles beyond the already established ones: The 9-1-1 clamp member HUS1 is known to promote end resection and to suppress A-EJ [123], thus through dual impairment of *Hus1* and *Prkdc*, we will gain insight into the fine tuning of the regulation between C-NHEJ, A-EJ and HRR.

3.3 Materials and Methods

Cell culture and treatments

MEFs of *Hus1*$^{-/-}$*p21*$^{-/-}$ and *Hus1*$^{+/+}$*p21*$^{-/-}$, *Hus1*$^{-/-}$*p53*$^{-/-}$ and *Hus1*$^{+/-}$ *p53*$^{-/-}$, cells were described before [95]. MEFs were grown in DMEM with 10% BCS cells and 1% Penicillin-Streptomycin, 1% NEA and 1% L-Glutamine. *Hus1*$^{-/-}$*p21*$^{-}$ transfected with mouse pCMV- *Hus1*-R4D+V151Y (PM4) (see chapter 2) were used in BRCA1 immunofluorescence staining. These cells were maintained in medium described above including 1.83 μg/ml puromycin.

Immunofluorescence

Hus1$^{-/-}$ and control MEF cells were seeded on 0.01 % gelatin-coated glass coverslips in 6 well dishes and allowed to attach for 24 hours. Then cells were treated with 10 Gy of IR or 1 μg/ml of MMC at indicated time points. For fixation cells were incubated with 4% PFA for 20 min at RT. Following fixation cells were washed in 1X PBS, then permeablized with 0.5% Triton-X 100 for staining. Cells were then blocked in 3% BSA for 1 hour and incubated in primary antibody solution at a concentration 1:500 overnight. Antibodies used were anti-BRCA1 provided by Dr. Lew Chodosh and 53BP1 purchased from Novus Biologicals. The next day, cells were triple rinsed in 1X PBS and incubated in a 1:1000 dilution of secondary antibody (Alexafluor 488 anti-rabbit or anti-mouse 488) for two hours in the dark. Cells were mounted in 0.05% DAPI containing mounting medium and imaged the same day using a Leica DMRE fluorescence microscope.

γH2AX FACS

Cells were grown in 10 cm dishes with the culturing methods described above. After treatment, cells were rinsed with 1X PBS once, then spun down and resuspended at a density of 1 x 10^6 cells per ml. Cells were then fixed in ice-cold 70% ethanol using about 5 ml per 15 ml conical tube. Cells were spun down and

washed in 3 ml of ice cold 1X TBS with 1 % BSA. After an additional spin, cells were resuspended and incubated in 1X TBS containing 1% BSA and .25% Triton-X 100 for 15 minutes on ice. Cells were then stained in 200 µl of antibody suspension (mouse anti-γH2AX Millipore) at a concentration of 1:500 in TBS containing 1% BSA and 10% goat serum overnight at 4^0 C. The next day, cells were washed once in TBS with 1% BSA then spun again and incubated with 200 µl conjugated anti-mouse Alexa Fluor 488 at a concentration of 1:400 for 30 min in the dark. Cells were then washed and spun again, and then resuspended in PI staining buffer (40mL Tris (pH 7.4), 0.8% NaCl, 21mM MgCl2, 0.05% NP-40 5.6 µg/ml PI, 10% RNAse A). The measurements were performed on a LSRII Flow cytometer using FACS DIVA software. The gates were normalized to the wild type negative control.

Animals

All mice in this study were handled in accordance with federal and institutional guidelines, under a protocol approved by the Cornell University Institutional Animal Care and Use Committee (IACUC). Mice were maintained in a 129S6 background. Crosses were generated using *Prkdc*$^{+/-}$ mice described in [197] and *Hus1*$^{+/\Delta 1}$ and *Hus1*$^{+/neo}$ mice described in [95, 288]. Heterozygote double crosses were set up to obtain the four genotypical groups. The double mutant mouse group form the experimental group and is represented by *Prkdc*$^{-/-}$*Hus1*$^{neo/\Delta 1}$. *Prkdc*$^{-/-}$ respectively *Hus1*$^{neo/\Delta 1}$ mice when heterozygote for the other gene, formed the single mutant control group. All other mice which were either wild type or heterozygote for both genes were placed in the wildtype control group. To obtain experimental and control mice, crosses paired a mouse of either sex with the *Prkdc*$^{+/-}$*Hus1*$^{neo/neo}$ or a *Prkdc*$^{+/-}$*Hus1*$^{+/neo}$ genotype with a mouse of *Prkdc*$^{+/-}$*Hus1*$^{+/\Delta 1}$ genotype. PCR was used to genotype mice from tail snip DNA, then mice in individual groups were counted.

Birth ratio

To test whether *Prkdc*$^{-/-}$*Hus1*$^{neo/\Delta 1}$ double mutant mice are underrepresented in the frequency of births, birth ratios were calculated for 413 mice in 73 litters. The expected Mendelian ratio to produce one *Prkdc*$^{-/-}$ *Hus1*$^{neo/\Delta 1}$ double mutant mouse was 1 in 16 pups. χ^2 with df=3 was calculated to determine the p-value.

Body weights

Mice were aged for 300 days, once per week beginning at weaning. The colony underwent dramatic changes in number of animals due to increased mortality in the groups *Prkdc*$^{-/-}$ and *Prkdc*$^{-/-}$ *Hus1*$^{neo/\Delta 1}$. The weights of the individual genotypical groups were averaged. Mice that fell sick were censored from the study at 20% weight loss (humane endpoint defined in animal user protocol) which accounts for the variability of mean weight for group between weeks 12-30. To test whether there is a statistically significant difference between genotypical groups, mice were analyzed at 10, 20, 30, and 40 weeks both with pooled and separated sexes. Shown is the mean of each group at the respective time point. For age analysis at ten 20, 30, and 40 weeks one-way ANOVA calculation was performed. Mean with SEM is shown. To test statistical significance between respective groups, an unpaired t-test was applied using Bonferroni correction.

***In vivo* survival**

For analysis of survival, 68 *Prkdc*$^{-/-}$ *Hus1*$^{neo/\Delta 1}$ and control mice were aged over the course of 300 days. Mice showing apathetic behavior with hunched body posture and pilorectic fur or when experiencing a body weight loss of 20% were euthanized as indicated on the mouse user protocol.

For *in vivo* MMC genotoxin sensitivity experiments Mice were injected IP with 4 mg/kg of MMC in sterile water which was obtained from the Cornell Small Animal Hospital Pharmacy. 9 *Prkdc*$^{-/-}$ *Hus1*$^{neo/\Delta 1}$ and control mice were monitored for 14 days but euthanized at the sign of clinical disease.

For analysis of radiation sensitivity mice were subjected to 9 Gy of γ-irradiation using a Mark 1 Model 68 137 CS source gamma irradiator. Mice were observed and weighed daily for 14 days and

euthanized when humane endpoint criteria as described above were reached. Survival was graphed in a Kaplan-Meier plot using Prism Graphpad. Statistical significance was calculated using Log-rank (Mantel-Cox) test and p-value correction according to Bonferroni.

Micronuclei assay

The measurement of micronuclei in peripheral blood was carried out as described in [289]. In brief, 6-8 week old *Prkdc*$^{-/-}$ *Hus1*$^{neo/\Delta1}$ and control mice were submitted to mandibular vein blood collection with immediate stabilization of the blood in heparin. Consequently, the samples were fixed in ice cold methanol at -80 °C overnight. The next day, samples were washed in bicarbonate buffer and subsequently stained with FITC-conjugated anti-CD71 antibody (Southern Biotech) for 45 min in the dark. After an additional rinse with bicarbonate buffer cells were stained with propidium iodide (PI) (Sigma-Aldrich) and subjected to FACS using an LSR II. Gating was standardized for accumulation of PI and FITC using FACS Diva software. χ^2 was used to determine statistical significance.

Lymphocyte maturity

Thymus was obtained from 12 week old *Prkdc*$^{-/-}$ *Hus1*$^{neo/\Delta1}$ and control mice. The tissues were kept on ice in RPMI completed medium, the volumes standardized for expected number of lymphocytes. The organs were individually disintegrated by mechanical force using the plunger of a 10 ml syringe and a 70 µm cell strainer size filter. The cell suspension was driven repeatedly through the filter until an even suspension was achieved. The concentration of lymphocytes was measured by using 50 µl of cell suspension in 10ml of 1X PBS in a Coulter counter. Then lymphocytes suspension was aliquoted and briefly spun down. The supernatant was discarded and the pellet resuspended to stain in a mix of the following fluorescent conjugated antibodies: PE FC, CD4, FITC CD8α, APC γδ, and APCCy7 TCRβ (BD). All antibodies were used at a dilution of 1:200 in 1X PBS. FC block was added to all samples at a concentration of 1:200. Single dye stains for compensation control were prepared using 0.5 µl of each dye, 0.5 µl of FC block and 100 µl of lymphocyte suspension. Counting was performed using a LSR II and FACS Diva software.

3.4 Results

3.4.1 9-1-1 coordinates recruitment of DSB repair associated proteins to the site of damage

First, to test for appropriate cell cycle arrest and damage recognition in *Hus1*-deficient cells, I tested γH2AX signaling and measured DNA content in cells treated with MMC using FACS. DNA content profiles measured by PI intensity showed profiles reminiscent of normal cell cycle transitions of cells, for both *Hus1*-deficient and *Hus1*-expressing cells. Next, after treatment with MMC for 24 hours, both *Hus1*-deficient and *Hus1*-expressing cells accumulated in the G2/M gate, indicating damage-induced cell cycle arrest. In the untreated groups *Hus1*-deficient or *Hus1*-espressing cells 33% respectively 23% of cells were in G2/M gate. After treatment 58.4 % of *Hus1*-deficient and 65.4 % of *Hus1*-espressing cells accumulated in G2/M. Similar numbers of γH2AX positive cells were detected when comparing untreated *Hus1*-deficient (2%) and *Hus1*-espressing cells (0.5%) to each other. After treatment those rates increased in both *Hus1*-deficient (58%) and *Hus1*-espressing cells (50.3%) (Fig. 3.3). This indicates that cells are proficient in detection of MMC-induced damage and G2/M arrest.

HUS1 has been implicated in HRR in cultured cells transfected with reporter plasmids [109]. To investigate functional interactions between 9-1-1 and BRCA1, I performed immunofluorescence staining using anti-BRCA1 antibody post MMC treatment (Fig 3.4). BRCA1 foci formed readily in cells expressing wild type HUS1 protein. In *Hus1*-deficient cells, the formation of BRCA1 foci was reduced after MMC treatment. When expressing surface altered mutant PM4- *Hus1* (see chapter 2) (Fig. 3.5), cells showed an intermediate amount of foci. After IR treatment, the formation of BRCA1 foci was greatly augmented in *Hus1*-deficient cells, but not in wild type cells (Fig. 3.4

To test whether HUS1 presence affects the upstream DSB repair regulator protein 53BP1, I carried out immunofluorescence staining in cells expressing wildtype and *Hus1*-deficient cells. There was no observable difference between the number of 53BP1 foci positive cells, wild type, mutant expressing or *Hus1*-deficient cells. This suggests a role for HUS1 in the regulation of repair proteins recruited to damage sites, which is regulated outside of 53BP1 (Fig. 3.6).

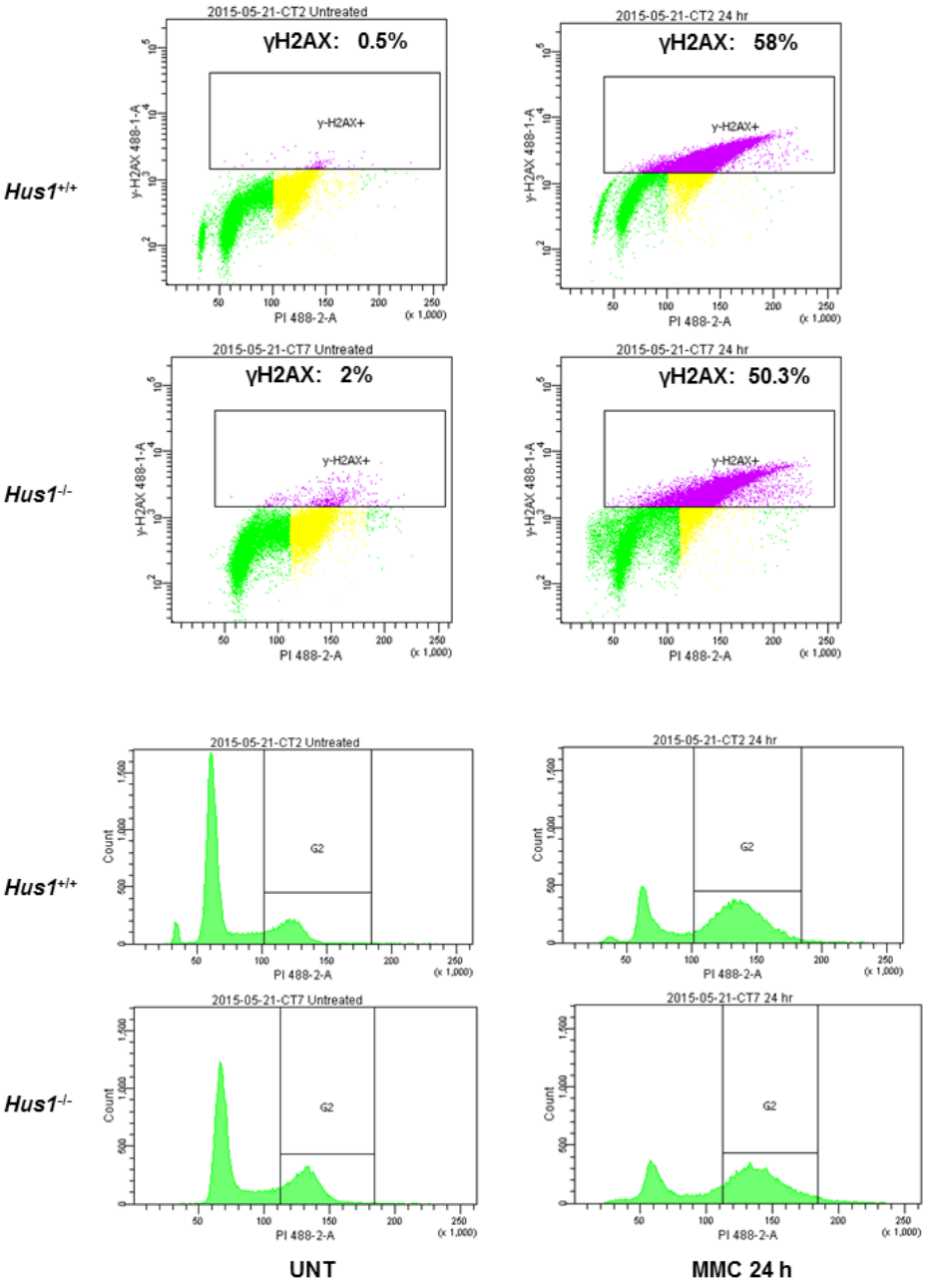

Figure 3.3. γH2AX staining reveals intact MMC-induced damage recognition and G2/M arrest in *Hus1*-deficient cells. MEFs were treated with MMC for 24 hours or mock treated. Staining for FITC-conjugated γH2AX and PI was performed followed by FACS.

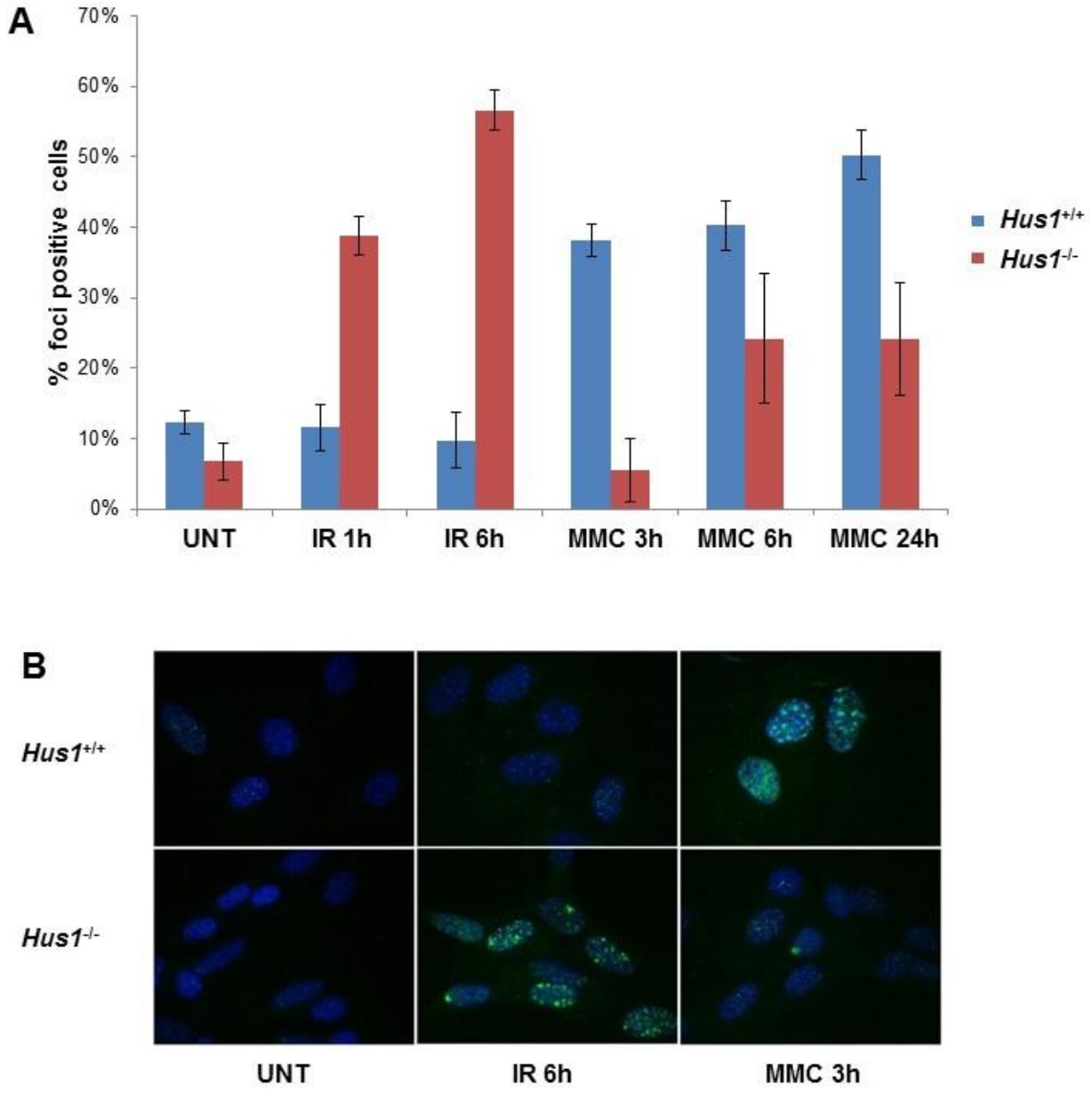

Figure 3.4. HUS1 deficiency promotes BRCA1 focus formation after IR treatment but not after MMC treatment. A and B. Immunofluorescence staining. Parental MEFs were genotoxin treated for indicated periods of time. IF staining against mouse BRCA1 was performed. 50 cells per condition counted, mean of positive cells per 40 X optical field with SEM is shown.

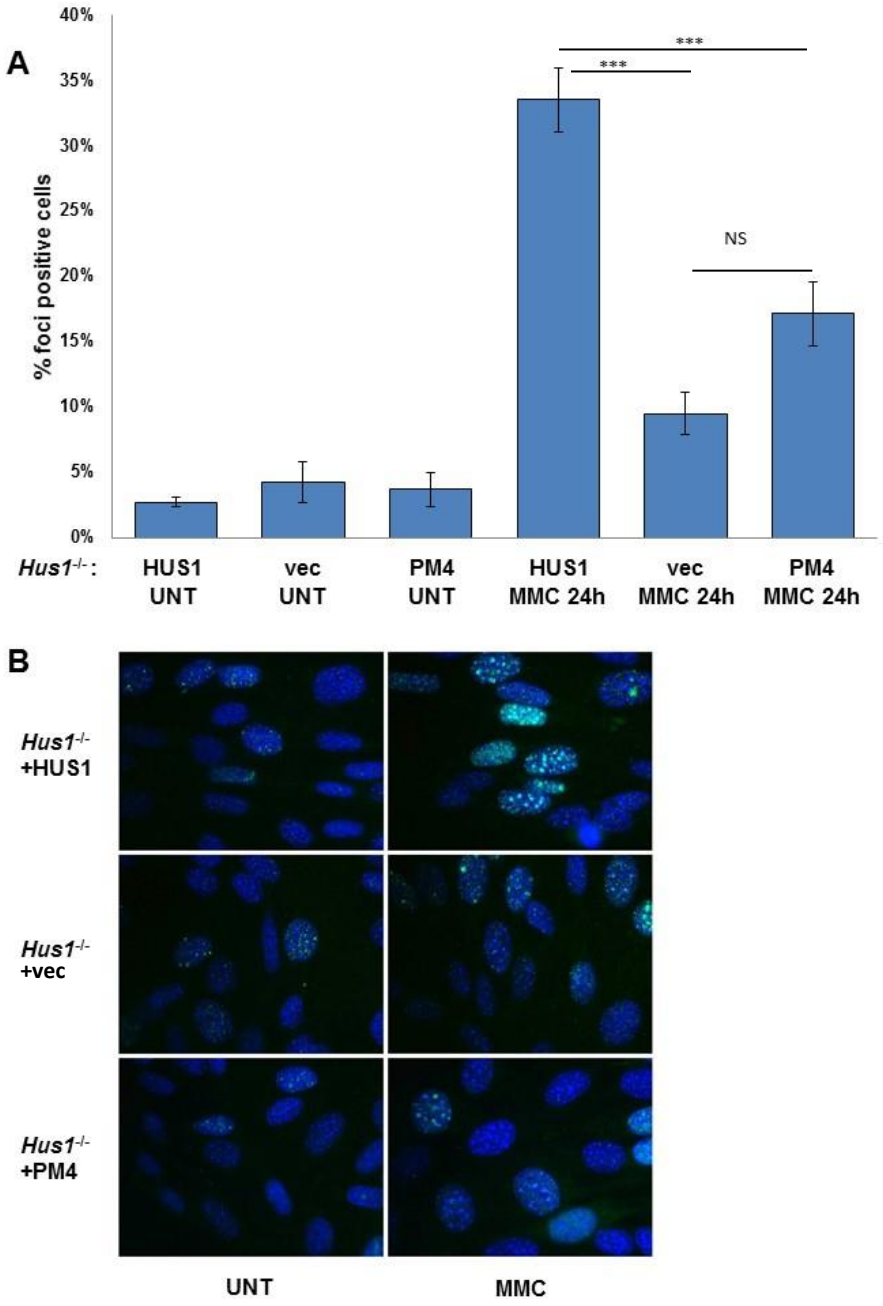

Figure 3.5. HUS1 promotes BRCA1 focus formation after MMC treatment but not after IR treatment. A and B. Immunofluorescence staining. *Hus*$^{-/-}$ MEFs complemented with wild type *Hus1*, PM4-*Hus1* or vector were treated with 1 μg/ml of MMC for 24h. IF staining against mouse BRCA1 was performed. 50 cells per condition counted, mean of positive cells per 40X optical field with SEM is shown.

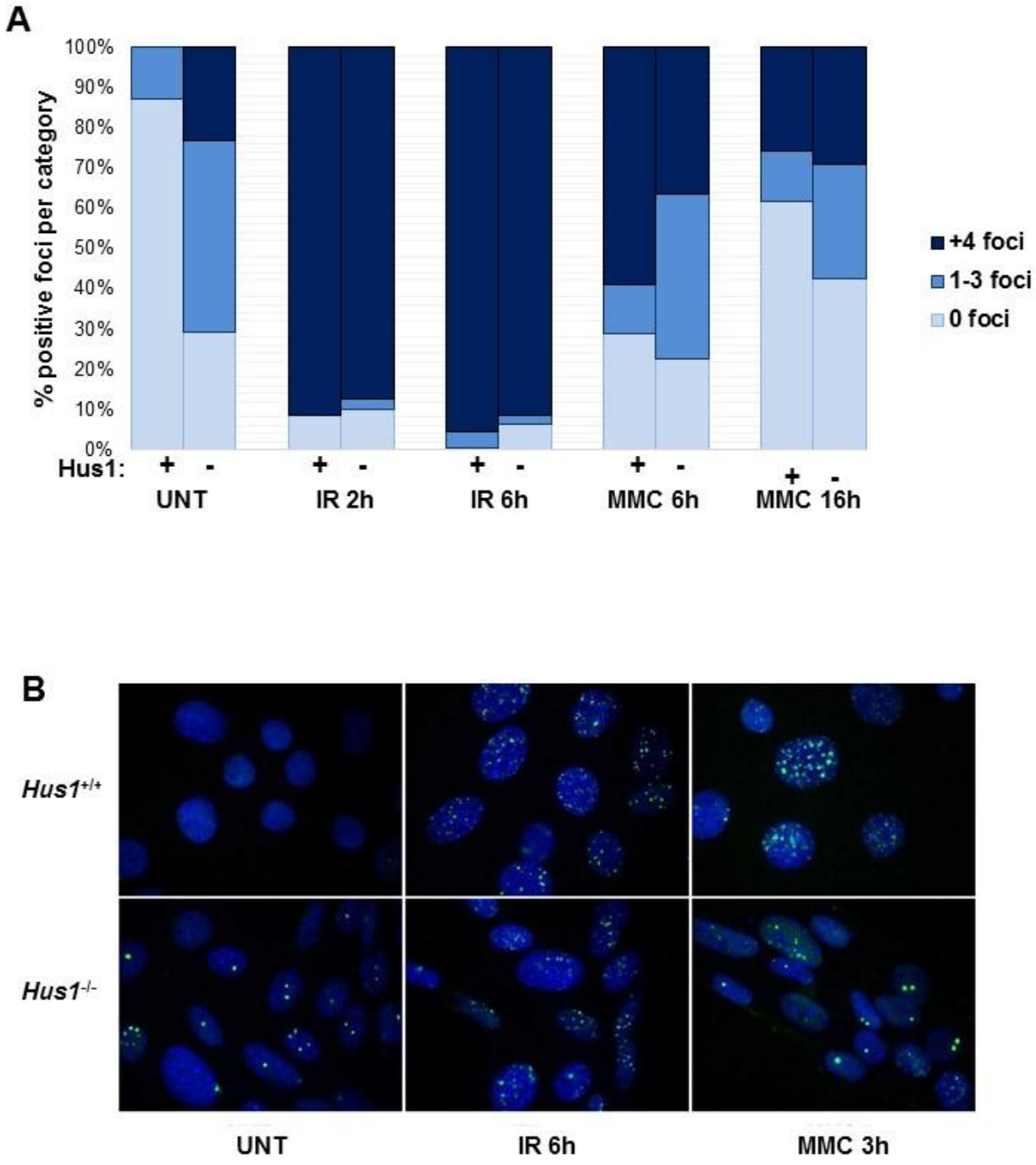

Figure 3.6. HUS1 deficiency promotes 53BP1 focus formation after IR treatment but not after MMC treatment. A and B. Immunofluorescence staining. Parental MEFs were genotoxin treated for indicated periods of time. IF staining against mouse 53BP1 was performed. 50 cells per condition counted, mean of positive cells per 40 X optical field with SEM is shown.

3.4.2 Partial *Hus1*-deficiency extends lifespan in *Prkdc*$^{-/-}$ mice

During embryonic development, cells undergo rapid proliferation, requiring protection from replication stress. Cells with elevated rates of replication stress may succumb to the consequences of genomic instability. This can result in altered morphology, small size or non-viable embryos. *Hus1*-deficiency confers spontaneous genomic instability in mice and cultures cells due to its known role in ATR checkpoint signaling and proposed roles in HRR. DNA-PK (*Prkdc*) is a member of the C-NHEJ pathway which is required for the repair of DSBs, often resulting from unabated replication stress. The simultaneous impairment of HUS1 and DNA-PK was predicted to pose a heavy burden on the genomic integrity of the developing mouse embryo. We hypothesized that the *Hus1*-deficiency in a C-NHEJ impaired background would result in synthetic lethal effects in mouse embryos on either a cellular or organismal level.

We selected *Prkdc*$^{-/-}$ as the C-NHEJ impaired background mice, as the more upstream players of DNA-PK, KU70 and KU80 have independent roles outside of C-NHEJ and confer a too dramatic phenotype when deleted [188, 290]. Synthetic-like interactions could be revealed by crossing mutant mice of these two pathways. *Hus1*$^{-/-}$ mice are embryonic lethal, thus we employed the *Hus1* allelic series to generate a *Prkdc*$^{-/-}$*Hus1*$^{neo/\Delta1}$ mouse.

We predicted that given the high necessity for intact DNA repair pathways during the phase of increased proliferation, the *Prkdc*$^{-/-}$*Hus1*$^{neo/\Delta1}$ double mutant mouse would be synthetic lethal. To test this hypothesis, we generated 413 mice and calculated the Mendelian ratio of the frequency for four defined genotypic group. To obtain *Prkdc*$^{-/-}$*Hus1*$^{neo/\Delta1}$ we crossed either *Prkdc*$^{+/-}$*Hus1*$^{neo/neo}$ or *Prkdc*$^{+/-}$*Hus1*$^{+/neo}$ mice to *Prkdc*$^{+/-}$*Hus1*$^{+/\Delta1}$ mice. The experimental group was defined as *Prkdc*$^{-/-}$*Hus1*$^{neo/\Delta1}$. *Prkdc*$^{+/+}$*Hus1*$^{neo/\Delta1}$ and *Prkdc*$^{+/-}$*Hus1*$^{neo/\Delta1}$ were considered the *Hus1* partially deficient single mutants. *Prkdc*$^{-/-}$*Hus1*$^{+/+}$, *Prkdc*$^{-/-}$*Hus1*$^{+/\Delta1}$ and *Prkdc*$^{-/-}$*Hus1*$^{+/neo/}$ mice formed the *Prkdc* single mutant group. All other mice were considered wild type controls. Out of 413 mice 38 *Prkdc*$^{-/-}$*Hus1*$^{neo/\Delta1}$ double mutants were born while 33.4 were expected. The result of χ^2 test equaled 0.96 at df=11 and p-value > 0.99. Therefore, there is no difference between the observed and expected ratio of events (Table. 3).

Table 3. Frequency of *Prkdc*$^{-/-}$*Hus1*$^{neo/\Delta1}$ offspring follows expected Mendelian ratios [a].

Prkdc	*Hus1*	Observed #	Exptected #
+/+	+/+	20	18.19
	+/neo	35	33.44
	+/Δ1	19	18.19
	neo/Δ1	41	33.44
+/-	+/+	32	36.38
	+/neo	67	66.88
	+/Δ1	35	36.38
	neo/Δ1	61	66.88
-/-	+/+	16	18.19
	+/neo	33	33.44
	+/Δ1	16	18.19
	neo/Δ1	38	33.44

[a] Mice were genotyped using PCR analysis at 3 weeks of age using DNA from tail tissue. Expected values represent the combined Mendelian ratios from crosses with different parental genotypes. The observed and expected genotype frequencies are not significantly different (p-value > 0.99 in χ^2 test).

To observe the mice for overt physical anomalies, mice were compared for body weight from weaning until 300 days of age. To test whether the *Prkdc*$^{-/-}$*Hus1*$^{neo/\Delta1}$ double mutant mice presented an altered size phenotype such as observed in *Atm*$^{-/-}$*Hus1*$^{neo/neo}$ [113] 68 mice were weighed weekly for the course of 300 days. The prediction for the *Prkdc*$^{-/-}$*Hus1*$^{neo/\Delta1}$ double mutant mice was for the group to be on average lighter than *Prkdc* single mutant mice, outweighed by *Hus1*$^{neo/\Delta1}$ and those in return outweighed by wild type group mice. (Figure 3.7A). As the mice aged, the number of animals enrolled in each group varied due to unexpected deaths. To test whether there was a difference between genotype groups at specific times, mice were analyzed at ten, twenty, thirty, and forty weeks post weaning. While at twenty, thirty, and forty weeks *Prkdc* single mutants and *Prkdc*$^{-/-}$*Hus1*$^{neo/\Delta1}$ double mutants were slightly lighter than wild types, *Prkdc*$^{-/-}$*Hus1*$^{neo/\Delta1}$ double mutant mice were only slightly lighter than *Prkdc* null mice. The differences were not statistically significant (ANOVA) (Figure 3.7B)

As the renewal of tissues requires intact replication cycles, early aging, increased mortality or tumor burden can be a sign of increased genomic instability. As we observed unexpected deaths of mice in the groups of *Prkdc*$^{-/-}$*Hus1*$^{neo/\Delta1}$ double mutant and *Prkdc* single mutant mice, we sought to determine if there were differences in mortality rates and mean survival between the groups. Physical examination and necropsy of mice suggested general inflammation of the gastro-intestinal tract as the cause of death, with no observable changes in histopathological examinations (visual inspection on the microscope). To test whether the *Prkdc*$^{-/-}$*Hus1*$^{neo/\Delta1}$ double mutant mice had an altered longevity, mice of the four genotypical groups were observed over the course of 300 days. The days from birth until the death of each mouse were quantified. (Figure 3.8). If a mouse reached humane endpoint criteria it was euthanized and counted as an event of death. While mice from both the wild type group or *Hus1*$^{neo/\Delta1}$ group died over the time course of 300 days, the *Prkdc* single mutant mice showed clinical signs of disease or died between the 80th and 220th day of the study with a median survival of 162 days and five mice alive at the end of the study. Contrary, the *Prkdc*$^{-/-}$*Hus1*$^{neo/\Delta1}$ double mutant mice showed a statistically significant extension in life span. The mice in this group died between days 180-290 of the study, with a median survival of 285 days and 8 mice alive at the end of the study.

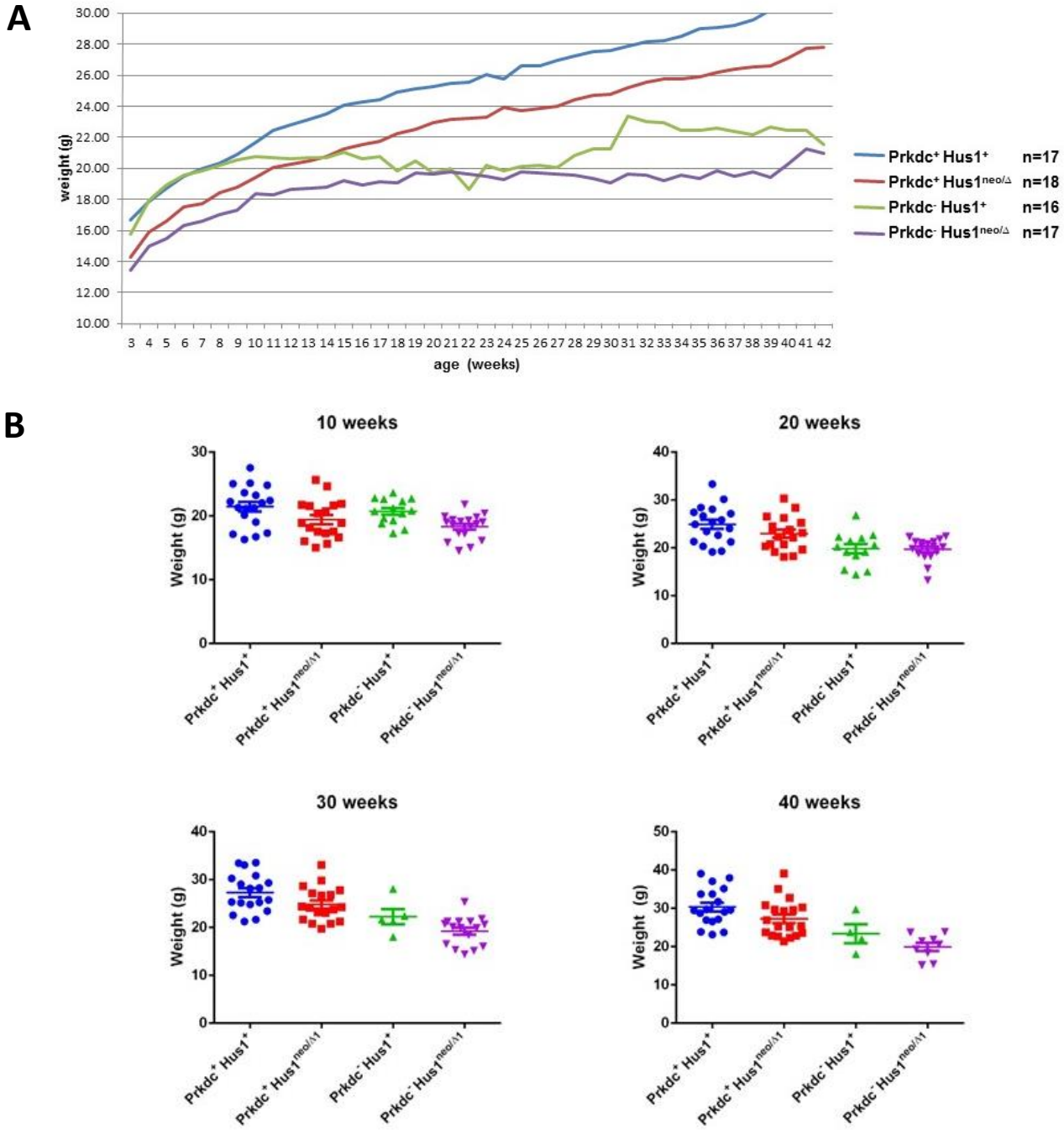

Figure 3.7. Body mass is grossly normal in adult *Prkdc*$^{-/-}$ *Hus1*$^{neo/\Delta 1}$ mice. **A.** 68 mice were weighed for 300 days weekly. Means are shown. **B.** Data from A was analyzed for indicated time points post weaning. Differences are not statistically significant (1-way Anova).

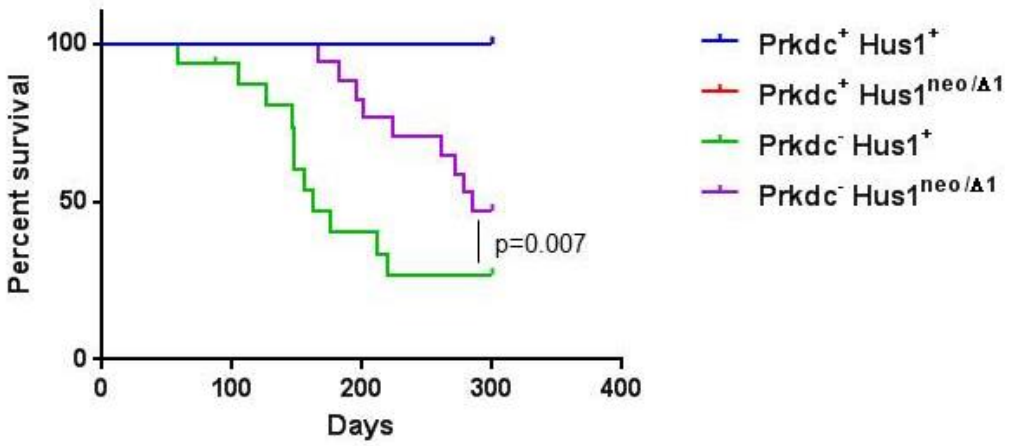

Figure 3.8. Body mass is grossly normal in adult *Prkdc*$^{-/-}$ *Hus1*$^{neo/\Delta1}$ mice. 68 mice were observed for 300 days. Mean survival shown. Differences not statistically significant by Gehan-Breslow-Wilcoxon test. P-value= 0.0072.

In an attempt to explain the surprising rescue of survival in the *Prkdc*$^{-/-}$*Hus1*$^{neo/\Delta1}$ double mutant group, we collected organs from all four genotype groups and weighed each organ as well as the whole mouse. The weights of the organs were calculated as percentage of each respective mouse and averaged to allow for comparison. Organs collected for measurement were liver, spleen, brain, kidneys, seminal vesical, and testes. As seen in figure 3.9 there was no difference between the organ weights among the genotype group, indicating grossly normal organ development. The livers were the exception with a 4% body mass for wild type and *Hus1*$^{neo/\Delta1}$ while *Prkdc*$^{-/-}$*Hus1*$^{neo/\Delta1}$ had a slight increased average liver weight (6%) and the *Prkdc*$^{-/-}$ single mutants had a reduced average liver mass at 1% body mass. However, the number of surviving animals in the groups *Prkdc*$^{-/-}$*Hus1*$^{neo/\Delta1}$ and *Prkdc*$^{-/-}$ was too small (n=3) to determine statistical significance. To better identify trends an earlier endpoint would be helpful.

3.4.3 *Hus1*-deficiency in a *Prkdc* background increases spontaneous genomic instability

To test whether there are differences among the genotype groups in regard to genomic instability, 8-12 week old mice were utilized for micronuclei (MN) assay. In this assay, erythrocytes obtained from peripheral blood are sorted by presence of CD71 reticulocyte markers and by DNA content. Maturing erythrocytes normally shed both the nucleus and CD71. Only if prior to expulsion of the nucleus DNA content was fragmented due to genomic instability, residual DNA in form of MN marked by PI staining can be detected in CD71 negative (mature) erythrocytes [289]. For measuring of MN the mice were bled, followed by PI and maturity marker staining of the red blood cells. *Hus1*$^{neo/\Delta1}$ mice were reported to have a percentage of micronuclei (0.37% ± 0.09%) [110]. Micronuclei data for *Prkdc*$^{-/-}$ have not been previously reported. In this study as well, *Hus1*$^{neo/\Delta1}$ showed elevated MN at a mean of (0.38% ± 0.04%). Interestingly, this was surpassed by the count of MN in the *Prkdc*$^{-/-}$*Hus1*$^{neo/\Delta1}$ double mutant group at (0.50% ± 0.03%). The increase of MN in the double mutants exceeded the sum of the MN count from the single mutant groups suggesting increased genomic instability in the *Prkdc*$^{-/-}$*Hus1*$^{neo/\Delta1}$ double mutant mice, likely stemming from synergistic effects from dual inactivation of *Hus1* and C-NHEJ (Fig. 3.10). The differences between groups were statistically significant as determined by single factor ANOVA (p-

value =3.58^{-12}). Pairwise comparison between *Hus1*$^{neo/\Delta1}$ and *Prkdc*$^{-/-}$*Hus1*$^{neo/\Delta1}$ confirmed the difference with p-value= 0.006 in two sample t-test.

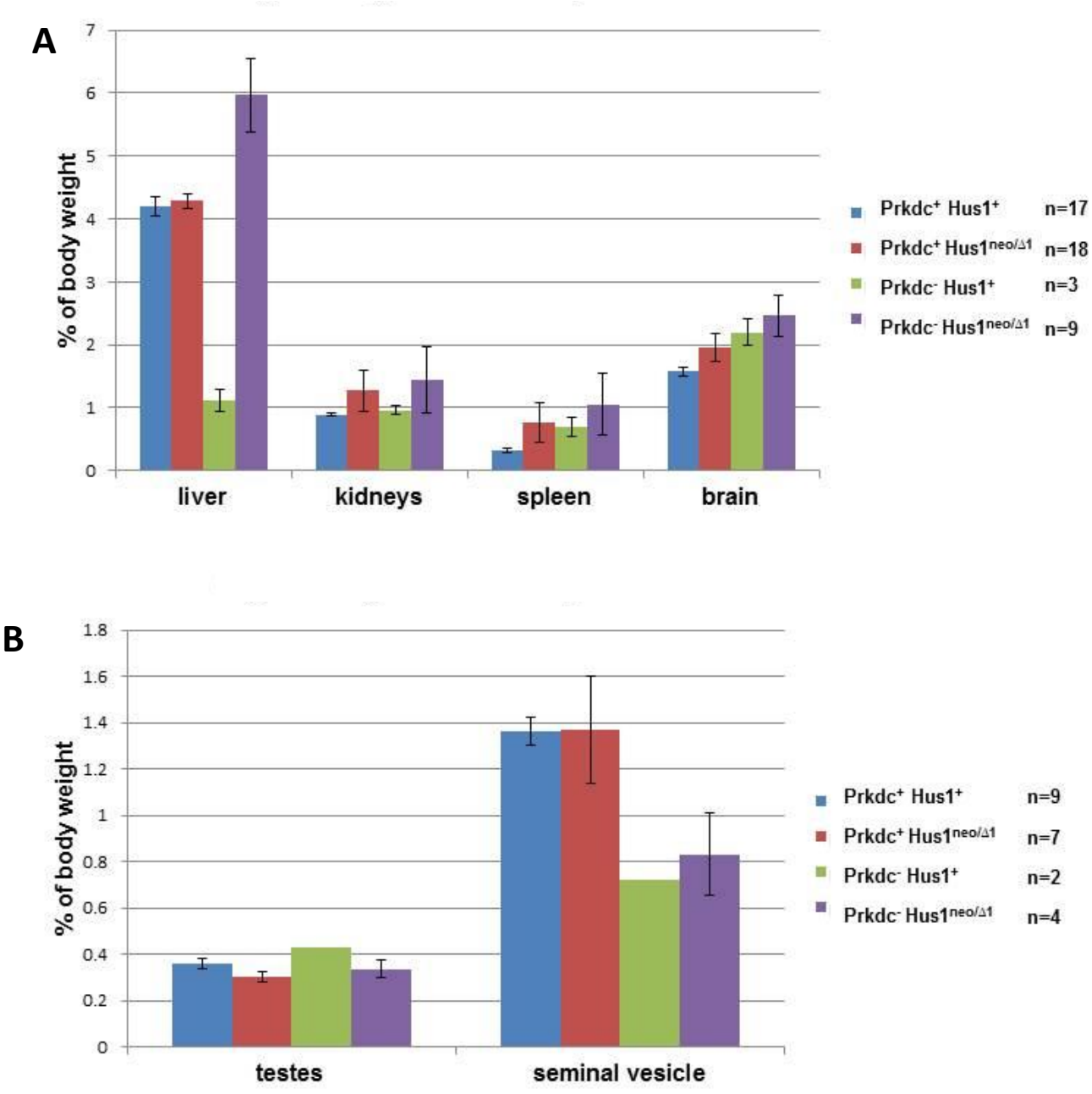

Figure 3.9. HUS1-deficiency does not affect gross organ weight in aging *Prkdc*$^{-/-}$ mice. A and B Organ weights. Organs were obtained from surviving 300 days old mice. Organs were weighed at sacrifice and presented as mean with SEM. The differences were not statistically significant (1-way Anova run for groups larger than n=3).

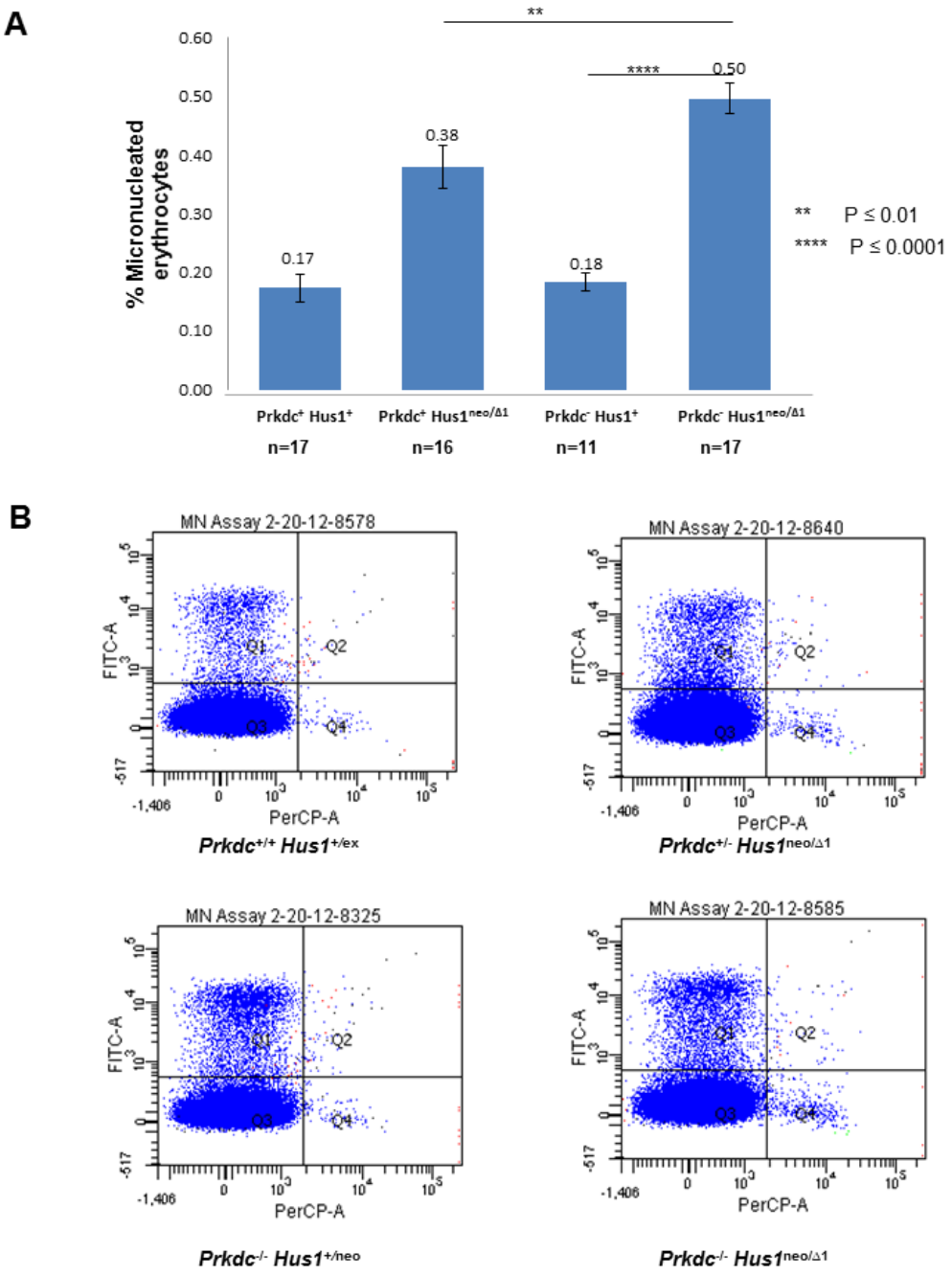

Figure 3.10. MN assay reveals elevated rates of genomic instability in *Prkdc*$^{-/-}$ *Hus1*$^{neo/\Delta1}$ mice. A and B. 6-8 weeks old mice were bled for MN assay. Staining for FITC-conjugated CD71 and PI was performed followed by FACS.

3.4.4 *Hus1*-deficiency and *Prkdc*-deficiency synergistically increase sensitivity to genotoxin treatment related DNA damage

Hus1$^{neo/\Delta 1}$ mice and control mice have been reported to display insignificant differences in sensitivity to IR at a dose of 9 Gy [115]. MEFs of *Prkdc*$^{-/-}$ genotype have displayed increased IR sensitivity [197, 285]. *Prkdc*^{SCID} mice (no data for *Prkdc*$^{-/-}$ mice whole body irradiation was available), which harbor a truncation mutation in *Prkdc*, are exquisitely sensitive to IR [291]. In order to test their genotoxin sensitivity, *Prkdc*$^{-/-}$*Hus1*$^{neo/\Delta 1}$ double mutant mice were treated with 9 Gy of full body exposure of ionizing radiation. Both weight loss in percent and survival were monitored. At that dose, there was no difference detectable between *Prkdc*$^{-/-}$*Hus1*$^{neo/\Delta 1}$ double mutant and *Prkdc*$^{-/-}$single mutant mice. Both these groups were however substantially more sensitive to IR than either *Hus1*$^{neo/\Delta 1}$ single mutant or wild type control mice, with no animal surviving the treatment (Fig. 3.11). This means that a regulatory role for HUS1 in repair of IR-induced DSB is less likely.

Hus1$^{neo/\Delta 1}$ mice were reported to have increased sensitivity towards MMC in comparison to wild type littermates [115]. *Prkdc*$^{-/-}$ MEFs showed no difference in MMC sensitivity when compared to control MEFs [292]. To compare MMC to IR sensitivity in *Prkdc*$^{-/-}$*Hus1*$^{neo/\Delta 1}$ double mutant mice 8-12 weeks old mice were injected with 4 mg/kg of MMC. Preliminary data suggest that *Prkdc*$^{-/-}$*Hus1*$^{neo/\Delta 1}$ double mutant are drastically more sensitive to MMC than their *Prkdc*$^{-/-}$, *Hus1*$^{neo/\Delta 1}$ and control mice. In two independent experiments, the *Prkdc*$^{-/-}$*Hus1*$^{neo/\Delta 1}$ double mutant mice died between days 4-6 (Fig. 3.12). The single mutant and control groups did not have losses due to treatment, however *Hus1*$^{neo/\Delta 1}$ showed weight loss as previously reported [115]. Repeat experiments are required as the sample size does not allow appropriate interpretation. If sensitivity of *Prkdc*$^{-/-}$, *Hus1*$^{neo/\Delta 1}$ mice was indeed higher than that of the single mutant controls it would suggest a cooperation between HUS1 and DNA-PK in repair of ICL-induced DSBs.

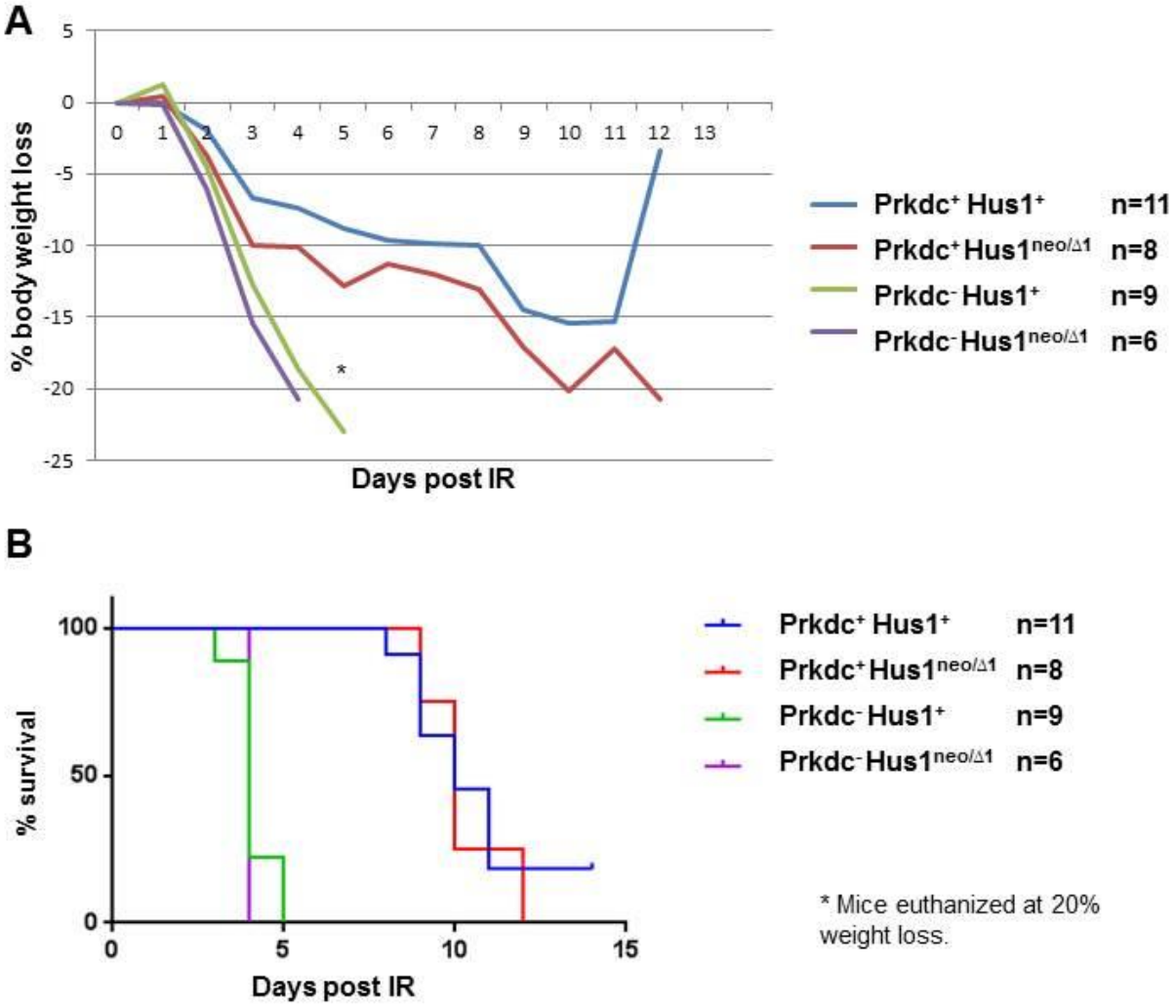

Figure 3.11. HUS1-deficiency modulates genotoxin sensitivity in *Prkdc*$^{-/-}$ mice. A. Weight loss analysis. Mice of indicated genotypes at age of 8-12 weeks were exposed to 9Gy full body irradiation. Weights were recorded daily and % of original weight calculated. Mice were euthanized when humane end criteria were reached. **B.** Kaplan-Meyer Survival plot. Mice from A were counted when found dead or when end criteria were reached.

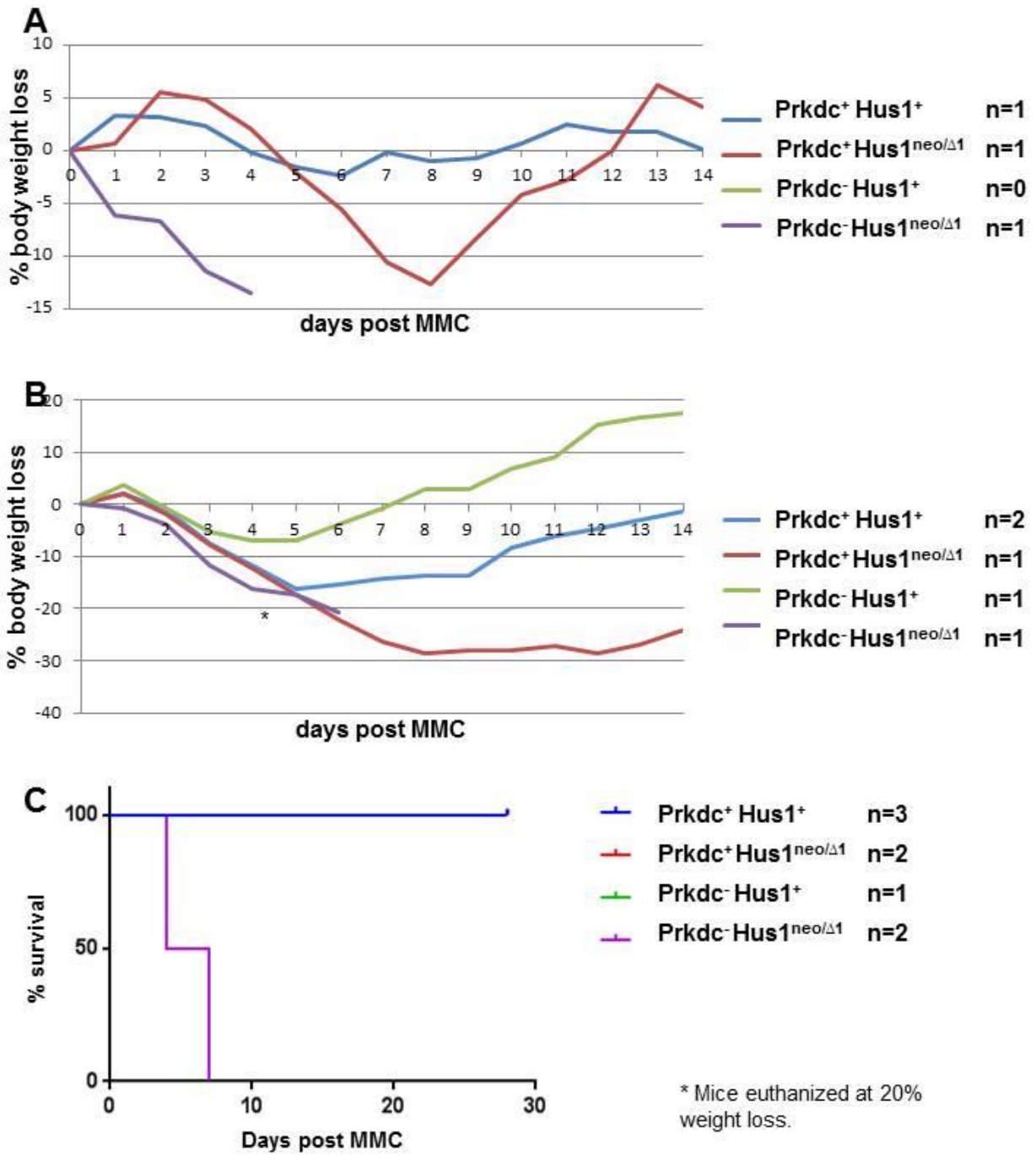

Figure 3.12. HUS1 deficiency modulates genotoxin sensitivity in *Prkdc*$^{-/-}$ mice. A. Weight loss analysis. Mice of indicated genotypes at age of 8-12 weeks old mice were injected with 4 mg/kg MMC in DMSO sc. or **B** in H2O ip. Weights were recorded daily and % of original weight calculated. Mice were euthanized when humane end criteria were reached. **C.** Kaplan-Meier Survival plot. Mice from A and B were counted when found dead or when end criteria were reached. Means are shown. The sample size was too low for statistical analysis.

3.4.5 HUS1-deficiency modulates lymphocyte maturity in Prkdc$^{-/-}$ mice

To test C-NHEJ proficiency via V(D)J recombination we analyzed mouse lymphocytes obtained from peripheral and central lymphatic organs can be grouped into stages of maturity analyzed. Briefly, single positive (SP) CD8 or CD4 represent mature immune-competent stages, double positive (DP) cells (CD8+, CD4+) are transitioning through the process of maturation and double negative (DN) cells are immature. *Prkdc*$^{-/-}$ have been reported to harbor no mature thymocytes at an age of up to 6 weeks as V(D)J recombination is required for TCR expression [197, 285]. To test C-NHEJ proficiency in my model, I analyzed lymphocyte maturity in *Prkdc*$^{-/-}$*Hus1*$^{neo/\Delta 1}$ and control groups (Fig. 3.13A). In the thymus, which is the primary site of T-cell development in the mouse, mostly immature and maturating stages of T-cells are expected. The preliminary results indicate, that the wild type control and *Hus1*$^{neo/\Delta 1}$ groups showed normal T-cell maturation (Fig. 3.13B): The DN stage was represented with 1-2% cells of the total population, the majority of cells was undergoing rearrangement in the DP group. SP cells were present at a normal CD4+ to CD8+ ratio of about 2, before migrating into peripheral organs. In our hands, *Prkdc*$^{-/-}$ single mutant mice reproduced the drastic phenotype seen by Gao et al. and Taccioli et al. [197, 285]. Thymocytes from both *Prkdc*$^{-/-}$ and *Prkdc*$^{-/-}$*Hus1*$^{neo/\Delta 1}$ animals displayed an accumulation of cells at the DN stage, however with striking differences in distribution between the *Prkdc*$^{-/-}$ and the *Prkdc*$^{-/-}$*Hus1*$^{neo/\Delta 1}$ double mutant. In the *Prkdc*$^{-/-}$ single mutant, the DN population made up 28.8% of the thymocytes and the DP harbored 57% of thymocytes. Neither mature stage was highly populated (2.8 and 3.9 % respectively). This indicates that the cells have struggled rearranging their TCRαβ resulting in halted progression at the immature stage. The number of cells that progressed into the CD4+ stage was reduced. Numbers of cells that progressed into the CD8+ stage were elevated likely to quality control detainment in the thymus. In the *Prkdc*$^{-/-}$*Hus1*$^{neo/\Delta 1}$ double mutant the DN stage makes up 34% of thymocytes, which is even further increased than in the *Prkdc* single mutant. The DP intermediate stage is surprisingly depleted at only 2.3% (83% in controls). This can mean that a portion of cells must proceed into the SP stage. Even though a greater portion of the cells (in comparison to the *Prkdc* single mutant) proceeds into the SP stage, further differentiation stages are at an abnormal ratio. Both CD4+ and CD8+ cells are drastically

elevated, likely due to reduced migration. To further analyze the DN population and to detect whether *Prkdc*$^{-/-}$*Hus1*$^{neo/\Delta1}$ manage to rescue early chain rearrangement events, TCRαβ positive cell were gated from the DN population. While TCRαβ staining (marked as TCRβ in figure 3.13C) was detected in the DN populations of control and *Hus1* hypomorph mice, the *Prkdc*$^{-/-}$ single mutant showed no presence of TCRαβ. Surprisingly, low levels of TCRαβ were restored in the *Prkdc*$^{-/-}$*Hus1*$^{neo/\Delta1}$ double mutant. A rescue in rearrangement of TCRαβ in *Prkdc*$^{-/-}$*Hus1*$^{neo/\Delta1}$ could provide an explanation for rescued survival in this group. The experiment described here was performed one time with two *Prkdc*$^{-/-}$*Hus1*$^{neo/\Delta1}$ mice (one mouse is shown, the other own showed indentical patterns) and one respective control mouse, thus requiring repeated experiments.

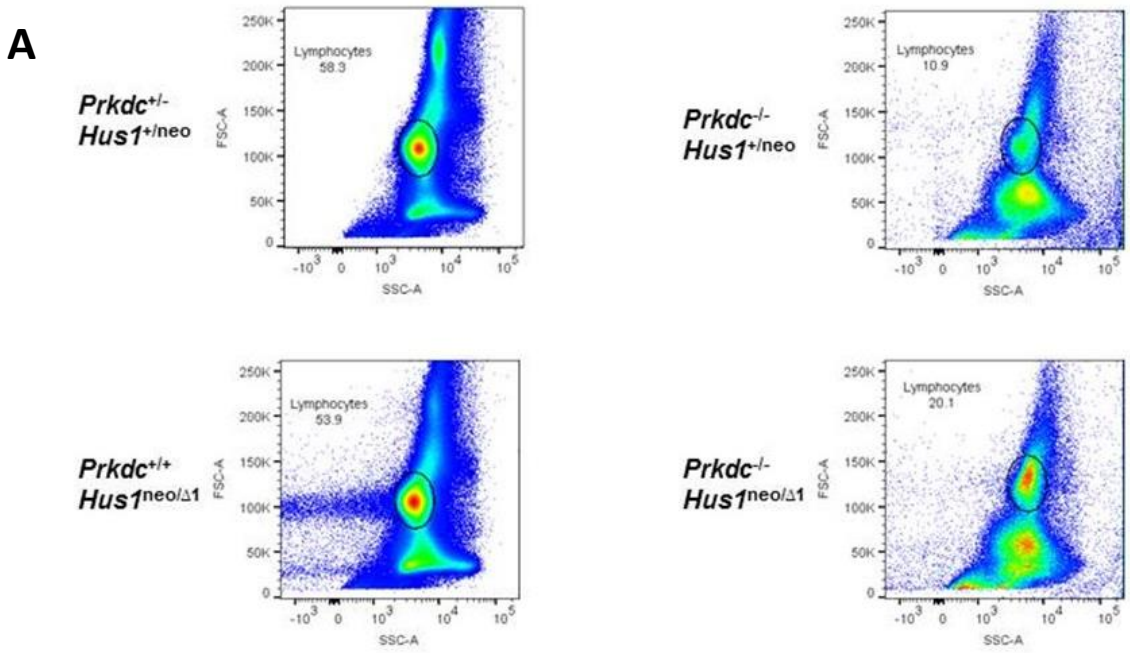

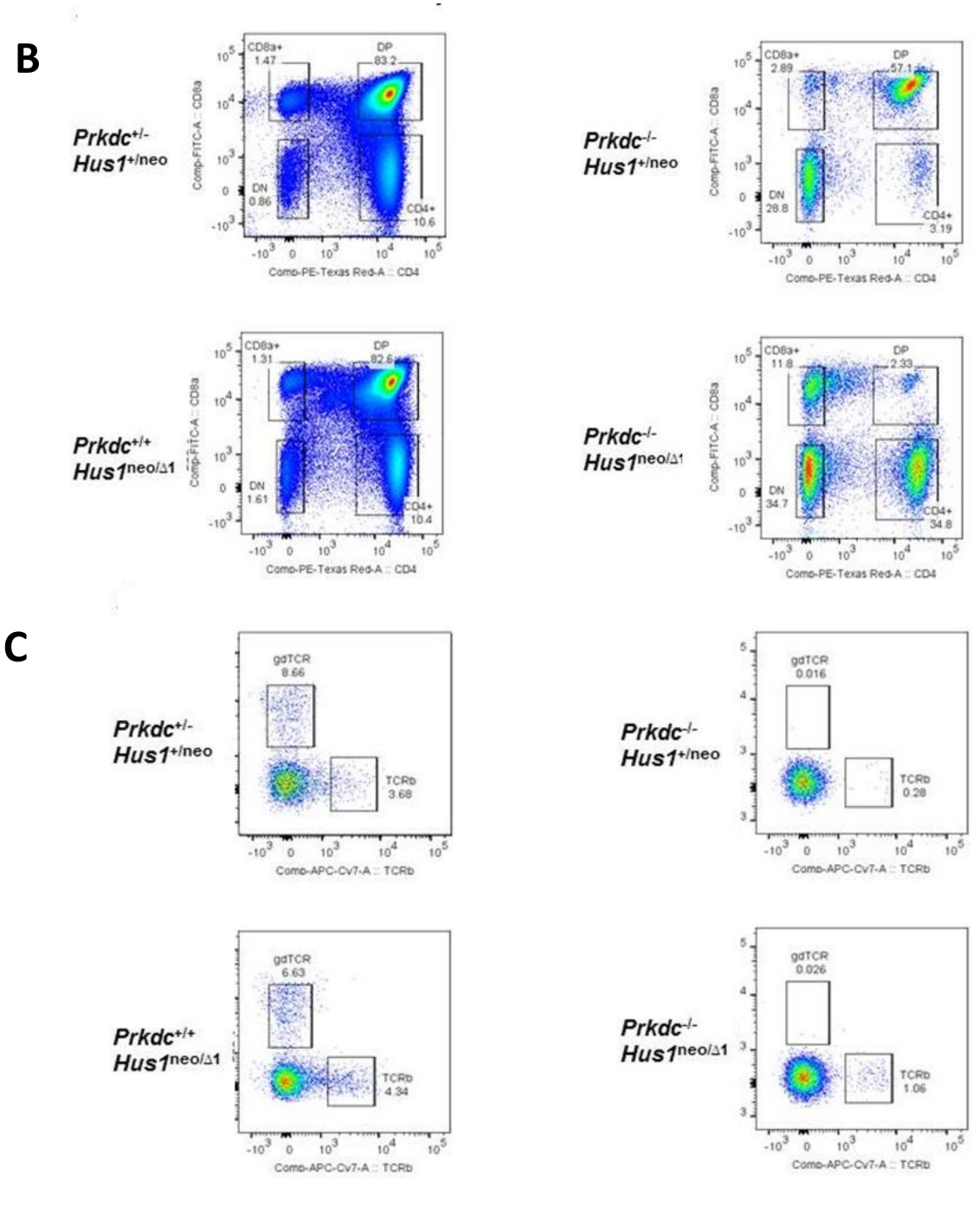

Figure 3.13. HUS1-deficiency modulates lymphocyte maturity in *Prkdc*$^{-/-}$ mice. A, B and C Thymus was obtained from 8-12 weeks old mice. Fluorescence-conjugated specific maturity markers CD4, CD8, TCRαβ and TCRγδ were used for FACS sorting. Genotypes and populations shown as indicated. This work was supported by Dr. Avery August and Nicholas Koylass. **A**. Overal population sorted by size. **B** CD4 by CD8 from within T-cell population. **C**. TCRαβ and TCRγδ from within DN population.

3.5 Discussion

In times of heightened proliferation such as during development, cells react particularly sensitive DNA damage resulting in replication stress. 9-1-1 is required for ATR- checkpoint activation [99] and has been proposed to carry out independent roles in DSB repair [109, 138]. I predicted dual inactivation of *Hus1* and *Prkdc* to increase genomic instability in mice to an extent that would overburden remaining repair mechanisms and therefore result in synthetic lethality of *Prkdc*$^{-/-}$*Hus1*$^{neo/\Delta1}$ embryos. However, *Prkdc*$^{-/-}$ *Hus1*$^{neo/\Delta1}$ double mutant mice were born at expected Mendelian ratios and were grossly normal, suggesting the presence of compensatory mechanisms. This however does not mean that the predicted synthetic interactions do not exist. There are chances that moderate effects exist which would be exacerbated by appropriate challenges.

A standard approach to characterize C-NHEJ proficiency in mutants of this and related pathways is the measurement of lymphocyte maturity. Lymphocytes, originating in the bone marrow and thymus undergo a maturation process in which they rearrange their DNA at specific DNA loci. The recombination of the TCRβ and TCRα gene loci while transitioning through maturation marker stages, is well documented [293]. Immature cells begin as CD4- and CD8- (DN). Then, with successful rearrangement at the TCRβ locus they express CD4+ and CD8+ surface markers (DP), later committing to just one of the two lines (SP). The expression of mature T-cell receptors requires V(D)J recombination, a process of cutting and recombining gene fragments at the T-cell receptor recognition site. This process requires C-NHEJ, thus conferring an immune deficiency phenotype to C-NHEJ impaired mice. In a so far unrepeated experiment, *Prkdc* null mice showed expected maturation defects in thymocytes, while the *Prkdc*$^{-/-}$*Hus1*$^{neo/\Delta1}$ double mutant mouse achieved generation of low levels of lymphocytes with TCRαβ expression.

Until this study, no role for HUS1 has been described in regard to lymphocyte maturation. Yet, in this study HUS1 reduction seems to positively affect survival and lymphocyte maturation in *Prkdc*$^{-/-}$ mice. The question emerges, as to why an organism would benefit from additional HUS1 reduction when already harboring a defect in C-NHEJ. The answer may lie in a possible regulatory role for 9-1-1 in the

decision making process between C-NHEJ, A-EJ and HRR. Wang et al. reported that *Hus1*-deficency reduces HRR rate, but not C-NHEJ rate [109]. Furthermore, Pandita et al. described a role for RAD9 in repair of DSBs through HRR [138]. 9-1-1 plays a role in promoting end-resection through stimulation of SGS1, DNA and EXO1 while at the same time suppressing A-EJ [123, 128]. In V(D)J recombination, A-EJ can step in the place of C-NHEJ for the rejoining steps in conditions when A-EJ is not suppressed [294]. As 9-1-1 has been shown to also suppress A-EJ, it is possible that in *Prkdc*-deficient thymocytes, the loci completely fail to rearrange: They cannot use neither C-NHEJ as it is disabled, nor A-EJ as it is suppressed (Figure 3.14). In this scenario, reduction of HUS1 could allow the cells to apply A-EJ for a make-shift rearrangement at the TCRαβ loci. This partial rescue could restore basic levels of adaptive immunity allowing for prolonged survival. Further repeats are required to confirm these results.

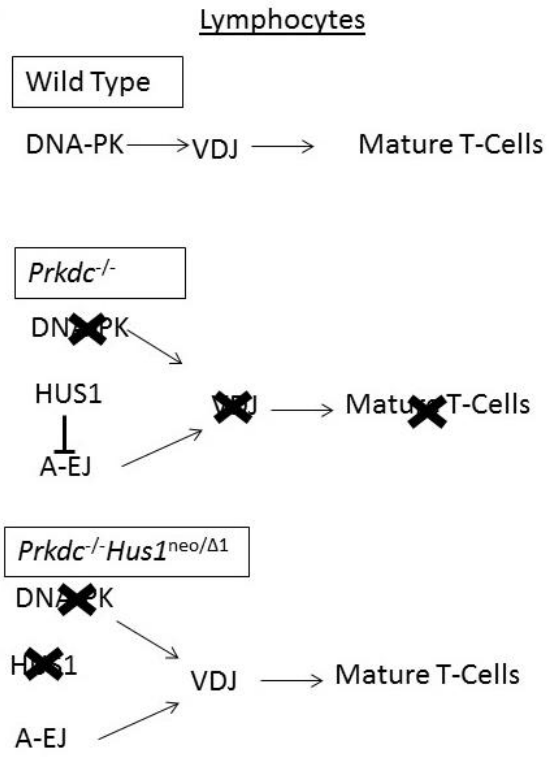

Figure 3.14. Model of compensatory A-EJ recombination in T-Cells in absence of HUS1. In wildtype mice, T-cells recombine their receptors using C-NHEJ and DNA-PK. In *Prkdc*$^{-/-}$ mice this pathway is inhibited. The back-up pathway using A-EJ is suppressed when HUS1 is active, thus impairing T-cell maturation. In the absence of HUS1, A-EJ provides partial rescue.

Whether this phenomenon can be observed in non-lymphatic cells as well, would require reporter plasmids for A-EJ, C-NHEJ and HRR to be used in *Prkdc*$^{-/-}$*Hus1*$^{neo/\Delta 1}$ and control MEFs. Sequencing of the respective receptor generating regions in the genome would allow to identify which joining process has been employed by the cells to generate the receptor region and whether the rearrangement and rejoining quality is sufficient for restoration of function.

Inside of lymphocyte maturation DSBs are introduced to enhance variability and during meiosis to assure accurate chromosome segregation. These are tightly controlled processes that manage to channel initiation of DSBs for the cell's advantage. Outside of these two processes, DSBs are usually toxic to genome integrity and require immediate and accurate repair. The astounding possible role of HUS1 in lymphocyte maturation might reverberate in unplanned DSB repair regulation scenarios.

Prkdc$^{-/-}$*Hus1*$^{neo/\Delta 1}$ double mutant mice display strong IR sensitivity on par with *Prkdc*$^{-/-}$ single mutants in comparison to *Hus1*$^{neo/\Delta 1}$ and normal controls. A preliminary interpretation would suggest that in regard to IR-induced DSB repair, the two proteins act independently, with both *Prkdc*-deficient groups succumbing to the burden of unrepaired DSBs. As IR-induced DSBs challenge the cell regardless of stage in cell cycle, the majority of the repair burden lies on C-NHEJ. It is possible, that at lower doses, *Prkdc*$^{-/-}$ *Hus1*$^{neo/\Delta 1}$ double mutant could be more sensitive than *Prkdc*$^{-/-}$ single mutant mice. This would reveal a partial overlap of roles for 9-1-1 and DNA-PK providing further evidence for a role of HUS1 in HRR.

A role for HUS1 in DSB repair is however more likely in the context of MMC-induced damage (fig 3.15). Preliminary data suggest that *Prkdc*$^{-/-}$*Hus1*$^{neo/\Delta 1}$ double mutant mice sensitivity to MMC is severely aggravated, supporting a strong role for HUS1 in MMC-induced ICL resolution. If dual inactivation of *Hus1* and *Prkdc* resulted in higher sensitivity to MMC-induced damage than partial inactivation of *Hus1* alone, then epistasis-like interactions could be involved. It would be crucial to carefully measure differences in sensitivity, in order to identify synergistic versus additive effects. If the sensitivity in *Prkdc*$^{-/-}$*Hus1*$^{neo/\Delta 1}$ double mutant mice was more than the combined sensitivity of the single mutant, then synergistic interaction would be likely, suggesting a cooperation of HUS1 and DNA-PK in the response to MMC-induced damage. To understand which exact role HUS1 plays in the coordination

of repair effort after MMC exposure, an analysis of HRR, NHEJ and ICL repair efficiency should be conducted, with the use of reporter plasmids as one possible way. If all repair mechanisms are impaired in *Hus1*-deficient cells, then a hypothesis of HUS1 within 9-1-1 acting as a molecular scaffold coordinating and regulating the repair of complex lesions becomes more likely. A comparison with the $Atm^{-/-}$ $Hus1^{neo/\Delta 1}$ mouse allows for interesting conclusions. ATM as one of the major DDR PIKK kinases, is an early sensor of DNA damage, including DSBs occurring from MMC damage [295]. ATM can function upstream from DNA-PK [296] and thus a dual inactivation of $Prkdc^{-/-}Hus1^{neo/\Delta 1}$ could be expected to show similar synergistic effects in response to MMC treatment as the $Atm^{-/-}$ $Hus1^{neo/\Delta 1}$ in regards to post-ICL DSBs. However, the lesions resulting from MMC are diverse and complex: Simple DSBs resulting from ICL excision form only a fraction of the lesions, bulky mono-adducts and ICLs can result in fork stalling, complex replication structures and fork collapse in the worst case [297, 298]. For these challenging and versatile lesions, a well-organized scaffolding structure might be required. Both dual inactivation models suggest that HUS1 as a member of 9-1-1 could be a central player in the coordination of high complexity repair jobs.

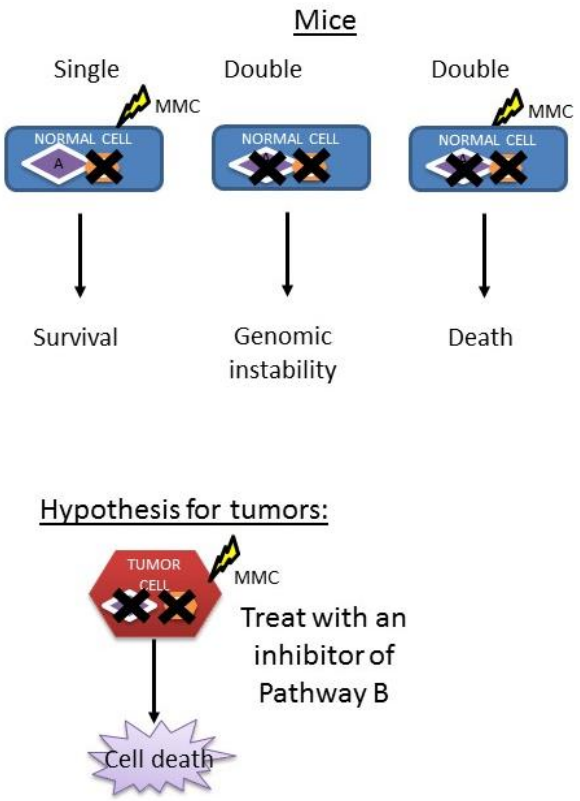

Figure 3.15. Model of genotoxin sensitivity caused by absence of HUS1 in a *Prkdc* null background. In cells with redundant DDR pathways, genotoxin challenge can be tolerated. Dual inactivation of related pathways causes increased genomic instability. When dual inactivation is combined with genotoxin challenge, viability is compromised. Similarly, selective toxicity in tumor cells harboring DDR defects can be achieved by combining DDR inhibitor treatment with genotoxin challenge.

I hypothesized that the 9-1-1 clamp member HUS1 plays a central role in coordinating DSBs and post-ICL DSBs. In the present study I described a possible cooperative role with DNA-PK in response to MMC treatment *in vivo* and a potential new role in life span reduction of immunosuppressed *Prkdc*$^{-/-}$ mice. Taken together, the *Prkdc*$^{-/-}$*Hus1*$^{neo/\Delta 1}$ double mutant mouse displays promise as a synthetic lethality drug cancer model as well as a tool in uncovering additional roles for HUS1 in lymphocyte maturation.

3.6 Acknowledgments

Dr. Pei Xin Lim and Tim Pierpont and Robert Weiss assisted with *in vivo* genotoxin treatment presented in this chapter. Dr. Pei Xin Lim and Dorian LaTocha assisted with FACS experiments. Dr. Avery August enabled and Nicholas Koylass assisted with the lymphocyte FACS experiment.

CHAPTER 4

SUMMARY AND FUTURE DIRECTIONS

4.1. Significance of DNA Damage Response research.

The role of 9-1-1, a heterotrimeric DNA sliding clamp composed of RAD9, HUS1 and RAD1, has been well established in the context of checkpoint signaling. However, it has been implied to harbor, functions going beyond that of an ATR activator alone: 9-1-1 functions as a regulatory platform in NER and BER pathways, where it interacts with multiple factors in a typical scaffolding manner and has been shown to enhance function of the pathways [121, 132, 299]. While 9-1-1 has been implied in ICL repair through an ICL repair-based proteomic screen [124] and in DSB repair through HRR reporter assays [109, 138], its molecular modus operandi remains in the dark. Attempts to elucidate the role of HUS1 in various repair pathways has proven difficult as 9-1-1 members, in fact, all major elements of the ATR pathway are essential genes. Knocking out *Hus1* results in early embryonic death in mice. MEFs made from embryos display cell cycle arrest and genomic instability [95]. One way to still study the role of *Hus1*-deficiency in live animals has been achieved through the generation of an allelic series: When combing a partial expressing $Hus1^{neo}$ allele with a null allele ($Hus1^{\Delta 1}$) mice are viable, while only marginal levels of HUS1 protein expression are detectable. This hypomorph mouse model and the *Hus1* null MEFs generated by simultaneous disabling of *p21* provide invaluable tools in discovering molecular interactions of HUS1 and DDR pathways [95, 288].

The interplay between DDR pathways has been well studied in the context of cancer therapy. As tumors often acquire mutations in DDR genes, hijacking and altering of these genes for purposes of their own proliferation, scientists began discovering the true potential in DDR research. Improving the general understanding of DDR genes such as HUS1 provides potential candidates in the search for drug targets. Tumors can be addicted or sensitive to the presence of certain DDR genes, which encouraged further research. Famous examples of DDR genes that have been altered are BRCA1/2 and P53, which have already reached a level of recognition among the lay population. Less recognized but promising, is a fairly sophisticated attempt of applying DDR knowledge onto the medical field: The exploitation of synthetic lethality. This concept takes advantage of known sensitivities of tumors that are consequences of shedding certain tumor suppressor functions. Simplified, after disabling one major DDR pathway to

allow for uncontrolled growth, cancer cells more heavily rely on a remaining DDR pathway to repair damage (Figure 3.15). When the remaining DDR pathway is now targeted by an inhibitory drug, the cancer cell is particularly sensitized to exogenous and endogenous damage. Following this approach, multiple DDR inhibitors are currently in pre-clinical or clinical trials, amongst these are DNA-PK, CHK1/CHK2, PARP, ATM, and P53 inhibitors [52-59].

Dual impairment of DDR genes can mimic a situation in which a certain cancer, which already harbors one DDR mutation, is challenged with the inhibition of another. Multiple dual inactivation models generated in our laboratory serve as powerful tools in understanding cellular requirements for 9-1-1 in resistance to genotoxic drugs. In further applications, these synthetic lethal interactions can be reproduced in tumor models harboring DDR defects to proof therapeutic efficacy.

9-1-1 which stands at the hub of multiple DDR pathways could emerge as a future drug target, if its molecular interactions were better understood. As a target in dual impairment models, it has proven to aggravate genotoxin sensitivity and reduce survival, promising signs of therapeutic application. The research described in this dissertation aims at elucidating molecular interactions between 9-1-1 and major repair pathways for later application for the benefits of medicine.

4.2. 9-1-1 modulates the DDR response to MMC-induced ICL lesions

Guided by previous findings describing increased MMC sensitivity in mice partially deficient for *Hus1* [115] we set out to investigate the role of HUS1 in MMC-induced cross link repair. We found a role for HUS1 in the maintenance of chromosomal stability. In *Hus1*-deficient cells, MMC treatment resulted in severe chromosomal aberrations including the formation of radial chromosomes. Radial chromosomes are a hallmark of the genome instability disorder FA, the pathway responsible for ICL resolution. Complementation of *Hus1*-deficient cells with wildtype or surface mutated HUS1 brought about a rescue of the phenotype in the former and partial rescue in the latter, suggesting a possible involvement of further HUS1, RAD9 or RAD1 residues in the prevention of radials. Including *Prkdc*$^{-/-}$*Hus1*$^{neo/\Delta 1}$ MEFs in this study alongside with their respective controls would possibly show, if the defect is indeed mediated

by C-NHEJ or A-EJ, as (DNA-PK) *Prkdc* has no known role in A-EJ. Furthermore, as RAD9 has been implied to partake in the decision making process between HRR and C-NHEJ as a promotor of resection [123], comparable surface mutants could indicate whether the chromosomal protection function is mediated through the checkpoint, the whole clamp or one of its members.

We have shown that 9-1-1 has interacted with multiple FA proteins, both functionally and physically: Functionally, 9-1-1 is required for metaphase radial prevention and MMC resistance. Physically, HUS1 interacts with FANCI, FANCD2 and FANCG in co-IP experiments. As our study was conducted in a mouse model, few reliable antibodies were available for endogenous protein localization and interaction studies. The generation of *Hus1* knockout human cell lines, which is under development in the lab, would allow us to include interaction studies for each single FA core complex protein and unveil a potential role of HUS1 in recruiting or stabilizing the complex. The study of HUS1 in human cells would allow for better predictions regarding cancer sensitizing approaches in *Hus1*-deficient cells in humans. Specifically, FA patients could benefit from this research, as by the nature of their disease, classic cancer drugs such as MMC cannot be used in the treatment of their tumors.

In the processing of the post-ICL DSBs multiple repair proteins, mostly members of the HRR pathway, have been shown to participate in the repair [140]. Our studies identified HUS1 as a major participant in ICL-induced DSB repair. During the process of the repair, RAD51 is required at the fork to stabilize the fork as well as to induce strand invasion after the ICL is excised. We showed that HUS1 is essential for the appropriate loading of RAD51 at the site of the ICL. In absence of HUS1, unrepaired damage continues to signal for activation of kinases. These kinases hyper-phosphorylate RPA, a state that is likely upheld by unrepaired damage delaying RAD51 loading to prevent stray strand invasion. However, some questions remain unanswered: Which kinases phosphorylate RPA at which sites specifically? Which sites on RPA are important for blocking or promoting RAD51 loading? How does HUS1 interject in these processes? Careful site mutagenesis studies will decipher the relationship between RPA phosphorylation sites, the responsible kinases and the regulatory effects on RAD51. An interesting follow up experiment to complement the DNA-PK and ATR inhibitor treatments would be to compare

RAD51 focus formation in regard to the role of HUS1 in a background of ATM-deficiency. A possible involvement of ATM in phosphorylation of RPA in *Hus1*-deficient cells could be tested. A recently emerged kinase, PLK1, which phosphorylates BRCA1 and RAD51, should be considered for interaction with 9-1-1 as well, possibly forming the missing link between HUS1 reduction and loss of RAD51 focus formation.

HRR and C-NHEJ players could be affected by HUS1 in the context of MMC-induced DSB repair. One of the most important regulators of RAD51 is BRCA2. Preliminary data showed a reduction of BRCA1 foci in *Hus1*-deficient cells. As BRCA1 is only an indirect regulator of RAD51, localization and interaction studies between HUS1 and BRCA2 would be most telling. I speculate that HUS1 and BRCA2 interact functionally, perhaps with 9-1-1 yet again taking on the protein scaffolding role.

I proposed that 9-1-1 has a regulatory role in ICL repair. In this study I described defects in ICL repair that were observed in absence of HUS1 in the form of radial chromosomes. I demonstrated co-localization of HUS1 and important ICL repair protein and showed defects in loading of some of these repair proteins onto chromatin. In summary, HUS1 emerged as a novel player in the ICL/DSB repair process. Its molecular fine tuning remains yet to be understood.

4.3. HUS1 modulates MMC sensitivity and lymphocyte maturity in NHEJ-deficient mice

In an attempt to unveil potential synthetic lethal interactions on the one hand and dissection of HRR and C-NHEJ crosstalk on the other hand, I designed a dual inactivation mutant mouse of 9-1-1 and C-NHEJ. The targeted genes of choice were *Hus1* in its hypomorphic manifestation and *Prkdc* as a major C-NHEJ member. Although predictions of synthetic mortality did not hold true, likely due to compensatory mechanisms, the double mutant mouse revealed interesting insight into the molecular crosstalk between 9-1-1 and NHEJ. In genomic instability assays measuring micronuclei formation, *Prkdc*$^{-/-}$*Hus1*$^{neo/\Delta 1}$ mice stood out with elevated levels of MN formation. These resemble a synergistic interaction, indicating that in this context the target proteins operate in independent pathways.

When aged over 300 days, *Prkdc*$^{-/-}$ single and *Prkdc*$^{-/-}$*Hus1*$^{neo/\Delta1}$ double mutant mice displayed increased mortality, with a more severe manifestation in the *Prkdc*$^{-/-}$ single mutant mice. As these mice suffer from immune deficiency, infections with opportunistic pathogens is a likely explanation for increased mortality, as discussed in chapter three. To test this hypothesis, mice could be aged in SPF conditions. Clinical tests to confirm possible infections and immune response in *Prkdc*$^{-/-}$single, *Prkdc*$^{-/-}$*Hus1*$^{neo/\Delta1}$ double mutant and control mice is advisable. To examine whether the reduced viability is due to genetic causes rather than infections, the generation of MEFs would be advantageous. In proliferation assays, early senescence could be revealed.

When challenged with MMC or IR radiation, *Prkdc* $^{-/-}$ *Hus* $^{neo/\Delta1}$ double mutant mice showed an exquisite sensitive reaction, that is more severe than that of the *Hus1*$^{neo/\Delta1}$ mice. While further studies are required, trends indicate that double mutant mice are synthetic lethal when challenged with MMC. In IR, the chosen dose did not allow for a dissection of sensitivity degrees between *Prkdc* single and double mutant mice: All mice in these two groups died within 72 hours of IR exposure, while control mice showed a gradual decline peaking at day 12. Further studies are required using lower doses to identify a potentially altered sensitivity to IR. Dose response tests would provide tolerable dose ranges for IR. Exposure of MEFs from the same four genotypical groups to IR and MMC would also reveal genotoxin sensitivity in quantifiable ways.

A standard approach to characterize C-NHEJ proficiency in mutants of this and related pathways is the measurement of lymphocyte maturity. Lymphocytes undergo a maturation process transitioning from a DN stage to a DP stage, then later shedding one of the CD4 and CD8 surface markers, thus differentiating [300]. The expression of mature T-cell receptors requires V(D)J recombination, which in turn heavily relies on C-NHEJ [301]. Strikingly, while *Prkdc* null mice showed practically no mature lymphocytes, the double mutant mouse achieves to generate low levels of TCRαβ expressing lymphocytes. Further repeats are required to confirm these results. Sequencing of the respective receptor generating regions in the genome would allow identifying which joining process has been employed by the cell to generate the receptor. As discussed in chapter three, HUS1 might be responsible for

suppression of A-EJ in *Prkdc* null mice leaving it with no alternatives to generate rearranged T-cell receptors. When HUS1 is absent, A-EJ is no longer being suppressed, thus partially rescues genetic rearrangement at the TCRαβ loci allowing for residual lymphocyte maturation. Sequencing of the TCRαβ gene loci would answer this question unequivocally. If confirmed by further analyses, this would be the first time a role for HUS1 in lymphocyte maturation is described. To test if this result is observable in lymphocytes only or globally, DSB repair fluorescent reporter plasmids should be used in *Prkdc*$^{-/-}$ *Hus1*$^{neo/\Delta 1}$ double mutant MEFs as well as in their single counterparts and controls. Then, by using specific A-EJ, C-NHEJ and HRR reporter plasmids, one could test if A-EJ is upregulated in *Prkdc*$^{-/-}$ *Hus1*$^{neo/\Delta 1}$ double mutant MEFs but suppressed in *Prkdc*$^{-/-}$ single mutants.

Concluding, HUS1 has been implied in genome integrity maintenance, in DSB and ICL repair and possibly in lymphocyte maturation through biochemical and genetic studies. HUS1 is indispensable for MMC related damage repair in regard to chromosomal integrity, ICL signaling, and the repair of the resulting DSBs, likely through coordinating DSB repair factors through direct and indirect interaction. In the decision making process between DSB repair mechanisms, HUS1 likely suppresses A-EJ, thus contributing to favoring of HRR outside of V(D)J recombination, and loss of recombination in V(D)J recombination. Further elucidating the role of HUS1 and its fellow clamp members in regulating DDR holds promise for future application in synthetic lethal cancer therapy.

REFERENCES

1. Maslov, A.Y. and J. Vijg, *Genome instability, cancer and aging.* Biochim Biophys Acta, 2009. **1790**(10): p. 963-9.

2. Lindahl, T., *Instability and decay of the primary structure of DNA.* Nature, 1993. **362**(6422): p. 709-715.

3. Lindahl, T. and B. Nyberg, *Rate of depurination of native deoxyribonucleic acid.* Biochemistry, 1972. **11**(19): p. 3610-3618.

4. Muller, S.J. and S. Caradonna, *Isolation and characterization of a human cDNA encoding uracil-DNA glycosylase.* Biochimica et Biophysica Acta (BBA) - Gene Structure and Expression, 1991. **1088**(2): p. 197-207.

5. Cooper, D. and H. Youssoufian, *The CpG dinucleotide and human genetic disease.* Human Genetics, 1988. **78**(2): p. 151-155.

6. Rideout, W.M., 3rd, et al., *5-Methylcytosine as an endogenous mutagen in the human LDL receptor and p53 genes.* Science, 1990. **249**(4974): p. 1288-90.

7. Yasui, M., et al., *Tracing the fates of site-specifically introduced DNA adducts in the human genome.* DNA Repair, 2014. **15**: p. 11-20.

8. Nishida, N., et al., *Reactive Oxygen Species Induce Epigenetic Instability through the Formation of 8-Hydroxydeoxyguanosine in Human Hepatocarcinogenesis.* Digestive Diseases, 2013. **31**(5-6): p. 459-466.

9. Swenberg, J.A., et al., *Endogenous versus exogenous DNA adducts: their role in carcinogenesis, epidemiology, and risk assessment.* Toxicol Sci, 2011. **120 Suppl 1**: p. S130-45.

10. De Bont, R. and N. van Larebeke, *Endogenous DNA damage in humans: a review of quantitative data.* Mutagenesis, 2004. **19**(3): p. 169-185.

11. Zeman, M.K. and K.A. Cimprich, *Causes and consequences of replication stress.* Nat Cell Biol, 2014. **16**(1): p. 2-9.

12. McMurray, C.T., *Mechanisms of trinucleotide repeat instability during human development.* Nat Rev Genet, 2010. **11**(11): p. 786-99.

13. Helmrich, A., et al., *Transcription-replication encounters, consequences and genomic instability.* Nat Struct Mol Biol, 2013. **20**(4): p. 412-8.

14. Lopes, M., et al., *The DNA replication checkpoint response stabilizes stalled replication forks.* Nature, 2001. **412**(6846): p. 557-61.

15. Tercero, J.A. and J.F. Diffley, *Regulation of DNA replication fork progression through damaged DNA by the Mec1/Rad53 checkpoint.* Nature, 2001. **412**(6846): p. 553-7.

16. Cobb, J.A., et al., *DNA polymerase stabilization at stalled replication forks requires Mec1 and the RecQ helicase Sgs1.* EMBO J, 2003. **22**(16): p. 4325-36.

17. Wang, S.Y. and A.J. Varghese, *Cytosine-thymine addition product from DNA irradiated with ultraviolet light.* Biochem Biophys Res Commun, 1967. **29**(4): p. 543-9.

18. Beukers, R. and W. Berends, *Isolation and identification of the irradiation product of thymine.* Biochim Biophys Acta, 1960. **41**: p. 550-1.

19. Kielbassa, C., L. Roza, and B. Epe, *Wavelength dependence of oxidative DNA damage induced by UV and visible light.* Carcinogenesis, 1997. **18**(4): p. 811-6.

20. Mouret, S., et al., *Cyclobutane pyrimidine dimers are predominant DNA lesions in whole human skin exposed to UVA radiation.* Proc Natl Acad Sci U S A, 2006. **103**(37): p. 13765-70.

21. Averbeck, D., D. Papadopoulo, and E. Moustacchi, *Repair of 4,5',8-trimethylpsoralen plus light-induced DNA damage in normal and Fanconi's anemia cell lines.* Cancer Res, 1988. **48**(8): p. 2015-20.

22. Tomasz, M., et al., *Isolation and structure of a covalent cross-link adduct between mitomycin C and DNA.* Science, 1987. **235**(4793): p. 1204-8.

23. Amos, B., *Lessons from the history of light microscopy.* Nat Cell Biol, 2000. **2**(8): p. E151-E152.

24. Nurse, P., *A Long Twentieth Century of the Cell Cycle and Beyond.* Cell. **100**(1): p. 71-78.

25. Garber, K., *Beyond the Nobel Prize: Cell Cycle Research Offers New View of Cancer.* Journal of the National Cancer Institute, 2001. **93**(23): p. 1766-1768.

26. Lee, M.G. and P. Nurse, *Complementation used to clone a human homologue of the fission yeast cell cycle control gene cdc2.* Nature, 1987. **327**(6117): p. 31-35.

27. Hartwell, L.H., et al., *Genetic Control of the Cell Division Cycle in Yeast: V. Genetic Analysis of cdc Mutants.* Genetics, 1973. **74**(2): p. 267-286.

28. Hartwell, L.H., et al., *Genetic Control of the Cell Division Cycle in Yeast.* A model to account for the order of cell cycle events is deduced from the phenotypes of yeast mutants, 1974. **183**(4120): p. 46-51.

29. Evans, T., et al., *Cyclin: a protein specified by maternal mRNA in sea urchin eggs that is destroyed at each cleavage division.* Cell, 1983. **33**(2): p. 389-96.

30. Pines, J. and T. Hunt, *Molecular cloning and characterization of the mRNA for cyclin from sea urchin eggs.* Embo j, 1987. **6**(10): p. 2987-95.

31. Lee, M.G. and P. Nurse, *Complementation used to clone a human homologue of the fission yeast cell cycle control gene cdc2.* Nature, 1987. **327**(6117): p. 31-5.

32. Weinert, T.A. and L.H. Hartwell, *Cell cycle arrest of cdc mutants and specificity of the RAD9 checkpoint.* Genetics, 1993. **134**(1): p. 63-80.

33. Bertoli, C., J.M. Skotheim, and R.A.M. de Bruin, *Control of cell cycle transcription during G1 and S phases.* Nat Rev Mol Cell Biol, 2013. **14**(8): p. 518-528.

34. Bartek, J. and J. Lukas, *Mammalian G1- and S-phase checkpoints in response to DNA damage.* Current Opinion in Cell Biology, 2001. **13**(6): p. 738-747.

35. Harper, J.W. and S.J. Elledge, *The DNA Damage Response: Ten Years After*. Molecular Cell, 2007. **28**(5): p. 739-745.

36. Michaels, M.L., et al., *A repair system for 8-oxo-7,8-dihydrodeoxyguanine.* Biochemistry, 1992. **31**(45): p. 10964-8.

37. de Laat, W.L., N.G. Jaspers, and J.H. Hoeijmakers, *Molecular mechanism of nucleotide excision repair.* Genes Dev, 1999. **13**(7): p. 768-85.

38. Li, G.-M., *Mechanisms and functions of DNA mismatch repair.* Cell Res, 2008. **18**(1): p. 85-98.

39. Czabotar, P.E., et al., *Control of apoptosis by the BCL-2 protein family: implications for physiology and therapy.* Nat Rev Mol Cell Biol, 2014. **15**(1): p. 49-63.

40. Hanahan, D. and Robert A. Weinberg, *Hallmarks of Cancer: The Next Generation.* Cell. **144**(5): p. 646-674.

41. Venkitaraman, A.R., *Cancer susceptibility and the functions of BRCA1 and BRCA2.* Cell, 2002. **108**(2): p. 171-82.

42. Digweed, M., A. Reis, and K. Sperling, *Nijmegen breakage syndrome: consequences of defective DNA double strand break repair.* Bioessays, 1999. **21**(8): p. 649-56.

43. Meyn, M.S., *Ataxia-telangiectasia, cancer and the pathobiology of the ATM gene.* Clin Genet, 1999. **55**(5): p. 289-304.

44. Gorgoulis, V.G., et al., *Activation of the DNA damage checkpoint and genomic instability in human precancerous lesions.* Nature, 2005. **434**(7035): p. 907-913.

45. Bartkova, J., et al., *DNA damage response as a candidate anti-cancer barrier in early human tumorigenesis.* Nature, 2005. **434**(7035): p. 864-870.

46. Bartkova, J., et al., *Oncogene-induced senescence is part of the tumorigenesis barrier imposed by DNA damage checkpoints.* Nature, 2006. **444**(7119): p. 633-637.

47. Di Micco, R., et al., *Oncogene-induced senescence is a DNA damage response triggered by DNA hyper-replication.* Nature, 2006. **444**(7119): p. 638-642.

48. Klein, T.A., et al., *Genetically Determined Differences in Learning from Errors.* Science, 2007. **318**(5856): p. 1642-1645.

49. Greenman, C., et al., *Patterns of somatic mutation in human cancer genomes.* Nature, 2007. **446**(7132): p. 153-158.

50. Bell, D.W., et al., *Heterozygous Germ Line hCHK2 Mutations in Li-Fraumeni Syndrome.* Science, 1999. **286**(5449): p. 2528-2531.

51. Halazonetis, T.D., V.G. Gorgoulis, and J. Bartek, *An Oncogene-Induced DNA Damage Model for Cancer Development.* Science, 2008. **319**(5868): p. 1352-1355.

52. Sarkaria, J.N., et al., *Inhibition of phosphoinositide 3-kinase related kinases by the radiosensitizing agent wortmannin.* Cancer Res, 1998. **58**(19): p. 4375-82.

53. Izzard, R.A., S.P. Jackson, and G.C. Smith, *Competitive and noncompetitive inhibition of the DNA-dependent protein kinase.* Cancer Res, 1999. **59**(11): p. 2581-6.

54. Hickson, I., et al., *Identification and characterization of a novel and specific inhibitor of the ataxia-telangiectasia mutated kinase ATM.* Cancer Res, 2004. **64**(24): p. 9152-9.

55. Golding, S.E., et al., *Improved ATM kinase inhibitor KU-60019 radiosensitizes glioma cells, compromises insulin, AKT and ERK prosurvival signaling, and inhibits migration and invasion.* Mol Cancer Ther, 2009. **8**(10): p. 2894-902.

56. Rainey, M.D., et al., *Transient inhibition of ATM kinase is sufficient to enhance cellular sensitivity to ionizing radiation.* Cancer Res, 2008. **68**(18): p. 7466-74.

57. Zhao, Y., et al., *Preclinical evaluation of a potent novel DNA-dependent protein kinase inhibitor NU7441*. Cancer Res, 2006. **66**(10): p. 5354-62.

58. Shinohara, E.T., et al., *DNA-dependent protein kinase is a molecular target for the development of noncytotoxic radiation-sensitizing drugs.* Cancer Res, 2005. **65**(12): p. 4987-92.

59. Ismail, I.H., et al., *SU11752 inhibits the DNA-dependent protein kinase and DNA double-strand break repair resulting in ionizing radiation sensitization.* Oncogene, 2004. **23**(4): p. 873-82.

60. Kaelin, W.G., Jr., *The concept of synthetic lethality in the context of anticancer therapy.* Nat Rev Cancer, 2005. **5**(9): p. 689-98.

61. Farmer, H., et al., *Targeting the DNA repair defect in BRCA mutant cells as a therapeutic strategy*. Nature, 2005. **434**(7035): p. 917-921.

62. McCabe, N., et al., *Deficiency in the Repair of DNA Damage by Homologous Recombination and Sensitivity to Poly(ADP-Ribose) Polymerase Inhibition.* Cancer Research, 2006. **66**(16): p. 8109-8115.

63. Bryant, H.E., et al., *Specific killing of BRCA2-deficient tumours with inhibitors of poly(ADP-ribose) polymerase.* Nature, 2005. **434**(7035): p. 913-917.

64. Lord, C.J. and A. Ashworth, *The DNA damage response and cancer therapy*. Nature, 2012. **481**(7381): p. 287-94.

65. Jiang, H., et al., *The combined status of ATM and p53 link tumor development with therapeutic response.* Genes & Development, 2009. **23**(16): p. 1895-1909.

66. Dietlein, F., et al., *A functional cancer genomics screen identifies a druggable synthetic lethal interaction between MSH3 and PRKDC.* Cancer Discov, 2014. **4**(5): p. 592-605.

67. Ellison, V. and B. Stillman, *Biochemical Characterization of DNA Damage Checkpoint Complexes: Clamp Loader and Clamp Complexes with Specificity for 5′ Recessed DNA.* PLoS Biol, 2003. **1**(2): p. e33.

68. Majka, J., et al., *Replication Protein A Directs Loading of the DNA Damage Checkpoint Clamp to 5′-DNA Junctions.* Journal of Biological Chemistry, 2006. **281**(38): p. 27855-27861.

69. Bermudez, V.P., et al., *Loading of the human 9-1-1 checkpoint complex onto DNA by the checkpoint clamp loader hRad17-replication factor C complex in vitro.* Proc Natl Acad Sci U S A, 2003. **100**(4): p. 1633-8.

70. Delacroix, S., et al., *The Rad9–Hus1–Rad1 (9–1–1) clamp activates checkpoint signaling via TopBP1.* Genes & Development, 2007. **21**(12): p. 1472-1477.

71. Lee, J., A. Kumagai, and W.G. Dunphy, *The Rad9-Hus1-Rad1 Checkpoint Clamp Regulates Interaction of TopBP1 with ATR.* Journal of Biological Chemistry, 2007. **282**(38): p. 28036-28044.

72. Greer, D.A., et al., *hRad9 Rapidly Binds DNA Containing Double-Strand Breaks and Is Required for Damage-dependent Topoisomerase IIβ Binding Protein 1 Focus Formation.* Cancer Research, 2003. **63**(16): p. 4829-4835.

73. Tibbetts, R.S., et al., *Functional interactions between BRCA1 and the checkpoint kinase ATR during genotoxic stress.* Genes & Development, 2000. **14**(23): p. 2989-3002.

74. Pichierri, P., F. Rosselli, and A. Franchitto, *Werner's syndrome protein is phosphorylated in an ATR/ATM-dependent manner following replication arrest and DNA damage induced during the S phase of the cell cycle.* Oncogene, 2003. **22**(10): p. 1491-500.

75. Davies, S.L., et al., *Phosphorylation of the Bloom's syndrome helicase and its role in recovery from S-phase arrest.* Mol Cell Biol, 2004. **24**(3): p. 1279-91.

76. Li, W., et al., *Absence of BLM leads to accumulation of chromosomal DNA breaks during both unperturbed and disrupted S phases.* J Cell Biol, 2004. **165**(6): p. 801-12.

77. al-Khodairy, F. and A.M. Carr, *DNA repair mutants defining G2 checkpoint pathways in Schizosaccharomyces pombe.* Embo j, 1992. **11**(4): p. 1343-50.

78. Enoch, T., A.M. Carr, and P. Nurse, *Fission yeast genes involved in coupling mitosis to completion of DNA replication.* Genes Dev, 1992. **6**(11): p. 2035-46.

79. Rowley, R., S. Subramani, and P.G. Young, *Checkpoint controls in Schizosaccharomyces pombe: rad1.* Embo j, 1992. **11**(4): p. 1335-42.

80. al-Khodairy, F., et al., *Identification and characterization of new elements involved in checkpoint and feedback controls in fission yeast.* Mol Biol Cell, 1994. **5**(2): p. 147-60.

81. Dean, F.B., L. Lian, and M. O'Donnell, *cDNA cloning and gene mapping of human homologs for Schizosaccharomyces pombe rad17, rad1, and hus1 and cloning of homologs from mouse, Caenorhabditis elegans, and Drosophila melanogaster.* Genomics, 1998. **54**(3): p. 424-36.

82. Kostrub, C.F., et al., *Hus1p, a conserved fission yeast checkpoint protein, interacts with Rad1p and is phosphorylated in response to DNA damage.* Embo j, 1998. **17**(7): p. 2055-66.

83. St Onge, R.P., et al., *The human G2 checkpoint control protein hRAD9 is a nuclear phosphoprotein that forms complexes with hRAD1 and hHUS1.* Mol Biol Cell, 1999. **10**(6): p. 1985-95.

84. Volkmer, E. and L.M. Karnitz, *Human Homologs of Schizosaccharomyces pombe Rad1, Hus1, and Rad9 Form a DNA Damage-responsive Protein Complex.* Journal of Biological Chemistry, 1999. **274**(2): p. 567-570.

85. Thelen, M.P., Č. Venclovas, and K. Fidelis, *A Sliding Clamp Model for the Rad1 Family of Cell Cycle Checkpoint Proteins.* Cell, 1999. **96**(6): p. 769-770.

86. Caspari, T., et al., *Characterization of Schizosaccharomyces pombeHus1: a PCNA-Related Protein That Associates with Rad1 and Rad9.* Molecular and Cellular Biology, 2000. **20**(4): p. 1254-1262.

87. Venclovas, C. and M.P. Thelen, *Structure-based predictions of Rad1, Rad9, Hus1 and Rad17 participation in sliding clamp and clamp-loading complexes.* Nucleic Acids Research, 2000. **28**(13): p. 2481-2493.

88. Onge, R.P.S., et al., *The Human G2 Checkpoint Control Protein hRAD9 Is a Nuclear Phosphoprotein That Forms Complexes with hRAD1 and hHUS1.* Molecular Biology of the Cell, 1999. **10**(6): p. 1985-1995.

89. Burtelow, M.A., et al., *Reconstitution and Molecular Analysis of the hRad9-hHus1-hRad1 (9-1-1) DNA Damage Responsive Checkpoint Complex.* Journal of Biological Chemistry, 2001. **276**(28): p. 25903-25909.

90. Kaur, R., C.F. Kostrub, and T. Enoch, *Structure-Function Analysis of Fission Yeast Hus1-Rad1-Rad9 Checkpoint Complex.* Molecular Biology of the Cell, 2001. **12**(12): p. 3744-3758.

91. Lindsey-Boltz, L.A., et al., *Purification and characterization of human DNA damage checkpoint Rad complexes.* Proceedings of the National Academy of Sciences, 2001. **98**(20): p. 11236-11241.

92. Shiomi, Y., et al., *Clamp and clamp loader structures of the human checkpoint protein complexes, Rad9-1-1 and Rad17-RFC.* Genes to Cells, 2002. **7**(8): p. 861-868.

93. Griffith, J.D., L.A. Lindsey-Boltz, and A. Sancar, *Structures of the Human Rad17-Replication Factor C and Checkpoint Rad 9-1-1 Complexes Visualized by Glycerol Spray/Low Voltage Microscopy.* Journal of Biological Chemistry, 2002. **277**(18): p. 15233-15236.

94. Weiss, R.S., et al., *Mouse Hus1, a homolog of the Schizosaccharomyces pombe hus1+ cell cycle checkpoint gene.* Genomics, 1999. **59**(1): p. 32-9.

95. Weiss, R.S., T. Enoch, and P. Leder, *Inactivation of mouse Hus1 results in genomic instability and impaired responses to genotoxic stress.* Genes Dev, 2000. **14**(15): p. 1886-98.

96. Weiss, R.S., et al., *Hus1 acts upstream of chk1 in a mammalian DNA damage response pathway.* Curr Biol, 2002. **12**(1): p. 73-7.

97. Roos-Mattjus, P., et al., *Phosphorylation of Human Rad9 Is Required for Genotoxin-activated Checkpoint Signaling.* Journal of Biological Chemistry, 2003. **278**(27): p. 24428-24437.

98. Zachos, G., M.D. Rainey, and D.A.F. Gillespie, *Chk1-deficient tumour cells are viable but exhibit multiple checkpoint and survival defects.* The EMBO Journal, 2003. **22**(3): p. 713-723.

99. Weiss, R.S., P. Leder, and C. Vaziri, *Critical role for mouse Hus1 in an S-phase DNA damage cell cycle checkpoint.* Mol Cell Biol, 2003. **23**(3): p. 791-803.

100. Green, C.M., et al., *A novel Rad24 checkpoint protein complex closely related to replication factor C.* Current Biology, 2000. **10**(1): p. 39-42.

101. Zou, L., D. Cortez, and S.J. Elledge, *Regulation of ATR substrate selection by Rad17-dependent loading of Rad9 complexes onto chromatin.* Genes & Development, 2002. **16**(2): p. 198-208.

102. Melo, J.A., J. Cohen, and D.P. Toczyski, *Two checkpoint complexes are independently recruited to sites of DNA damage in vivo.* Genes & Development, 2001. **15**(21): p. 2809-2821.

103. Kondo, T., et al., *Recruitment of Mec1 and Ddc1 Checkpoint Proteins to Double-Strand Breaks Through Distinct Mechanisms.* Science, 2001. **294**(5543): p. 867-870.

104. Jones, R.E., et al., *XRad17 Is Required for the Activation of XChk1 But Not XCds1 during Checkpoint Signaling in Xenopus.* Molecular Biology of the Cell, 2003. **14**(9): p. 3898-3910.

105. St.Onge, R.P., et al., *A Role for the Phosphorylation of hRad9 in Checkpoint Signaling.* Journal of Biological Chemistry, 2003. **278**(29): p. 26620-26628.

106. Paulovich, A.G., C.D. Armour, and L.H. Hartwell, *The Saccharomyces cerevisiae RAD9, RAD17, RAD24 and MEC3 genes are required for tolerating irreparable, ultraviolet-induced DNA damage.* Genetics, 1998. **150**(1): p. 75-93.

107. Kai, M. and T.S. Wang, *Checkpoint activation regulates mutagenic translesion synthesis.* Genes Dev, 2003. **17**(1): p. 64-76.

108. Aylon, Y. and M. Kupiec, *The Checkpoint Protein Rad24 of Saccharomyces cerevisiae Is Involved in Processing Double-Strand Break Ends and in Recombination Partner Choice.* Molecular and Cellular Biology, 2003. **23**(18): p. 6585-6596.

109. Wang, X., et al., *The effect of Hus1 on ionizing radiation sensitivity is associated with homologous recombination repair but is independent of nonhomologous end-joining.* Oncogene, 2006. **25**(13): p. 1980-3.

110. Levitt, P.S., et al., *Genome Maintenance Defects in Cultured Cells and Mice following Partial Inactivation of the Essential Cell Cycle Checkpoint Gene Hus1*. Molecular and Cellular Biology, 2007. **27**(6): p. 2189-2201.

111. Meyerkord, C.L., et al., *Loss of Hus1 sensitizes cells to etoposide-induced apoptosis by regulating BH3-only proteins.* Oncogene, 2008. **27**(58): p. 7248-7259.

112. Yazinski, S.A., et al., *Dual inactivation of Hus1 and p53 in the mouse mammary gland results in accumulation of damaged cells and impaired tissue regeneration.* Proc Natl Acad Sci U S A, 2009. **106**(50): p. 21282-7.

113. Balmus, G., et al., *Disease severity in a mouse model of ataxia telangiectasia is modulated by the DNA damage checkpoint gene Hus1.* Hum Mol Genet, 2012. **21**(15): p. 3408-20.

114. Lyndaker, A.M., et al., *Conditional Inactivation of the DNA Damage Response Gene <italic>Hus1</italic> in Mouse Testis Reveals Separable Roles for Components of the RAD9-RAD1-HUS1 Complex in Meiotic Chromosome Maintenance.* PLoS Genet, 2013. **9**(2): p. e1003320.

115. Balmus, G., et al., *HUS1 regulates in vivo responses to genotoxic chemotherapies.* Oncogene, 2015.

116. Lim, P.X., et al., *Genome Protection by the 9-1-1 Complex Subunit HUS1 Requires Clamp Formation, DNA Contacts, and ATR Signaling-Independent Effector Functions.* J Biol Chem, 2015.

117. Sasaki, M.S. and A. Tonomura, *A high susceptibility of Fanconi's anemia to chromosome breakage by DNA cross-linking agents.* Cancer Res, 1973. **33**(8): p. 1829-36.

118. Toueille, M., et al., *The human Rad9/Rad1/Hus1 damage sensor clamp interacts with DNA polymerase β and increases its DNA substrate utilisation efficiency: implications for DNA repair.* Nucleic Acids Research, 2004. **32**(11): p. 3316-3324.

119. Wang, W., et al., *The human Rad9–Rad1–Hus1 checkpoint complex stimulates flap endonuclease 1.* Proceedings of the National Academy of Sciences of the United States of America, 2004. **101**(48): p. 16762-16767.

120. Shi, G., et al., *Physical and functional interactions between MutY glycosylase homologue (MYH) and checkpoint proteins Rad9-Rad1-Hus1.* Biochem J, 2006. **400**(1): p. 53-62.

121. Smirnova, E., et al., *The human checkpoint sensor and alternative DNA clamp Rad9-Rad1-Hus1 modulates the activity of DNA ligase I, a component of the long-patch base excision repair machinery.* Biochem J, 2005. **389**(Pt 1): p. 13-7.

122. Bai, H., et al., *Interaction between human mismatch repair recognition proteins and checkpoint sensor Rad9-Rad1-Hus1.* DNA Repair (Amst), 2010. **9**(5): p. 478-87.

123. Tsai, F.L. and M. Kai, *The checkpoint clamp protein Rad9 facilitates DNA-end resection and prevents alternative non-homologous end joining.* Cell Cycle, 2014. **13**(21): p. 3460-4.

124. Raschle, M., et al., *DNA repair. Proteomics reveals dynamic assembly of repair complexes during bypass of DNA cross-links.* Science, 2015. **348**(6234): p. 1253671.

125. Wang, X., et al., *Involvement of nucleotide excision repair in a recombination-independent and error-prone pathway of DNA interstrand cross-link repair.* Mol Cell Biol, 2001. **21**(3): p. 713-20.

126. Kai, M., *Role of the Checkpoint Clamp in DNA Damage Response.* Biomolecules, 2013. **3**(1): p. 75-84.

127. Karras, Georgios I., et al., *Noncanonical Role of the 9-1-1 Clamp in the Error-Free DNA Damage Tolerance Pathway.* Molecular Cell, 2013. **49**(3): p. 536-546.

128. Ngo, G.H., et al., *The 9-1-1 checkpoint clamp stimulates DNA resection by Dna2-Sgs1 and Exo1*. Nucleic Acids Res, 2014.

129. Dufault, V.M., et al., *Identification and characterization of RAD9B, a paralog of the RAD9 checkpoint gene.* Genomics, 2003. **82**(6): p. 644-51.

130. Hang, H., et al., *Identification and characterization of a paralog of human cell cycle checkpoint gene HUS1*. Genomics, 2002. **79**(4): p. 487-92.

131. Chang, D.-Y. and A.-L. Lu, *Interaction of Checkpoint Proteins Hus1/Rad1/Rad9 with DNA Base Excision Repair Enzyme MutY Homolog in Fission Yeast, Schizosaccharomyces pombe.* Journal of Biological Chemistry, 2005. **280**(1): p. 408-417.

132. Gembka, A., et al., *The checkpoint clamp, Rad9-Rad1-Hus1 complex, preferentially stimulates the activity of apurinic/apyrimidinic endonuclease 1 and DNA polymerase β in long patch base excision repair.* Nucleic Acids Research, 2007. **35**(8): p. 2596-2608.

133. Zhao, J., et al., *Mismatch repair and nucleotide excision repair proteins cooperate in the recognition of DNA interstrand crosslinks.* Nucleic Acids Res, 2009. **37**(13): p. 4420-9.

134. He, W., et al., *Rad9 plays an important role in DNA mismatch repair through physical interaction with MLH1*. Nucleic Acids Res, 2008. **36**(20): p. 6406-17.

135. Sabbioneda, S., et al., *The 9-1-1 checkpoint clamp physically interacts with polzeta and is partially required for spontaneous polzeta-dependent mutagenesis in Saccharomyces cerevisiae.* J Biol Chem, 2005. **280**(46): p. 38657-65.

136. Giannattasio, M., et al., *Correlation between checkpoint activation and in vivo assembly of the yeast checkpoint complex Rad17-Mec3-Ddc1*. J Biol Chem, 2003. **278**(25): p. 22303-8.

137. De Haro, L.P., et al., *Metnase promotes restart and repair of stalled and collapsed replication forks.* Nucleic Acids Res, 2010. **38**(17): p. 5681-91.

138. Pandita, R.K., et al., *Mammalian Rad9 Plays a Role in Telomere Stability, S- and G2-Phase-Specific Cell Survival, and Homologous Recombinational Repair.* Molecular and Cellular Biology, 2006. **26**(5): p. 1850-1864.

139. Wang, Y., et al., *FANCM and FAAP24 maintain genome stability via cooperative as well as unique functions.* Mol Cell, 2013. **49**(5): p. 997-1009.

140. Williams, H.L., M.E. Gottesman, and J. Gautier, *The differences between ICL repair during and outside of S phase.* Trends in Biochemical Sciences, 2013. **38**(8): p. 386-393.

141. Long, D.T., et al., *Mechanism of RAD51-dependent DNA interstrand cross-link repair.* Science, 2011. **333**(6038): p. 84-7.

142. Clauson, C., O.D. Schärer, and L. Niedernhofer, *Advances in Understanding the Complex Mechanisms of DNA Interstrand Cross-Link Repair.* Cold Spring Harbor Perspectives in Biology, 2013. **5**(10).

143. Lobitz, S. and E. Velleuer, *Guido Fanconi (1892-1979): a jack of all trades.* Nat Rev Cancer, 2006. **6**(11): p. 893-8.

144. Huang, Y., et al., *Modularized Functions of the Fanconi Anemia Core Complex.* Cell Rep, 2014.

145. Huang, M., et al., *Human MutS and FANCM complexes function as redundant DNA damage sensors in the Fanconi Anemia pathway.* DNA Repair (Amst), 2011. **10**(12): p. 1203-12.

146. Ciccia, A., et al., *Identification of FAAP24, a Fanconi anemia core complex protein that interacts with FANCM.* Mol Cell, 2007. **25**(3): p. 331-43.

147. Singh, T.R., et al., *ATR-dependent phosphorylation of FANCM at serine 1045 is essential for FANCM functions.* Cancer Res, 2013. **73**(14): p. 4300-10.

148. Kim, J.M., et al., *Cell cycle-dependent chromatin loading of the Fanconi anemia core complex by FANCM/FAAP24.* Blood, 2008. **111**(10): p. 5215-22.

149. Ishiai, M., et al., *FANCI phosphorylation functions as a molecular switch to turn on the Fanconi anemia pathway.* Nat Struct Mol Biol, 2008. **15**(11): p. 1138-46.

150. Wang, W., *A major switch for the Fanconi anemia DNA damage-response pathway.* Nat Struct Mol Biol, 2008. **15**(11): p. 1128-30.

151. Chen, Y.H., et al., *ATR-Mediated Phosphorylation of FANCI Regulates Dormant Origin Firing in Response to Replication Stress.* Mol Cell, 2015. **58**(2): p. 323-38.

152. Collins, N.B., et al., *ATR-dependent phosphorylation of FANCA on serine 1449 after DNA damage is important for FA pathway function.* Blood, 2009. **113**(10): p. 2181-90.

153. Qiao, F., et al., *Phosphorylation of fanconi anemia (FA) complementation group G protein, FANCG, at serine 7 is important for function of the FA pathway.* J Biol Chem, 2004. **279**(44): p. 46035-45.

154. Wang, X., et al., *Chk1-mediated phosphorylation of FANCE is required for the Fanconi anemia/BRCA pathway.* Mol Cell Biol, 2007. **27**(8): p. 3098-108.

155. Garcia-Higuera, I., et al., *Interaction of the Fanconi anemia proteins and BRCA1 in a common pathway.* Mol Cell, 2001. **7**(2): p. 249-62.

156. Rajendra, E., et al., *The genetic and biochemical basis of FANCD2 monoubiquitination.* Mol Cell, 2014. **54**(5): p. 858-69.

157. Pace, P., et al., *FANCE: the link between Fanconi anaemia complex assembly and activity.* EMBO J, 2002. **21**(13): p. 3414-23.

158. de Winter, J.P., et al., *The Fanconi anemia protein FANCF forms a nuclear complex with FANCA, FANCC and FANCG.* Hum Mol Genet, 2000. **9**(18): p. 2665-74.

159. Cybulski, K.E. and N.G. Howlett, *FANCP/SLX4: A Swiss army knife of DNA interstrand crosslink repair.* Cell Cycle, 2011. **10**(11): p. 1757-1763.

160. Huang, M. and A.D. D'Andrea, *A new nuclease member of the FAN club.* Nat Struct Mol Biol, 2010. **17**(8): p. 926-928.

161. Liu, T., et al., *FAN1 acts with FANCI-FANCD2 to promote DNA interstrand cross-link repair.* Science, 2010. **329**(5992): p. 693-6.

162. MacKay, C., et al., *Identification of KIAA1018/FAN1, a DNA repair nuclease recruited to DNA damage by monoubiquitinated FANCD2.* Cell, 2010. **142**(1): p. 65-76.

163. Smogorzewska, A., et al., *A genetic screen identifies FAN1, a Fanconi anemia-associated nuclease necessary for DNA interstrand crosslink repair.* Mol Cell, 2010. **39**(1): p. 36-47.

164. Klein Douwel, D., et al., *XPF-ERCC1 acts in Unhooking DNA interstrand crosslinks in cooperation with FANCD2 and FANCP/SLX4.* Mol Cell, 2014. **54**(3): p. 460-71.

165. Takata, M., et al., *The Fanconi anemia pathway promotes homologous recombination repair in DT40 cell line.* Subcell Biochem, 2006. **40**: p. 295-311.

166. Newell, A.E., et al., *Interstrand crosslink-induced radials form between non-homologous chromosomes, but are absent in sex chromosomes.* DNA Repair (Amst), 2004. **3**(5): p. 535-42.

167. Hanlon Newell, A.E., et al., *Loss of homologous recombination or non-homologous end-joining leads to radial formation following DNA interstrand crosslink damage.* Cytogenet Genome Res, 2008. **121**(3-4): p. 174-80.

168. van Gent, D.C., J.H. Hoeijmakers, and R. Kanaar, *Chromosomal stability and the DNA double-stranded break connection.* Nat Rev Genet, 2001. **2**(3): p. 196-206.

169. Chapman, J.R., Martin R.G. Taylor, and Simon J. Boulton, *Playing the End Game: DNA Double-Strand Break Repair Pathway Choice.* Molecular Cell, 2012. **47**(4): p. 497-510.

170. Mao, Z., et al., *Comparison of nonhomologous end joining and homologous recombination in human cells.* DNA Repair, 2008. **7**(10): p. 1765-1771.

171. Bunting, S.F. and A. Nussenzweig, *End-joining, translocations and cancer.* Nat Rev Cancer, 2013. **13**(7): p. 443-454.

172. Deriano, L. and D.B. Roth, *Modernizing the nonhomologous end-joining repertoire: alternative and classical NHEJ share the stage.* Annu Rev Genet, 2013. **47**: p. 433-55.

173. Symington, L.S. and J. Gautier, *Double-Strand Break End Resection and Repair Pathway Choice.* Annual Review of Genetics, 2011. **45**(1): p. 247-271.

174. Heyer, W.-D., K.T. Ehmsen, and J. Liu, *Regulation of homologous recombination in eukaryotes.* Annual review of genetics, 2010. **44**: p. 113-139.

175. Williams, G.J., et al., *Structural insights into NHEJ: Building up an integrated picture of the dynamic DSB repair super complex, one component and interaction at a time.* DNA Repair, 2014. **17**: p. 110-120.

176. Ochi, T., Q. Wu, and T.L. Blundell, *The spatial organization of non-homologous end joining: From bridging to end joining.* DNA Repair, 2014. **17**: p. 98-109.

177. Grundy, G.J., et al., *One ring to bring them all—The role of Ku in mammalian non-homologous end joining.* DNA Repair, 2014. **17**: p. 30-38.

178. Errami, A., et al., *Ku86 defines the genetic defect and restores X-ray resistance and V(D)J recombination to complementation group 5 hamster cell mutants.* Molecular and Cellular Biology, 1996. **16**(4): p. 1519-26.

179. Getts, R.C. and T.D. Stamato, *Absence of a Ku-like DNA end binding activity in the xrs double-strand DNA repair-deficient mutant.* J Biol Chem, 1994. **269**(23): p. 15981-4.

180. Rathmell, W.K. and G. Chu, *Involvement of the Ku autoantigen in the cellular response to DNA double-strand breaks.* Proceedings of the National Academy of Sciences, 1994. **91**(16): p. 7623-7627.

181. Rathmell, W.K. and G. Chu, *A DNA end-binding factor involved in double-strand break repair and V(D)J recombination.* Molecular and Cellular Biology, 1994. **14**(7): p. 4741-4748.

182. Smider, V., et al., *Restoration of X-ray resistance and V(D)J recombination in mutant cells by Ku cDNA.* Science, 1994. **266**(5183): p. 288-91.

183. Gu, Y., et al., *Ku70-deficient embryonic stem cells have increased ionizing radiosensitivity, defective DNA end-binding activity, and inability to support V(D)J recombination.* Proceedings of the National Academy of Sciences, 1997. **94**(15): p. 8076-8081.

184. Mimitou, E.P. and L.S. Symington, *Ku prevents Exo1 and Sgs1-dependent resection of DNA ends in the absence of a functional MRX complex or Sae2.* EMBO J, 2010. **29**(19): p. 3358-69.

185. Mari, P.-O., et al., *Dynamic assembly of end-joining complexes requires interaction between Ku70/80 and XRCC4.* Proceedings of the National Academy of Sciences, 2006. **103**(49): p. 18597-18602.

186. Boulton, S.J. and S.P. Jackson, *Saccharomyces cerevisiae Ku70 potentiates illegitimate DNA double-strand break repair and serves as a barrier to error-prone DNA repair pathways.* EMBO J, 1996. **15**(18): p. 5093-103.

187. Chen, S., et al., *Accurate in Vitro End Joining of a DNA Double Strand Break with Partially Cohesive 3'-Overhangs and 3'-Phosphoglycolate Termini: EFFECT OF Ku ON REPAIR FIDELITY.* Journal of Biological Chemistry, 2001. **276**(26): p. 24323-24330.

188. Nussenzweig, A., et al., *Hypersensitivity of Ku80-deficient cell lines and mice to DNA damage: The effects of ionizing radiation on growth, survival, and development.* Proceedings of the National Academy of Sciences, 1997. **94**(25): p. 13588-13593.

189. Difilippantonio, M.J., et al., *DNA repair protein Ku80 suppresses chromosomal aberrations and malignant transformation.* Nature, 2000. **404**(6777): p. 510-514.

190. Ferguson, D.O., et al., *The nonhomologous end-joining pathway of DNA repair is required for genomic stability and the suppression of translocations.* Proceedings of the National Academy of Sciences, 2000. **97**(12): p. 6630-6633.

191. Lovejoy, C.A. and D. Cortez, *Common mechanisms of PIKK regulation.* DNA Repair, 2009. **8**(9): p. 1004-1008.

192. Douglas, P., et al., *Identification of in vitro and in vivo phosphorylation sites in the catalytic subunit of the DNA-dependent protein kinase.* Biochem J, 2002. **368**(Pt 1): p. 243-51.

193. Chan, D.W., et al., *Autophosphorylation of the DNA-dependent protein kinase catalytic subunit is required for rejoining of DNA double-strand breaks.* Genes & Development, 2002. **16**(18): p. 2333-2338.

194. Yu, Y., et al., *DNA-PK phosphorylation sites in XRCC4 are not required for survival after radiation or for V(D)J recombination.* DNA Repair, 2003. **2**(11): p. 1239-1252.

195. Chen, B.P.C., et al., *Cell Cycle Dependence of DNA-dependent Protein Kinase Phosphorylation in Response to DNA Double Strand Breaks.* Journal of Biological Chemistry, 2005. **280**(15): p. 14709-14715.

196. Douglas, P., et al., *The DNA-dependent protein kinase catalytic subunit is phosphorylated in vivo on threonine 3950, a highly conserved amino acid in the protein kinase domain.* Mol Cell Biol, 2007. **27**(5): p. 1581-91.

197. Gao, Y., et al., *A targeted DNA-PKcs-null mutation reveals DNA-PK-independent functions for KU in V(D)J recombination.* Immunity, 1998. **9**(3): p. 367-76.

198. Mahaney, Brandi L., K. Meek, and Susan P. Lees-Miller, *Repair of ionizing radiation-induced DNA double-strand breaks by non-homologous end-joining.* Biochemical Journal, 2009. **417**(3): p. 639-650.

199. Ochi, T., et al., *DNA repair. PAXX, a paralog of XRCC4 and XLF, interacts with Ku to promote DNA double-strand break repair.* Science, 2015. **347**(6218): p. 185-8.

200. Costantini, S., et al., *Interaction of the Ku heterodimer with the DNA ligase IV/Xrcc4 complex and its regulation by DNA-PK.* DNA Repair, 2007. **6**(6): p. 712-722.

201. Hsu, H.-L., S.M. Yannone, and D.J. Chen, *Defining interactions between DNA-PK and ligase IV/XRCC4.* DNA Repair, 2002. **1**(3): p. 225-235.

202. Yano, K.-i., et al., *Ku recruits XLF to DNA double-strand breaks.* EMBO Reports, 2008. **9**(1): p. 91-96.

203. Reynolds, P., et al., *The dynamics of Ku70/80 and DNA-PKcs at DSBs induced by ionizing radiation is dependent on the complexity of damage.* Nucleic Acids Research, 2012. **40**(21): p. 10821-10831.

204. Datta, K., et al., *Molecular analysis of base damage clustering associated with a site-specific radiation-induced DNA double-strand break.* Radiat Res, 2006. **166**(5): p. 767-81.

205. Feng, L. and J. Chen, *The E3 ligase RNF8 regulates KU80 removal and NHEJ repair.* Nat Struct Mol Biol, 2012. **19**(2): p. 201-206.

206. Langerak, P., et al., *Release of Ku and MRN from DNA Ends by Mre11 Nuclease Activity and Ctp1 Is Required for Homologous Recombination Repair of Double-Strand Breaks.* PLoS Genet, 2011. **7**(9): p. e1002271.

207. Neale, M.J., J. Pan, and S. Keeney, *Endonucleolytic processing of covalent protein-linked DNA double-strand breaks.* Nature, 2005. **436**(7053): p. 1053-1057.

208. Wu, D., L.M. Topper, and T.E. Wilson, *Recruitment and Dissociation of Nonhomologous End Joining Proteins at a DNA Double-Strand Break in Saccharomyces cerevisiae.* Genetics, 2008. **178**(3): p. 1237-1249.

209. Brown, Jessica S., et al., *Neddylation Promotes Ubiquitylation and Release of Ku from DNA-Damage Sites.* Cell Reports, 2015. **11**(5): p. 704-714.

210. Frit, P., et al., *Alternative end-joining pathway(s): Bricolage at DNA breaks.* DNA Repair, 2014. **17**: p. 81-97.

211. Wang, H., et al., *Biochemical evidence for Ku-independent backup pathways of NHEJ.* Nucleic Acids Research, 2003. **31**(18): p. 5377-5388.

212. Betermier, M., P. Bertrand, and B.S. Lopez, *Is non-homologous end-joining really an inherently error-prone process?* PLoS Genet, 2014. **10**(1): p. e1004086.

213. Guirouilh-Barbat, J., S. Huck, and B.S. Lopez, *S-phase progression stimulates both the mutagenic KU-independent pathway and mutagenic processing of KU-dependent intermediates, for nonhomologous end joining.* Oncogene, 2007. **27**(12): p. 1726-1736.

214. Rothkamm, K., et al., *Pathways of DNA Double-Strand Break Repair during the Mammalian Cell Cycle.* Molecular and Cellular Biology, 2003. **23**(16): p. 5706-5715.

215. Liang, F., et al., *Chromosomal double-strand break repair in Ku80-deficient cells.* Proceedings of the National Academy of Sciences, 1996. **93**(17): p. 8929-8933.

216. Kabotyanski, E.B., et al., *Double-strand break repair in Ku86- and XRCC4-deficient cells.* Nucleic Acids Research, 1998. **26**(23): p. 5333-5342.

217. Kent, T., et al., *Mechanism of microhomology-mediated end-joining promoted by human DNA polymerase θ.* Nat Struct Mol Biol, 2015. **22**(3): p. 230-237.

218. Jazayeri, A., et al., *ATM- and cell cycle-dependent regulation of ATR in response to DNA double-strand breaks.* Nat Cell Biol, 2006. **8**(1): p. 37-45.

219. Fukushima, T., et al., *Genetic analysis of the DNA-dependent protein kinase reveals an inhibitory role of Ku in late S-G2 phase DNA double-strand break repair.* J Biol Chem, 2001. **276**(48): p. 44413-8.

220. Chen, L., et al., *Cell Cycle-dependent Complex Formation of BRCA1·CtIP·MRN Is Important for DNA Double-strand Break Repair.* Journal of Biological Chemistry, 2008. **283**(12): p. 7713-7720.

221. Panier, S. and S.J. Boulton, *Double-strand break repair: 53BP1 comes into focus.* Nat Rev Mol Cell Biol, 2014. **15**(1): p. 7-18.

222. Cimprich, K.A. and D. Cortez, *ATR: an essential regulator of genome integrity.* Nat Rev Mol Cell Biol, 2008. **9**(8): p. 616-27.

223. Gurley, K.E. and C.J. Kemp, *Synthetic lethality between mutation in Atm and DNA-PK(cs) during murine embryogenesis.* Curr Biol, 2001. **11**(3): p. 191-4.

224. Mills, K.D., et al., *Rad54 and DNA Ligase IV cooperate to maintain mammalian chromatid stability*. Genes Dev, 2004. **18**(11): p. 1283-92.

225. Barnes, D.E., et al., *Targeted disruption of the gene encoding DNA ligase IV leads to lethality in embryonic mice.* Curr Biol, 1998. **8**(25): p. 1395-8.

226. Frank, K.M., et al., *Late embryonic lethality and impaired V(D)J recombination in mice lacking DNA ligase IV*. Nature, 1998. **396**(6707): p. 173-7.

227. Essers, J., et al., *Disruption of mouse RAD54 reduces ionizing radiation resistance and homologous recombination.* Cell, 1997. **89**(2): p. 195-204.

228. Couedel, C., et al., *Collaboration of homologous recombination and nonhomologous end-joining factors for the survival and integrity of mice and cells.* Genes Dev, 2004. **18**(11): p. 1293-304.

229. Raschle, M., et al., *Mechanism of replication-coupled DNA interstrand crosslink repair*. Cell, 2008. **134**(6): p. 969-80.

230. Jasin, M. and R. Rothstein, *Repair of Strand Breaks by Homologous Recombination.* Cold Spring Harbor Perspectives in Biology, 2013. **5**(11).

231. Rothfuss, A. and M. Grompe, *Repair Kinetics of Genomic Interstrand DNA Cross-Links: Evidence for DNA Double-Strand Break-Dependent Activation of the Fanconi Anemia/BRCA Pathway*. Molecular and Cellular Biology, 2004. **24**(1): p. 123-134.

232. Eichinger, C.S. and S. Jentsch, *9-1-1: PCNA's specialized cousin.* Trends Biochem Sci, 2011. **36**(11): p. 563-8.

233. Liu, Q., et al., *Chk1 is an essential kinase that is regulated by Atr and required for the G(2)/M DNA damage checkpoint*. Genes & Development, 2000. **14**(12): p. 1448-1459.

234. Wagner, J.M. and L.M. Karnitz, *Cisplatin-Induced DNA Damage Activates Replication Checkpoint Signaling Components that Differentially Affect Tumor Cell Survival.* Molecular Pharmacology, 2009. **76**(1): p. 208-214.

235. Houghtaling, S., et al., *Epithelial cancer in Fanconi anemia complementation group D2 (Fancd2) knockout mice.* Genes & Development, 2003. **17**(16): p. 2021-2035.

236. Wong, J.C.Y., et al., *Targeted disruption of exons 1 to 6 of the Fanconi Anemia group A gene leads to growth retardation, strain-specific microphthalmia, meiotic defects and primordial germ cell hypoplasia.* Human Molecular Genetics, 2003. **12**(16): p. 2063-2076.

237. Xu, J., *Preparation, Culture, and Immortalization of Mouse Embryonic Fibroblasts*, in *Current Protocols in Molecular Biology*. 2001, John Wiley & Sons, Inc.

238. Simons, A., L.G. Shaffer, and R.J. Hastings, *Cytogenetic Nomenclature: Changes in the ISCN 2013 Compared to the 2009 Edition.* Cytogenet Genome Res, 2013. **141**(1): p. 1-6.

239. Méndez, J. and B. Stillman, *Chromatin Association of Human Origin Recognition Complex, Cdc6, and Minichromosome Maintenance Proteins during the Cell Cycle: Assembly of Prereplication Complexes in Late Mitosis.* Molecular and Cellular Biology, 2000. **20**(22): p. 8602-8612.

240. Barrios-Rodiles, M., et al., *High-Throughput Mapping of a Dynamic Signaling Network in Mammalian Cells.* Science, 2005. **307**(5715): p. 1621-1625.

241. Taipale, M., et al., *Quantitative Analysis of Hsp90-Client Interactions Reveals Principles of Substrate Recognition.* Cell, 2012. **150**(5): p. 987-1001.

242. Muniandy, P., et al., *DNA INTERSTRAND CROSSLINK REPAIR IN MAMMALIAN CELLS: STEP BY STEP.* Critical reviews in biochemistry and molecular biology, 2010. **45**(1): p. 23-49.

243. Auerbach, A.D., *Fanconi Anemia and its Diagnosis.* Mutation research, 2009. **668**(1-2): p. 4-10.

244. Krejci, L., et al., *Homologous recombination and its regulation.* Nucleic Acids Research, 2012.

245. Liaw, H., D. Lee, and K. Myung, *DNA-PK-Dependent RPA2 Hyperphosphorylation Facilitates DNA Repair and Suppresses Sister Chromatid Exchange.* PLoS ONE, 2011. **6**(6): p. e21424.

246. Andreassen, P.R., A.D. D'Andrea, and T. Taniguchi, *ATR couples FANCD2 monoubiquitination to the DNA-damage response.* Genes Dev, 2004. **18**(16): p. 1958-63.

247. Chen, X., et al., *The Fanconi Anemia Proteins FANCD2 and FANCJ Interact and Regulate Each Other's Chromatin Localization.* Journal of Biological Chemistry, 2014.

248. Schlacher, K., H. Wu, and M. Jasin, *A Distinct Replication Fork Protection Pathway Connects Fanconi Anemia Tumor Suppressors to RAD51-BRCA1/2.* Cancer Cell, 2012. **22**(1): p. 106-116.

249. Somyajit, K., et al., *Mammalian RAD51 paralogs protect nascent DNA at stalled forks and mediate replication restart.* Nucleic Acids Research, 2015.

250. Lim, D.S. and P. Hasty, *A mutation in mouse rad51 results in an early embryonic lethal that is suppressed by a mutation in p53.* Mol Cell Biol, 1996. **16**(12): p. 7133-43.

251. Adam, J., B. Deans, and J. Thacker, *A role for Xrcc2 in the early stages of mouse development.* DNA Repair (Amst), 2007. **6**(2): p. 224-34.

252. Deans, B., et al., *Xrcc2 is required for genetic stability, embryonic neurogenesis and viability in mice.* EMBO J, 2000. **19**(24): p. 6675-85.

253. Pittman, D.L. and J.C. Schimenti, *Midgestation lethality in mice deficient for the RecA-related gene, Rad51d/Rad51l3.* Genesis, 2000. **26**(3): p. 167-73.

254. Shu, Z., et al., *Disruption of muREC2/RAD51L1 in mice results in early embryonic lethality which can Be partially rescued in a p53(-/-) background.* Mol Cell Biol, 1999. **19**(12): p. 8686-93.

255. Tsuzuki, T., et al., *Targeted disruption of the Rad51 gene leads to lethality in embryonic mice.* Proc Natl Acad Sci U S A, 1996. **93**(13): p. 6236-40.

256. Kuznetsov, S., et al., *RAD51C deficiency in mice results in early prophase I arrest in males and sister chromatid separation at metaphase II in females.* The Journal of Cell Biology, 2007. **176**(5): p. 581-592.

257. Ying, S., F.C. Hamdy, and T. Helleday, *Mre11-Dependent Degradation of Stalled DNA Replication Forks Is Prevented by BRCA2 and PARP1.* Cancer Research, 2012. **72**(11): p. 2814-2821.

258. Lord, C.J. and A. Ashworth, *RAD51, BRCA2 and DNA repair: a partial resolution.* Nat Struct Mol Biol, 2007. **14**(6): p. 461-462.

259. Gravells, P., et al., *Reduced FANCD2 influences spontaneous SCE and RAD51 foci formation in uveal melanoma and Fanconi anaemia.* Oncogene, 2013. **32**(46): p. 5338-46.

260. Digweed, M., et al., *Attenuation of the formation of DNA-repair foci containing RAD51 in Fanconi anaemia.* Carcinogenesis, 2002. **23**(7): p. 1121-1126.

261. Yamamoto, K., et al., *Fanconi anemia protein FANCD2 promotes immunoglobulin gene conversion and DNA repair through a mechanism related to homologous recombination.* Mol Cell Biol, 2005. **25**(1): p. 34-43.

262. Ohashi, A., et al., *Fanconi anemia complementation group D2 (FANCD2) functions independently of BRCA2- and RAD51-associated homologous recombination in response to DNA damage.* J Biol Chem, 2005. **280**(15): p. 14877-83.

263. Anantha, R.W., E. Sokolova, and J.A. Borowiec, *RPA phosphorylation facilitates mitotic exit in response to mitotic DNA damage.* Proc Natl Acad Sci U S A, 2008. **105**(35): p. 12903-8.

264. Vassin, V.M., et al., *Human RPA phosphorylation by ATR stimulates DNA synthesis and prevents ssDNA accumulation during DNA-replication stress.* J Cell Sci, 2009. **122**(Pt 22): p. 4070-80.

265. Murphy, A.K., et al., *Phosphorylated RPA recruits PALB2 to stalled DNA replication forks to facilitate fork recovery.* J Cell Biol, 2014. **206**(4): p. 493-507.

266. Shi, W., et al., *The role of RPA2 phosphorylation in homologous recombination in response to replication arrest.* Carcinogenesis, 2010. **31**(6): p. 994-1002.

267. Zou, Y., et al., *Functions of human replication protein A (RPA): from DNA replication to DNA damage and stress responses.* J Cell Physiol, 2006. **208**(2): p. 267-73.

268. Binz, S.K., A.M. Sheehan, and M.S. Wold, *Replication Protein A phosphorylation and the cellular response to DNA damage.* DNA Repair, 2004. **3**(8–9): p. 1015-1024.

269. Lee, D.-H., et al., *A PP4 phosphatase complex dephosphorylates RPA2 to facilitate DNA repair via homologous recombination.* Nat Struct Mol Biol, 2010. **17**(3): p. 365-372.

270. Tomida, J., et al., *A novel interplay between the Fanconi anemia core complex and ATR-ATRIP kinase during DNA cross-link repair.* Nucleic Acids Res, 2013. **41**(14): p. 6930-41.

271. Guervilly, J.H., G. Mace-Aime, and F. Rosselli, *Loss of CHK1 function impedes DNA damage-induced FANCD2 monoubiquitination but normalizes the abnormal G2 arrest in Fanconi anemia.* Hum Mol Genet, 2008. **17**(5): p. 679-89.

272. Guirouilh-Barbat, J., et al., *Impact of the KU80 Pathway on NHEJ-Induced Genome Rearrangements in Mammalian Cells.* Molecular Cell. **14**(5): p. 611-623.

273. Sonoda, E., et al., *Differential usage of non-homologous end-joining and homologous recombination in double strand break repair.* DNA Repair (Amst), 2006. **5**(9-10): p. 1021-9.

274. Moynahan, M.E., et al., *Brca1 controls homology-directed DNA repair.* Mol Cell, 1999. **4**(4): p. 511-8.

275. Kinner, A., et al., *Gamma-H2AX in recognition and signaling of DNA double-strand breaks in the context of chromatin.* Nucleic Acids Res, 2008. **36**(17): p. 5678-94.

276. Zou, L., D. Liu, and S.J. Elledge, *Replication protein A-mediated recruitment and activation of Rad17 complexes.* Proceedings of the National Academy of Sciences, 2003. **100**(24): p. 13827-13832.

277. Yan, S. and W.M. Michael, *TopBP1 and DNA polymerase-alpha directly recruit the 9-1-1 complex to stalled DNA replication forks.* J Cell Biol, 2009. **184**(6): p. 793-804.

278. Helt, C.E., et al., *Evidence that DNA damage detection machinery participates in DNA repair.* Cell Cycle, 2005. **4**(4): p. 529-32.

279. Balakrishnan, L., et al., *Long patch base excision repair proceeds via coordinated stimulation of the multienzyme DNA repair complex.* J Biol Chem, 2009. **284**(22): p. 15158-72.

280. Wang, L.C. and J. Gautier, *The Fanconi anemia pathway and ICL repair: implications for cancer therapy.* Critical Reviews in Biochemistry and Molecular Biology, 2010. **45**(5): p. 424-439.

281. Auerbach, A.D. and S.R. Wolman, *Susceptibility of Fanconi's anaemia fibroblasts to chromosome damage by carcinogens.* Nature, 1976. **261**(5560): p. 494-6.

282. Blier, P.R., et al., *Binding of Ku protein to DNA. Measurement of affinity for ends and demonstration of binding to nicks.* Journal of Biological Chemistry, 1993. **268**(10): p. 7594-7601.

283. Yoo, S. and W.S. Dynan, *Geometry of a complex formed by double strand break repair proteins at a single DNA end: Recruitment of DNA-PKcs induces inward translocation of Ku protein.* Nucleic Acids Research, 1999. **27**(24): p. 4679-4686.

284. Downs, J.A. and S.P. Jackson, *A means to a DNA end: the many roles of Ku.* Nat Rev Mol Cell Biol, 2004. **5**(5): p. 367-78.

285. Taccioli, G.E., et al., *Targeted disruption of the catalytic subunit of the DNA-PK gene in mice confers severe combined immunodeficiency and radiosensitivity.* Immunity, 1998. **9**(3): p. 355-66.

286. Kuhfittig-Kulle, S., et al., *The mutagenic potential of non-homologous end joining in the absence of the NHEJ core factors Ku70/80, DNA-PKcs and XRCC4-LigIV.* Mutagenesis, 2007. **22**(3): p. 217-233.

287. Germain, R.N., *T-cell development and the CD4-CD8 lineage decision.* Nat Rev Immunol, 2002. **2**(5): p. 309-322.

288. Levitt, P.S., et al., *Conditional inactivation of the mouse Hus1 cell cycle checkpoint gene.* Genomics, 2005. **86**(2): p. 212-24.

289. Shima, N., et al., *Phenotype-based identification of mouse chromosome instability mutants.* Genetics, 2003. **163**(3): p. 1031-40.

290. Gu, Y., et al., *Growth Retardation and Leaky SCID Phenotype of Ku70-Deficient Mice.* Immunity, 1997. **7**(5): p. 653-665.

291. Biedermann, K.A., et al., *scid mutation in mice confers hypersensitivity to ionizing radiation and a deficiency in DNA double-strand break repair.* Proceedings of the National Academy of Sciences of the United States of America, 1991. **88**(4): p. 1394-1397.

292. Zhang, S., et al., *Congenital bone marrow failure in DNA-PKcs mutant mice associated with deficiencies in DNA repair.* J Cell Biol, 2011. **193**(2): p. 295-305.

293. Woodsworth, D.J., M. Castellarin, and R.A. Holt, *Sequence analysis of T-cell repertoires in health and disease.* Genome Med, 2013. **5**(10): p. 98.

294. Corneo, B., et al., *Rag mutations reveal robust alternative end joining.* Nature, 2007. **449**(7161): p. 483-6.

295. Marechal, A. and L. Zou, *DNA damage sensing by the ATM and ATR kinases.* Cold Spring Harb Perspect Biol, 2013. **5**(9).

296. Chen, B.P., et al., *Ataxia telangiectasia mutated (ATM) is essential for DNA-PKcs phosphorylations at the Thr-2609 cluster upon DNA double strand break.* J Biol Chem, 2007. **282**(9): p. 6582-7.

297. Tomasz, M., *Mitomycin C: small, fast and deadly (but very selective).* Chem Biol, 1995. **2**(9): p. 575-9.

298. Zellweger, R., et al., *Rad51-mediated replication fork reversal is a global response to genotoxic treatments in human cells.* The Journal of Cell Biology, 2015. **208**(5): p. 563-579.

299. Zheng, H., et al., *Nucleotide Excision Repair- and Polymerase η-Mediated Error-Prone Removal of Mitomycin C Interstrand Cross-Links.* Molecular and Cellular Biology, 2003. **23**(2): p. 754-761.

300. Germain, R.N., *T-cell development and the CD4-CD8 lineage decision.* Nat Rev Immunol, 2002. **2**(5): p. 309-22.

301. Malu, S., et al., *Role of non-homologous end joining in V(D)J recombination.* Immunol Res, 2012. **54**(1-3): p. 233-46.